

**ISTANBUL TECHNICAL UNIVERSITY ★ GRADUATE SCHOOL OF SCIENCE**  
**ENGINEERING AND TECHNOLOGY**

**SATELLITE ORBIT DETERMINATION VIA OPTICAL AND RADAR  
SYSTEMS**

**M.Sc. THESIS**

**Derya BAŞ**

**Department of Aeronautical and Astronautical Engineering**

**Aeronautics and Astronautics Engineering Programme**

**DECEMBER 2015**



**ISTANBUL TECHNICAL UNIVERSITY ★ GRADUATE SCHOOL OF SCIENCE**  
**ENGINEERING AND TECHNOLOGY**

**SATELLITE ORBIT DETERMINATION VIA OPTICAL AND RADAR  
SYSTEMS**

**M.Sc. THESIS**

**Derya BAŞ**

**511121160**

**Department of Aeronautical and Astronautical Engineering**

**Aeronautics and Astronautics Engineering Programme**

**Thesis Advisor: Prof. Dr. Cengiz Hacızade**

**DECEMBER 2015**



**İSTANBUL TEKNİK ÜNİVERSİTESİ ★ FEN BİLİMLERİ ENSTİTÜSÜ**

**OPTİK VE RADAR SİSTEMLERİNE DAYALI OLARAK UYDU  
YÖRÜNGESİNİN BELİRLENMESİ**

**YÜKSEK LİSANS TEZİ**

**DERYA BAŞ**

**511121160**

**Uçak ve Uzay Mühendisliği Anabilim Dalı**

**Uçak ve Uzay Mühendisliği Programı**

**Tez Danışmanı: Prof. Dr. Cengiz Hacıoade**

**ARALIK 2015**



Derya BAŞ, a M.Sc. student of ITU Aeronautics and Astronautics Engineering Programme of Graduate School Of Science Engineering And Technology student ID 511121160, successfully defended the thesis entitled “SATELLITE ORBIT DETERMINATION VIA OPTICAL AND RADAR SYSTEMS”, which she prepared after fulfilling the requirements specified in the associated legislations, before the jury whose signatures are below.

**Thesis Advisor :**     **Prof. Dr. Cengiz Hacızade**  
Istanbul Technical University

**Jury Members :**     **Assist. Prof. Dr. Cuma Yarım**  
Istanbul Technical University

**Assist. Prof. Dr. Sıddık Murat Yeşiloğlu**  
Istanbul Technical University

**Date of Submission : 23 November 2015**

**Date of Defense : 25 December 2015**





*To my family,*



## **FOREWORD**

I would like to begin with expressing my deepest gratitude to my thesis advisor Prof. Dr. Cengiz Hacızade for his guidance, support and understanding throughout this study.

I want to thank to my colleagues Ahmet Ekinici, Ali Nur Nurbaki, Cemal Şakacı, Hasan Hüseyin Ertok and Dr. Kemal Sarı from Turksat for their encouragements, guidance and support throughout my master study.

At last but not least, I thank my family for being a great source of energy and motivation.

January 2015

Derya BAŞ

(Aeronautical Engineer)



## TABLE OF CONTENTS

	<u>Page</u>
<b>FOREWORD</b> .....	<b>ix</b>
<b>TABLE OF CONTENTS</b> .....	<b>xi</b>
<b>ABBREVIATIONS</b> .....	<b>xiii</b>
<b>LIST OF FIGURES</b> .....	<b>xvii</b>
<b>SUMMARY</b> .....	<b>xix</b>
<b>ÖZET</b> .....	<b>xxi</b>
<b>1. INTRODUCTION</b> .....	<b>1</b>
1.1. Literature Review .....	1
1.2. Purpose of Thesis .....	6
1.3. Turksat Satellite Fleet .....	8
<b>2. TWO BODY PROBLEM</b> .....	<b>11</b>
2.1. Introduction .....	11
2.2. Angular Momentum and the Orbit Formulas .....	11
2.3. Circular Orbits ( $e = 0$ ) .....	19
2.4. Elliptical Orbits ( $0 < e < 1$ ) .....	21
2.5. Perifocal Frame .....	26
2.6. The Lagrange Coefficients .....	29
<b>3. ORBITS IN THREE DIMENSIONS</b> .....	<b>39</b>
3.1. Introduction .....	39
3.2. Geocentric Right Ascension Declination Frame .....	39
3.3. State Vector and the Geocentric Equatorial Frame .....	42
3.4. Orbital Elements and the State Vector .....	44
3.5. Effects of The Earth's Oblateness .....	47
<b>4. PRELIMINARY ORBIT DETERMINATION</b> .....	<b>51</b>

4.1.	Introduction .....	51
4.2.	Three Position Vectors and Time - Gibbs Method .....	51
4.3.	Two Position Vectors and Time - Lambert's Problem .....	55
4.4.	Sidereal Time .....	62
4.5.	Topocentric Coordinate System .....	64
4.6.	Topocentric Equatorial Coordinate System .....	67
4.7.	Topocentric Horizon Coordinate System .....	68
4.8.	Orbit Determination from Angle and Range Measurements .....	70
4.9.	Angles-only Observations .....	74
4.9.1.	Gauss method .....	75
4.9.2.	Laplace's method .....	83
4.9.3.	Double r-iteration .....	86
<b>5.</b>	<b>EXAMPLES USING GAUSS and GIBBS METHODS .....</b>	<b>91</b>
5.1.	Telescope and Antenna Characteristics.....	91
5.2.	Gauss and Gibbs Methods Examples .....	93
<b>6.</b>	<b>CONCLUSION AND RECOMMENDATIONS .....</b>	<b>105</b>
	<b>REFERENCES .....</b>	<b>107</b>
	<b>APPENDICES .....</b>	<b>111</b>
	<b>CURRICULUM VITAE .....</b>	<b>145</b>
	<b>.....</b>	<b>145</b>

## **ABBREVIATIONS**

<b>BC</b>	: Before Christ
<b>COMS</b>	: Communication Ocean and Meteorological Satellite
<b>Dec</b>	: Declination
<b>EKF</b>	: Extended Kalman Filter
<b>ENZ</b>	: East-North-Zenith
<b>GEO</b>	: Geostationary Earth Orbit
<b>GPS</b>	: Global Positioning System
<b>ISS</b>	: International Space Station
<b>JD</b>	: Julian Day
<b>LEO</b>	: Low Earth Orbit
<b>NASA</b>	: National Aeronautics and Space Administration
<b>NEZ</b>	: North-East-Zenith
<b>OD</b>	: Orbit Determination
<b>OOD</b>	: Operational Orbit Determination
<b>OSNE</b>	: Onboard Satellite Navigation Equipment
<b>POD</b>	: Precise Orbit Determination
<b>RA</b>	: Right Ascension
<b>RMS</b>	: Root Mean Square
<b>SATRE</b>	: SATellite Time and Ranging Equipment
<b>SEZ</b>	: South-East-Zenith
<b>STK</b>	: Systems Tool Kit
<b>TLE</b>	: Two Line Element
<b>TWTT</b>	: Two-Way Time Transfer
<b>UKF</b>	: Unscented Kalman Filter
<b>US</b>	: United States
<b>UT</b>	: Universal Time





## LIST OF TABLES

	<u>Page</u>
Table 1.1: Turksat satellites general information [31]. .....	9
Table 3.1: Oblateness and second zonal harmonics [32]. .....	47
Table 5.1: Characteristics of Turksat-3A ranging antenna. ....	92
Table 5.2: ISS orbit comparison. ....	97
Table 5.3: Characteristic of GEO satellite.....	98
Table 5.4: State vectors of Turksat-4A on 20 October 2015. ....	99
Table 5.5: Orbital parameters of Turksat-4A on 20 October 2015.....	99
Table 5.6: State vectors of Turksat-3A on 20 October 2015. ....	100
Table 5.7: Orbital parameters of Turksat-3A on 20 October 2015.....	100
Table 5.8: State vectors of Turksat-3A on 26 October 2015. ....	101
Table 5.9: Orbital parameters of Turksat-3A on 26 October 2015.....	101
Table 5.10: State vectors of Turksat-2A on 20 October 2015. ....	102
Table 5.11: Orbital parameters of Turksat-2A on 20 October 2015.....	102
Table 5.12: Short time period and long time period on 13 August 2015. ....	103
Table 5.13: State vectors of Cosmos 2397 on 20 October 2015.....	103
Table 5.14: Orbital parameters of Cosmos 2397 on 20 October 2015. ....	103



## LIST OF FIGURES

	<u>Page</u>
Figure 2.1: Path of $m_2$ around $m_1$ [32].	12
Figure 2.2: Components of the velocity of $m_2$ [32].	12
Figure 2.3: Differential area $dA$ [32].	13
Figure 2.4: $\theta$ is the angle between $e$ and $r$ [32].	16
Figure 2.5: Position and velocity of $m_2$ in polar coordinates at $m_1$ [32].	17
Figure 2.6: Illustration of latus rectum, semilatus rectum $p$ , and chord [32].	18
Figure 2.7: $m_1$ is at the focus $F$ . $F'$ is the unoccupied empty focus [32].	22
Figure 2.8: Cartesian coordinate description of the orbit [32].	23
Figure 2.9: Since same major axis, periods and energies are identical [32].	25
Figure 2.10: Perifocal frame $pqw$ [32].	27
Figure 2.11: Position and velocity relative to the perifocal frame [32].	27
Figure 3.1: The earth's orbit around the sun [32].	39
Figure 3.2: Secondary (perturbing) gravitational forces on the earth [32].	40
Figure 3.3: Grid lines of right ascension and declination [32].	41
Figure 3.4: The geocentric equatorial frame [32].	42
Figure 3.5: Geocentric equatorial frame and the orbital elements [32].	44
Figure 4.1: Any one of a set of three coplanar vectors ( $r_1, r_2, r_3$ ) [32].	52
Figure 4.2: Lambert's problem [32].	56
Figure 4.3: Schematic of the relationship among $\theta G O$ , $\theta G$ , $\Lambda$ and $\theta$ [32].	64
Figure 4.4: Oblate spheroidal earth (exaggerated) [32].	65
Figure 4.5: Geocentric latitude ( $\varphi'$ ) and geodetic latitude ( $\varphi$ ) [32].	66
Figure 4.6 Topocentric equatorial coordinate system [32].	67

Figure 4.7: Topocentric horizon ( $xyz$ ) coordinate system [32]. .....	68
Figure 4.8: Earth-orbiting body $B$ tracked by an observer $O$ [32]. .....	70
Figure 4.9: Center of attraction $C$ , observer $O$ and tracked body $B$ [32]. .....	76
Figure 5.1: Observatory building and control office of Turksat observatory. ....	91
Figure 5.2: Telescopes with 50 cm and 8 cm diameters. ....	92
Figure 5.3: Turksat-3A ranging antenna. ....	93
Figure 5.4: Display image of Gauss method in the beginning. ....	94
Figure 5.5: Display image of Gauss method for the results. ....	94
Figure 5.6: Display image of Gibbs method in the beginning. ....	95
Figure 5.7: Display image of Gibbs method for the results. ....	95
Figure 5.8: Display image of Stellarium software for Turksat-3A [33]. ....	96
Figure 5.9: ISS orbit according to NASA [34]. ....	96
Figure 5.10: ISS orbit according to Stellarium [33]. ....	97
Figure 5.11: Display image of GORDAM software [35]. ....	98

# **SATELLITE ORBIT DETERMINATION VIA OPTICAL AND RADAR SYSTEMS**

## **SUMMARY**

Orbit determination is very important subject for astronomers and satellite operators. Orbit determination can be used for providing safe operation, security of satellites, identification of an uncatalogued spacecraft and detect enemy satellite.

Turksat satellite fleet, which is the only communication satellites of Turkey, is explained in detail in introduction. All Turksat satellites are located in Geostationary Earth Orbit (GEO) and designed to provide services for voice, data, internet, TV and radio broadcasting. Therefore, orbit determination is very significant for Turksat Company and for me as a Turksat employee. Turksat-2A, Turksat-3A and Turksat-4A satellite data are used in this thesis.

Two-body problem and orbits in 3D are described item by item to understand the essential points of orbital mechanics in chapter two and three, respectively.

Satellite is placed in the planned mission orbit via launcher and then propulsion system of satellite. However, satellite is in tendency to slip to the unsteady points because of orbital perturbations such as atmospheric drag, gravitational perturbations, solar radiation pressure, lunar gravity and solar gravity. Therefore, satellite maneuvering must be done regularly to correct the position of satellites and continue the mission victoriously. Hence, perturbation effects are kept in mind while estimating orbit with precise orbit determination methods such as least square method, Kalman filter and GPS.

Moreover, preliminary orbit determination methods are detailed in four. Then, the best preliminary orbit determination methods for optical and radar systems are selected to apply to the inputs for this thesis. Success of Gauss method is proved for angle only data orbital problems and Gibbs method is the best orbit determining method for radar systems.

Orbit determination code is written for Gauss and Gibbs method in Matlab. Right ascension and declination data for the specified time are measured by telescope in Turksat Main Campus. Then, these data are used as input for Gauss method, so orbital parameters and state vectors are found. Likewise, range, azimuth and elevation data of the Turksat satellites for the specified time are measured by antenna in Turksat Main Campus. Then, these data are used as input for Gibbs method, so orbital parameters and state vectors are found. There is selection button for using telescope and antenna data in Gauss method Matlab code to find orbital parameters and just compare the results and reliability of telescope and antenna data. For this reason, right ascension and declination is calculated in the code by using azimuth and

elevation data for antenna choice. Furthermore, a free open source planetarium software Stellarium that shows 3D simulation of sky and gives angle and position data is utilized to compare results that are calculated using the measured data in Turksat. Additionally, GORDAM software orbital parameter results, that was used by Turksat for orbit determination, was obtained for comparison.

Optical measurements of Turksat-2A, Turksat-3A, Turksat-4A, Russian communication satellite Cosmos 2397 in GEO are done using telescope in Turksat. In addition, Turksat-2A, Turksat-3A and Turksat-4A data are obtained using Stellarium software and GORDAM software. Furthermore, Turksat-2A, Turksat-3A and Turksat-4A data acquired using antenna in Turksat.

Data that is measured by Turksat telescope and data that is obtained from Stellarium software are estimated via Gauss method and used to make a comparison with GORDAM results. In addition, antenna data is utilized as input for Gauss and Gibbs methods to compare accuracy of the methods with GORDAM results. Moreover, Gauss method results for telescope and antenna data in the same specific time are contrasted.

As a conclusion, weather conditions and human errors have an effect upon sensibility of telescope for optical measurements. Moreover, antenna is more accurate than telescope and can measure ranging value, so Gibbs method gives more sensible results than Gauss method. Stellarium is independent from weather conditions and human errors, so input data always gives good results. GORDAM uses least square method, so it gives the best results. Gauss method using antenna data gives better results than Gauss method using telescope data. Furthermore, short period time measurements give better results because Gauss method works robust especially once data is separated by  $10^\circ$  or less (so by 40 minutes or less). Gauss method is the best method for angle only observations while Gibbs method is the best method for ranging data in order to determine preliminary orbit.

## OPTİK VE RADAR SİSTEMLERİNE DAYALI OLARAK UYDU YÖRÜNGESİNİN BELİRLENMESİ

### ÖZET

İlk yapay uydu olan Sputnik, 4 Ekim 1957’ de fırlatılmıştır ve devamında bir çok ülke yapay uydu üretmeye ve işletmeye başlamıştır. Böylece, yörünge belirleme, gök bilimciler ve uydu işletmecileri için çok önemli bir konu haline gelmiştir. Radar, lazer, teleskop gibi metotlarla yörünge belirleme ve iyileştirme çalışmaları yapılmıştır. Teleskop sadece karanlıkta kullanılabildiğinden ve hava koşullarına bağlı olduğundan kullanım kısıtlaması vardır. Ancak, teleskop ölçümleri ile kabul edilebilir sağlam sonuçlara ulaşılabilirdiği bir çok kez ispatlanmıştır. Yörünge belirleme ile güvenli operasyon ve uydunun düşman uydulara karşı güvenliği sağlanabilir. Ayrıca, kataloglanmamış uydular ve gök cisimleri tanımlanabilir. Ek olarak, askeriye ve ülkenin güvenliği için düşman uydular tespit edilebilir.

Türkiye’ nin haberleşme uydularına sahip tek şirketi olan Türksat A.Ş.’ nin uydu filosu giriş bölümünde detaylı olarak anlatılmıştır. Tüm Türksat uyduları, yer sabit yörüngede konumlanmıştır ve ses, data, internet, TV ile radyo yayıncılığı servisleri vermektedir. Bu yüzden, Türksat şirketi ve bir Türksat çalışanı olarak benim için yörünge belirleme konusu çok önemlidir. Bu tezde şu an aktif olarak kullanılmakta olan Türksat-2A, Türksat-3A ve Türksat-4A uydularının teleskop ve anten ile ölçülüp elde edilmiş açıl ve mesafe verileri kullanılmıştır.

Yörünge mekaniğinin temellerini ve yörünge yapısını anlamak amacıyla iki cisim problemi ve üç boyutta yörünge konuları sırasıyla ikinci ve üçüncü bölümlerde detaylı olarak açıklanmıştır.

Uydu fırlatıcısı, sonrasında uydunun itki sistemi ve yönelim belirleme sistemi ile uydu önceden planlanmış görev yörüngesine yerleştirilir. Ancak uydu, atmosfer direnci, yerçekimi ile ilgili perturbasyonlar, solar radyasyon basıncı, Ay çekim kuvveti ve Güneş çekim kuvveti gibi yörüngesel perturbasyonlardan dolayı düzensiz bölgelere kayma eğilimi gösterir. Bu yüzden, uydunun pozisyonunu düzeltmek ve göreve başarıyla devam edebilmesini sağlamak amacıyla düzenli olarak uydu manevraları yapılmalıdır. Bundan dolayı, en küçük kareler yöntemi, Kalman filtresi ve GPS gibi hassas yörünge tahmini yapan metotlar yörüngesel perturbasyonları dikkate almaktadır.

Ek olarak, ilk yörünge tahmini metotları sırasıyla dördüncü bölümde detaylı olarak işlenmiştir. Sonrasında bu tez için kullanılacak olan ölçüm verilerine en uygun ilk yörünge tahmini metotları seçilmiştir. Yörünge belirleme konusunda, şimdiye kadar yapılmış çalışmalar ve tecrübeler ışığında, sadece açı verilerinin olduğu yörünge belirleme problemleri için, Gauss metodu en uygun seçimdir. Ayrıca, radar sistemleri

yani mesafe ölçümü ile elde edilebilen veriler için ise en uygun metot Gibbs metodudur.

Gauss ve Gibbs metotları için Matlab program dilinde kod yazılmıştır. Kod için gerekli üç ölçüm girdileri metin belgesine yazılmıştır ve kod çalıştırıldığında kullanıcıdan girdi dosyasını seçmesi istenmiştir. Uyduların belirli bir tarihte ve saatte bulundukları konumdaki sağ açıklık ve dik açıklık verileri, Türksat Ana Kampüsü'nde bulunan teleskop ile ölçülmüştür. Sonrasında bu veriler Gauss metodu kodunda girdi olarak kullanılmıştır ve bu açılara karşılık gelen yörünge parametreleri ile durum vektörü hesaplanmıştır. Dahası, uyduların belirli bir tarihte ve saatte bulundukları konumdaki mesafe, azimut açısı (güney açısı) ve elevasyon (yükseklik) açısı verileri Türksat Ana Kampüsü'nde bulunan anten ile ölçülmüştür. Sonrasında, benzer olarak bu veriler Gibbs metodu kodunda girdi olarak kullanılmıştır ve bu açılara karşılık gelen yörünge parametreleri ile durum vektörü hesaplanmıştır. Sadece, teleskop ve anten aracılığı ile elde edilmiş verilerden hesaplanan yörünge parametreleri ve durum vektörlerini karşılaştırma amacıyla, Gauss metodu için hazırlanmış Matlab koduna teleskop ve anten seçeneği eklenmiştir. Kullanıcı ilk başta teleskop mu ya da anten verisi mi kullanacağını seçmek zorundadır. Bu amaçla, anten azimut ve elevasyon değerlerinin, açılım ve yükselim açıları değeri karşılığı, kodun içinde dönüşüm matrisleri kullanılarak otomatik olarak hesaplanmaktadır. Kullanıcı sadece girdi dosyasına açılım ve yükselim açıları yerine azimut ve elevasyon değerlerini yazmalıdır.

Ek olarak, gökyüzünü üç boyutlu gösterebilen ve uydu ile gök cisimlerinin açı ile pozisyon değerlerini verebilen, bir ücretsiz açık kod planetarium yazılımı olan Stellarium kullanılmıştır. Stellarium verileri elde edilirken, Türksat Kampüsü ile aynı enlem, boylam ve denizden yükseklik değerleri ayarlanmıştır. Böylece, Türksat teleskop ve antenlerinden elde edilen veriler ile Stellarium yazılımından elde edilen verilerin hassasiyeti karşılaştırılabilmiştir.

Dahası, Türksat'ın yörünge belirlemek için kullandığı GORDAM yazılımından yörünge parametreleri elde edilmiştir ve ölçümlerden elde edilen sonuçlar ile karşılaştırılmıştır. GORDAM yazılımı, en küçük kareler metodu ile yörünge belirlemektedir.

Türksat-2A, Türksat-3A, Türksat-4A, yer sabit yörüngede bulunan Rus haberleşme uydusu Kozmoz 2397' nin optik ölçümleri Türksat' da bulunan teleskop ile yapılmıştır. Ek olarak, Türksat-2A, Türksat-3A, Türksat-4A uydularının verileri Stellarium ve GORDAM yazılımları ile elde edilmiştir. Dahası, Türksat-2A, Türksat-3A, Türksat-4A uydularının ölçümleri Türksat' da bulunan anten ile yapılmıştır.

Türksat' da bulunan teleskop ile ölçülmüş veriler ile Stellarium' dan elde edilmiş veriler, Gauss metodu ile hesaplanmıştır ve sonucunda bulunan yörünge parametreleri ile durum vektörleri GORDAM sonuçlarıyla da karşılaştırılmıştır. Ayrıca, Türksat' da bulunan anten ile ölçülmüş veriler, Gauss ve Gibbs metotları ile hesaplanmıştır ve sonuçta elde edilen yörünge parametreleri ile durum vektörleri GORDAM sonuçlarıyla da karşılaştırılmıştır. Dahası, önceden belirlenmiş aynı saatte alınmış teleskop ve anten verileri, Gauss metodu ile hesaplanıp karşılaştırılmıştır.

Sonuç olarak, hava koşulları ve insan kaynaklı hatalar, optik ölçümler yapılırken teleskop hassasiyetini önemli ölçüde etkilemektedir. Dahası, anten teleskoba göre daha doğru ölçüm alır ve mesafe bilgisini ölçebilir, bu yüzden Gibbs metodu, Gauss metoduna göre daha hassas sonuçlar vermektedir. Stellarium yazılımı, hava koşulları ve insan kaynaklı hatalardan etkilenmediği için, her zaman daha iyi ölçüm verileri



elde edilebilir. GORDAM yazılımı ise hassas yörünge tahmini yaptığından ve en küçük kareler metodunu kullandığından en iyi sonuçları vermektedir.

Anten verilerini kullanan Gauss metodu, teleskop verilerini kullanan Gauss metoduna göre daha iyi sonuçlar vermektedir. Ek olarak, özellikle veriler  $10^\circ$  veya daha az aralıklı olduğunda (yani 40 dakika veya daha az), Gauss metodu daha sağlıklı sonuçlar vermektedir. Netice itibariyle, sadece açısal ölçümler söz konusu olduğunda Gauss, mesafe verisinin de elde edildiği durumlarda Gibbs, ilk yörünge belirlenirken en iyi metotlardır. İki metodun da, ilk yörünge belirleme konusunda kabul edilebilir derecede doğru sonuçlar verdiği görülmüştür.



## **1. INTRODUCTION**

### **1.1. Literature Review**

Johann Kepler (1571-1630) performed the first initial orbit determination produced astronomical tables of the positions of the planets and stars known as Rudolphine Tables in 1627. The conjunctions of Mercury and the Sun were been predicted enough accurately within five hours in 1631. The first practical method to find the orbit of a body from three observations was been devised and expressed by Newton. The first true determination of a comet of 1680's parabolic orbit from three observations was done by Newton. Successive graphical approximations were used to determine a parabolic orbit from observations [1].

Leonhard Euler (1707-1783) found the first completely analytical method to solve same problem discovered the equation that connecting two radius vectors and the subtended chord of the parabola with the interval of time resulted complex but accurate infinite series. Euler's formulas were generalized consisting of elliptical and hyperbolic orbits by Johann H. Lambert (1728-1779). Moreover, Joseph Louis Lagrange (1736-1813) found the Lagrange expansion theorem providing a series representation of Kepler's equation for the stable solutions of the three-body problem. In addition, Pierre-Simon de Laplace (1749-1827) discovered completely a new method of orbit determination that depended only on angles gave not insignificant solution supremely without computers doing complex calculations [1].

Karl Friedrich Gauss (1777-1855) developed a practical technique for initial orbit determination that is pertinent today as it was in 1802 due to using the right ascension and declination at three observation times to determine orbit. Furthermore, Josiah Gibbs (1839-1903) found a geometrical solution for initial calculations that can solve for very short time spans, so it is required for modern radar systems and dense observational data [1].

Then, data that is more precise was needed and new methods are developed for precise orbit determination. Adrian Marie Legendre (1752-1833) found the least

square method. Another famous precise orbit determination method, Kalman filtering was developed by Rudolf E. Kalman (1930- ). Kalman filtering is more popular than least squares method today, but it is just fundamentals variation of Legendre [1]. Reliable functional and stochastic models specify the performance of a Kalman filter. In other words, the reliability of dynamic models and observational information should be accurately defined by model errors and their covariance matrices [2].

Global Positioning System (GPS) satellites firstly obtained their orbits precisely using GPS receiver. TOPEX/Poseidon altimeter satellite (1992) is the first user satellite to fly a precise GPS receiver [3]. According to Wettergren et al, “At least four GPS signals are tracked to determine the code and carrier ranges, from which the position can be derived. The accuracy improves when using more GPS satellites and by averaging over many measurements” [4].

There are two master’s theses about orbital determination in Turkey. Seda Aydın Duru who was a master student of Department of Astronomy and Space Sciences of Ankara University wrote a thesis about orbit determination and verification of satellite and space debris via ground-based optical systems. In this thesis, orbit determination of artificial satellites and space debris in the Low Earth Orbit (LEO) based on observational methods with small telescope using Gauss and Gibbs methods in JAVA were studied. In addition, STK (Systems Tool Kit) was used via TLE (Two Line Element) data to confirm orbital parameters that were obtained from measurement results [5]. Hakan Abacı who was a master student of Department of Electrical and Electronics Engineering of Hacettepe University wrote a thesis about satellite orbit simulation and orbit determination using TLE data to obtain state vectors in Matlab [6].

Additionally, there are several articles about orbit determination. Arroyo et al improved a new high order method to evaluate nonlinear system solutions and determine orbit of celestial body. At the end of the tests, decrease in number of iterations that made process faster was observed, and so more tolerances that are limited could be used for improving accuracy without increasing much more the number of iterations [7].

According to Montojo et al, “Orbit determination can be improved by taking into consideration the data from other stations, such as angular observations alone or

together with ranging measurements to the satellite”. Orbit Determination Tool Kit was utilized as software for determining precise orbits of geostationary satellites [8].

As reported by Cao et al, “A more precise orbit and prediction can be obtained compared to common short arc methods when observations starting 1 day prior the maneuver and 2 h after the maneuver are adopted in POD (Precise Orbit Determination)” [9].

Moreover, initial orbit determination by a genetic algorithm using two well-known solutions for the Lambert’s problem: universal variable method and Battin method was improved in Kyushu University. Orbit was estimated with a little better performance than Gauss’s methods and Escobal’s method by 120 km while the rotational angle result was closer to the osculating orbit elements than the mean orbit elements [10].

Hui et al used SATRE (SATellite Time and Ranging Equipment) to determine orbit for geostationary satellite. According to Hui et al, “All the experiments indicate that a meter-level accuracy of orbit determination for geostationary satellite is achievable” [11].

Japanese first Mars explorer NOZOMI was used to determine orbit without telemetry by using unusual range and Doppler data [12]. This is an impressive and strange orbit determination example. Although satellite cannot perform the planned mission, it can be still used for other researches.

Furthermore, a new GEO combined precise orbit determination (POD) strategy that combines pseudorange data and C-band transfer ranging data was researched in China. As reported by Rui et al, “Even for the combination of one C-band transfer ranging station and 4 pseudorange stations, POD is able to achieve a reasonable accuracy with the radial error of 0.280 m and the 2-h predicted radial error of 0.888 m [13].

Moreover, orbit determination using only differenced ranges between master station and slave stations conjunction with C-band ranging was studied in China. According to Yang et al, “The accuracy of orbit determination and orbit precision is limited by the length of baselines between master station and slave stations. In order to improve the orbit accuracy, the baselines of differenced ranges should be lengthened” [14].

Satellite laser ranging was used to determine precise orbit of Haiyang-2. At the end, 3D orbital accuracy about 12.5 cm and radial accuracy is better than 3 cm was acquired [15].

Wang utilized least absolute deviation estimation to prevent unreliable results of least square error estimation due to outliers happen in the observation [16]. Wang noted that

For the problem of orbit improvement, the least absolute deviation estimation has no advantage, because the method based on the least square estimation may provide fine result both in efficiency and quality when fairly good initial values are available, and it is also not suitable for the routine data processing because of the restriction of computing amount. When observational data and initial values are not so satisfactory, and orbit improvement is impeded, the method proposed in this paper may be applied to obtaining reliable initial values and to the pretreatment of data, so that the noise immunity of former iterations will be raised in the course of orbit improvement [16].

The reduced dynamic technique was firstly proved on the TOPEX/ Poseidon mission in 1992 and further work have use this technique in the satellite positioning field like improvements in dynamic models and processing efficiencies because of achievement of the technique [17]. For instance, reduced dynamic orbit determination tool that depends on GPS utilizing accelerometer data was improved to analyze GRACE and CHAMP data [18]. The first reliable dual-band spaceborne GPS receivers were carried on board by CHAMP satellite [19]. At the end of the researches, more stable scale and bias factors, and high-quality orbit were obtained. Moreover, it was shown that accelerometer measurements was more beneficial while days of high solar activity [18].

Position and velocity of SMART-1 and C-EOR were obtained via extended Kalman filter (EKF) and unscented Kalman filter (UKF) in case of range measurements are not available. Average localization errors for both estimators were within the bounds of possibility and the same order of magnitude while UKF had better performance [20].

A new method was developed to improve geostationary satellite navigation accuracy by using dynamic Two-Way Time Transfer (TWTT) measurements. Dainty et al improved a simulation for satellites in GEO orbits with GPS receivers onboard generated a position with 1) GPS with a crystal clock, 2) GPS with an onboard atomic clock, 3) GPS with TWTT to a ground-based atomic clock, and 4) GPS with

TWTT to a ground-based clock synchronized to GPS time for comparison. 21-38% improvement in the 3-D RMS position accuracy over the standard GPS case (case 1) was obtained for cases 2 and 3 (including atomic clock) while 60%-70% improvement in 3-D RMS positioning accuracy was acquired for case 4 [21].

Mikhailov and Vasil'ev developed onboard satellite navigation equipment (OSNE) and procedures for space based radio navigation receivers [22]. According to Mikhailov and Vasil'ev,

- (1) The GEO navigation using GPS provides sufficient accuracy ( $1\sigma \sim 10-40$  m), even in the case of moderate stability 10-9 quartz oscillators used as onboard clocks.
- (2) The time to the first fix is about 12 h for GEO applications. Availability of the GEO initial elements is a necessary condition for the working capacity of the proposed algorithm.
- (3) The proposed OD [orbit determination] method can be applied not only to GEO, but also for LEO, HEO, and Geostationary Transfer Orbit.
- (4) A unified algorithm like this can significantly reduce the cost of navigation software development [22].

Operational orbit determination (OD) of geostationary Communication, Ocean, and Meteorological Satellite (COMS) mission was performed using ranging and tracking data from a single ground station for correcting satellite positioning knowledge to accomplish image navigation registration on the ground. Then, a method was evaluated to prevent singularity due to small longitude difference between the satellite and tracking site via the ranging and tracking data of two stations. Three-sigma position accuracy on the order of 1.5 km root-sumsquare was obtained applying only single-station data with the correction of the azimuth bias achieved by two stations [23].

Helmert variance component estimation method was used for the combined orbit determination (transmitting data and pseudo range data) of GEO satellites using different observations, and usability of this method was shown [24].

Some problems shown up while processing on-board GPS data of Shenzhou 4 via Kalman filter algorithm were examined [25]. According to Jia and Xiong,

- (1) The theoretical criterion for the selection of the variance matrix of model error lies in that the adjustable parameters  $Q_S$ ,  $Q_T$ ,  $Q_W$ ,  $Q_n$  and  $Q_b$  should be the minimum values which can make the filter run steadily and smoothly for a long time and that the mean square error of the (O - C) sequence in its stable state should match the theoretical mean square error. During the actual operation a conservative method may be adopted, by selecting a set of slightly larger parameter values.

- (2) It is guaranteed that the filter can operate normally after a 3 hour interruption of the signal when the discrimination threshold of the outliers is increased up to 6 or 8 times the mean square error.
- (3) According to several characteristics of the filter divergence, autonomous monitoring of the running state of the filter on the satellite may be realized [25].

Orbit determination system of KOMPSAT-2 Mission Control Element was developed using GPS. For this purpose, GPS navigation solution data was used to perform Operational Orbit Determination (OOD) for the normal satellite mission operations while GPS raw measurement such as C/A code pseudorange and L1 carrier phase data was utilized to achieve Precise Orbit Determination (POD) for the satellite image product enhancement. TOPEX/POSEDON and CHAMP satellite was used to carry out functional and performance tests of the POD via two methods that GRAPHIC technique uses C/A code pseudorange and L1 carrier phase data once TEC estimation technique uses only L1 carrier phase data. As a result, C/A code performance was a major factor to the accuracy assessment showed by POD results via GRAPHIC technique. Moreover, altitude of the CHAMP satellite was lower than that of the KOMPSAT-2, so TEC scale factor estimation technique could be applied [26].

## **1.2. Purpose of Thesis**

Sputnik that was launched on October 4, 1957 is the first artificial satellite. Then, various countries have launched satellites; hence, orbit determination and identification of each satellite have been important to provide safe operation and security of satellites. Various equipment such radar, lasers and optical telescopes are utilized for determining or improving orbits of satellites via signals from satellites or observation data. Although weather or lighting conditions limit the observation time of optical observation, it is useful to obtain accurate satellite position determination [27].

Preliminary orbit determination for solar system bodies like comets and minor planets has great significance to detect them. On the other hand, its importance for satellite orbits is restricted by regular tracking campaigns for most satellites and orbital element databases of reasonable accuracy. However, launcher injection errors



or the identification of an uncatalogued spacecraft can be done using preliminary orbit determination [28].

Moreover, space debris has strong effect on the safety of present and future space missions in the high inclination Low Earth Orbit (LEO) region containing sun-synchronous orbits. Thus, orbit determination is an important subject for developing the planning of collision avoidance maneuvers and reducing the impact risk [29].

Orbital position changes due to anomalies and so orbital maneuvers must be done regularly to correct the position of satellite. Otherwise, mission cannot accomplish. Thus, orbit determination is very important for artificial satellites.

Moreover, enemy satellite can be detected using orbit determination methods and satellite period can be estimated. In this way, this data that obtained via quality telescope or ranging method can be used for military missions.

Angular observations can be used alone to determine orbit for angle only observations. On the other hand, ranging measurements can be utilized to determine orbit more robustly. Gibbs method and Lambert's problem are used with ranging measurement while Gauss method, Laplace's problem and double r-iteration are used for angle only observations in order to determine preliminary orbit. Furthermore, least square method, Kalman filters and GPS are used for precise orbit determination.

Laplace method is convenient only middle point even though it is close to other data points. However, Gauss method adjusts data to all three points and is reliable for all data. On the other hand, double r-iteration is efficient for large spreads in data for multiple observing locations. Therefore, Gauss method is the most suitable for orbit determination of Turksat satellites for angle only observation. Furthermore, Gauss developed Gauss method really to improve Lambert's problem [1]. Thus, Gibbs method is used in thesis because Gauss method has already used and there is no need for less improved Lambert's problem.

Preliminary orbit determination results are utilized as an initial condition for precise orbit determination [30]. Thus, accuracy of preliminary orbit determination results are very significant to obtain as much as possible accurate orbit.

As a conclusion, aim of this thesis is to obtain initial condition values for orbit determination via preliminary orbit determination methods.

### **1.3. Turksat Satellite Fleet**

There are four Turksat communication satellites are in Geostationary Orbit (GEO), which Turksat-2A, Turksat-3A, Turksat-4A and Turksat-4B. The general information of each Turksat satellites are seen in Table 1.1 [31].

**Table 1.1: Turksat satellites general information [31].**

	<b>Turksat-2A</b>	<b>Turksat-3A</b>	<b>Turksat-4A</b>	<b>Turksat-4B</b>
<b>Manufacturer</b>	Alcatel Alenia Space Industries	Alcatel Alenia Space Industries	Mitsubishi Electric Corporation	Mitsubishi Electric Corporation
<b>Platform</b>	SpaceBus 3000B3	SpaceBus 3000B3	DS2000	DS2000
<b>Stabilization type</b>	3 Axial Control	3 Axial Control	3 Axial Control	3 Axial Control
<b>Date of service commencement</b>	2001	2008	2013	2015
<b>Location of orbit</b>	42° Eastern Longitude	42° Eastern Longitude	42° Eastern Longitude	50° Eastern Longitude
<b>Payload general characteristics</b>	<b>Uplink Coverage Areas</b> East, West Steerable S1 and S2	<b>Uplink Coverage Areas</b> Turkey, East and West	<b>Ku Band BSS Coverage Areas</b> Turkey, West (Turkey, North Africa, Europe) and East (Turkey, Middle East, Asia)	<b>Ku Band Coverage Areas</b> Turkey, West (Turkey, North Africa, Europe) and East (Turkey, Middle East, Asia)
	<b>Downlink Coverage Areas</b> East, West Steerable S1 and S2	<b>Downlink Coverage Areas</b> West and East	<b>Ku Band FSS/Ka Band Coverage Areas</b> Africa/Turkey and Europe	<b>Ka Band Coverage Areas</b> Beams over Turkey, Middle East, Europe and Asia
	<b>Number of Transponders</b> 32	<b>Number of Transponders</b> 24	<b>Number of Transponders</b> 30	<b>C Band Coverage Areas</b> Africa and Turkey
	<b>Total Band Width</b> 1092 MHz	<b>Total Band Width</b> 1296 MHz	<b>Total Band Width</b> 1750 MHz	<b>Number of Transponders</b> 43 <b>Total Band Width</b> 3400 MHz
<b>Platform technical specs</b>	<b>Nominal Launching Weight</b> 3400 kg <b>Maximum Power To Be Consumed</b> 4100 Watt	<b>Nominal Launching Weight</b> 3110 kg <b>Maximum Power To Be Consumed</b> 6126.9 Watt	<b>Nominal Launching Weight</b> 4910 kg <b>Maximum Power To Be Consumed</b> 7670 Watt	<b>Nominal Launching Weight</b> 4977 kg <b>Maximum Power To Be Consumed</b> 7600 Watt
<b>Launcher</b>	Ariane 4	Ariane 5	Proton-M	Proton-M



## 2. TWO BODY PROBLEM

### 2.1. Introduction

Previous Lunar missions and new scientific results have shown that operating in the lunar environment and exploring the Moon still have major challenges for manned and robotic missions. Regarding lunar surface and its environment, the effects of them are still unknowns scientifically; however, scientific data is available from the recent missions to have an idea for preparing for future exploration [32].

### 2.2. Angular Momentum and the Orbit Formulas

The angular momentum of body  $m_2$  relative to  $m_1$  is the moment of  $m_2$ 's relative linear momentum  $m_2\dot{\mathbf{r}}$  is  $\mathbf{H}_{2/1} = \mathbf{r} \times m_2\dot{\mathbf{r}}$ , where the velocity of  $m_2$  relative to  $m_1$  is  $\dot{\mathbf{r}} = \mathbf{v}$ . Divide this equation through by  $m_2$  and let  $\mathbf{h} = \mathbf{H}_{2/1}/m_2$  [32],

$$\mathbf{h} = \mathbf{r} \times \dot{\mathbf{r}} \quad (2.1)$$

$\mathbf{h}$  is the relative angular momentum of  $m_2$  per unit mass, specific relative angular momentum and units of  $\mathbf{h}$  are square kilometers per second. Taking the time derivative of  $\mathbf{h}$  gives:  $\frac{d\mathbf{h}}{dt} = \dot{\mathbf{r}} \times \dot{\mathbf{r}} + \mathbf{r} \times \ddot{\mathbf{r}}$ . However,  $\dot{\mathbf{r}} \times \dot{\mathbf{r}} = 0$  and  $\ddot{\mathbf{r}} = -\left(\frac{\mu}{r^3}\right)\mathbf{r}$ , hence  $\mathbf{r} \times \ddot{\mathbf{r}} = \mathbf{r} \times \left(-\frac{\mu}{r^3}\right)\mathbf{r} = -\frac{\mu}{r^3}(\mathbf{r} \times \mathbf{r}) = 0$ . Thus, angular momentum is conserved [32],

$$\frac{d\mathbf{h}}{dt} = 0 \quad (\text{or } \mathbf{r} \times \dot{\mathbf{r}} = \text{constant}) \quad (2.2)$$

On condition that the position vector  $\mathbf{r}$  and the velocity vector  $\dot{\mathbf{r}}$  are parallel, Eqn (2.1) and accordingly Eqn (2.2) yield zero. Rectilinear trajectories whereon  $m_2$  moves toward or away from  $m_1$  in a straight line are characterized by zero angular momentum [32].

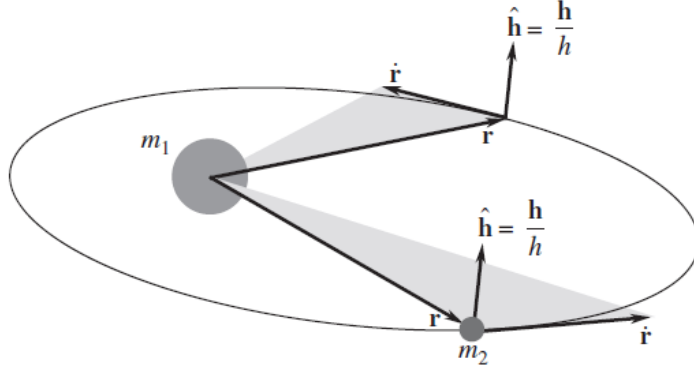


**Figure 2.1: Path of  $m_2$  around  $m_1$  [32].**

As seen in Figure 2.1, the position vector  $\mathbf{r}$  and the velocity vector  $\dot{\mathbf{r}}$  lie in the same plane at any point of a curvilinear trajectory.  $\mathbf{r} \times \dot{\mathbf{r}} = \mathbf{h}$  and the unit vector normal to the plane is [32],

$$\hat{\mathbf{h}} = \frac{\mathbf{h}}{h} \quad (2.3)$$

This unit vector is constant due to the conservation of angular momentum (Eqn (2.2)). Therefore, the path of  $m_2$  around  $m_1$  lies in a single plane [32].

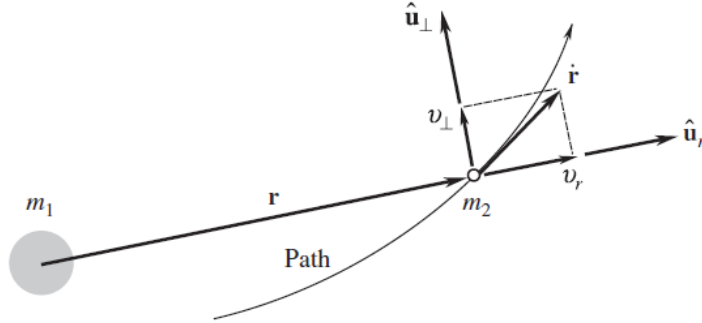


**Figure 2.2: Components of the velocity of  $m_2$  [32].**

As seen in Figure 2.2, it is convenient to orient oneself above that plane and look down upon the path because the orbit of  $m_2$  around  $m_1$  forms a plane. Resolve the relative velocity vector  $\dot{\mathbf{r}}$  into components  $\mathbf{v}_r = v_r \hat{\mathbf{u}}_r$  and  $\mathbf{v}_\perp = v_\perp \hat{\mathbf{u}}_\perp$  along the outward radial from  $m_1$  and perpendicular to it where  $\hat{\mathbf{u}}_r$  and  $\hat{\mathbf{u}}_\perp$  are the radial and perpendicular (azimuthal) unit vectors. Thus Eqn (2.28) can be written as  $\mathbf{r} \times \mathbf{v} = r \hat{\mathbf{u}}_r \times (v_r \hat{\mathbf{u}}_r + v_\perp \hat{\mathbf{u}}_\perp) = r v_\perp \hat{\mathbf{h}}$ . That is [32],

$$h = r v_\perp \quad (2.4)$$

Obviously, the angular momentum only hinges on the azimuthal component of the relative velocity [32].

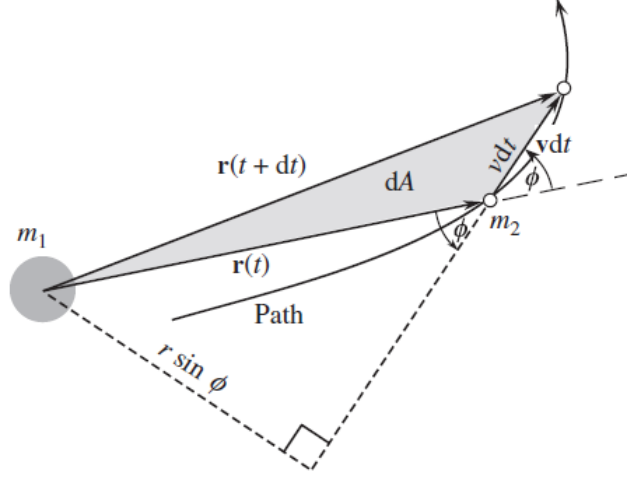


**Figure 2.3: Differential area  $dA$  [32].**

As seen in Figure 2.3, during the differential time interval  $dt$  the position vector  $r$  sweeps out an area  $dA$ . The triangular area  $dA$  is given by  $dA = \frac{1}{2} \times \text{base} \times \text{altitude} = \frac{1}{2} \times v dt \times r \sin \phi = \frac{1}{2} r (v \sin \phi) dt = \frac{1}{2} r v_{\perp} dt$  [8].

Thus, utilizing Eqn (2.4) [32],

$$\frac{dA}{dt} = \frac{h}{2} \quad (2.5)$$

$dA/dt$  is described as areal velocity and according to Eqn (2.5) it is constant. This result is known as Kepler's second law that equal areas are swept out in equal times. Use the bac-cab rule to proceed with an effort [32]:

$$\mathbf{A} \times (\mathbf{B} \times \mathbf{C}) = \mathbf{B}(\mathbf{A} \cdot \mathbf{C}) - \mathbf{C}(\mathbf{A} \cdot \mathbf{B}) \quad (2.6)$$

Using [32]

$$\mathbf{r} \cdot \mathbf{r} = r^2 \quad (2.7)$$

Thus  $\frac{d}{dt}(\mathbf{r} \cdot \mathbf{r}) = 2\mathbf{r} \frac{d\mathbf{r}}{dt}$  but  $\frac{d}{dt}(\mathbf{r} \cdot \mathbf{r}) = \mathbf{r} \cdot \frac{d\mathbf{r}}{dt} + \frac{d\mathbf{r}}{dt} \cdot \mathbf{r} = 2\mathbf{r} \frac{d\mathbf{r}}{dt}$  so obtain the important identity [32]

$$\mathbf{r} \cdot \dot{\mathbf{r}} = r \dot{r} \quad (2.8a)$$

For the reason that  $\dot{\mathbf{r}} = \mathbf{v}$  and  $r = \|\mathbf{r}\|$ , this can be written as [32]

$$\mathbf{r} \cdot \mathbf{v} = \|\mathbf{r}\| \frac{d\|\mathbf{r}\|}{dt} \quad (2.8b)$$

Take crossproduct of both sides of  $\ddot{\mathbf{r}} = -\frac{\mu}{r^3} \mathbf{r}$  with the specific angular momentum  $\mathbf{h}$  [32]:

$$\ddot{\mathbf{r}} \times \mathbf{h} = -\frac{\mu}{r^3} \mathbf{r} \times \mathbf{h} \quad (2.9)$$

For the reason that  $\frac{d}{dt}(\dot{\mathbf{r}} \times \mathbf{h}) = \ddot{\mathbf{r}} \times \mathbf{h} + \dot{\mathbf{r}} \times \dot{\mathbf{h}}$ , the left side can be written as  $\ddot{\mathbf{r}} \times \mathbf{h} = \frac{d}{dt}(\dot{\mathbf{r}} \times \mathbf{h}) - \dot{\mathbf{r}} \times \dot{\mathbf{h}}$ . However, the angular momentum is constant ( $\dot{\mathbf{h}} = 0$ ) according to Eqn (2.2), in this way this reduce to [32]

$$\ddot{\mathbf{r}} \times \mathbf{h} = \frac{d}{dt}(\dot{\mathbf{r}} \times \mathbf{h}) \quad (2.10)$$

The right side of Eqn (2.8) can be transformed by the following sequence of substitutions [32]:

$$\begin{aligned} \frac{1}{r^3} \mathbf{r} \times \mathbf{h} &= \frac{1}{r^3} [\mathbf{r} \times (\mathbf{r} \times \dot{\mathbf{r}})] \quad ([\mathbf{h} = \mathbf{r} \times \dot{\mathbf{r}}]) \\ &= \frac{1}{r^3} [\mathbf{r}(\mathbf{r} \cdot \dot{\mathbf{r}}) - \dot{\mathbf{r}}(\mathbf{r} \cdot \mathbf{r})] \quad ([\text{bac-cab rule}]) \\ &= \frac{1}{r^3} [\mathbf{r}(r\dot{r}) - \dot{\mathbf{r}}r^2] \\ &= \frac{\mathbf{r}\dot{r} - \dot{\mathbf{r}}r}{r^2} \end{aligned}$$

However,  $\frac{d}{dt}\left(\frac{\mathbf{r}}{r}\right) = \frac{r\dot{\mathbf{r}} - \dot{\mathbf{r}}r}{r^2} = -\frac{r\dot{r} - \dot{\mathbf{r}}r}{r^2}$ . Thus [32],

$$\frac{1}{r^3} \mathbf{r} \times \mathbf{h} = -\frac{d}{dt}\left(\frac{\mathbf{r}}{r}\right) \quad (2.11)$$

Substituting Eqn (2.10) and (2.11) into Eqn (2.9), get  $\frac{d}{dt}(\dot{\mathbf{r}} \times \mathbf{h}) = \frac{d}{dt}\left(\mu \frac{\mathbf{r}}{r}\right)$  or  $\frac{d}{dt}\left(\dot{\mathbf{r}} \times \mathbf{h} - \mu \frac{\mathbf{r}}{r}\right) = 0$ . That is [32],

$$\dot{\mathbf{r}} \times \mathbf{h} - \mu \frac{\mathbf{r}}{r} = \mathbf{C} \quad (2.12)$$



where the vector  $\mathbf{C}$  that is called the Laplace vector is a constant having the dimensions of  $\mu$ . Eqn (2.12) is the first integral of the equation of motion,  $\ddot{\mathbf{r}} = -\left(\frac{\mu}{r^3}\right)\mathbf{r}$ . Taking the dot product of both sides of Eqn (2.12) with the vector  $\mathbf{h}$  gives  $(\dot{\mathbf{r}} \times \mathbf{h}) \cdot \mathbf{h} - \mu \frac{\mathbf{r} \cdot \mathbf{h}}{r} = \mathbf{C} \cdot \mathbf{h}$  [32].

$(\dot{\mathbf{r}} \times \mathbf{h}) \cdot \mathbf{h} = 0$  due to  $\dot{\mathbf{r}} \times \mathbf{h}$  is perpendicular to both  $\dot{\mathbf{r}}$  and  $\mathbf{h}$ . Similarly,  $\mathbf{r} \cdot \mathbf{h} = 0$  due to  $\mathbf{h} = \mathbf{r} \times \dot{\mathbf{r}}$  is perpendicular to both  $\mathbf{r}$  and  $\dot{\mathbf{r}}$ . Thus  $\mathbf{C} \cdot \mathbf{h} = 0$ , that means  $\mathbf{C}$  is perpendicular to  $\mathbf{h}$  that is normal to the orbital plane and the Laplace vector must lie in the orbital plane. Rearrange Eqn (2.12) and write it as [32]

$$\frac{\mathbf{r}}{r} + \mathbf{e} = \frac{\dot{\mathbf{r}} \times \mathbf{h}}{\mu} \quad (2.13)$$

Where  $\mathbf{e} = \mathbf{C}/\mu$  and the dimensionless vector  $\mathbf{e}$  is called the eccentricity vector. The line defined by the vector  $\mathbf{e}$  is commonly described as the apse line. Take the dot product of both sides of Eqn (2.13) with  $\mathbf{r}$  to obtain a scalar equation [32].

$$\frac{\mathbf{r} \cdot \mathbf{r}}{r} + \mathbf{r} \cdot \mathbf{e} = \frac{\mathbf{r} \cdot (\dot{\mathbf{r}} \times \mathbf{h})}{\mu} \quad (2.14)$$

Simplify the right side by employing the vector identity [32]

$$\mathbf{A} \cdot (\mathbf{B} \times \mathbf{C}) = (\mathbf{A} \times \mathbf{B}) \cdot \mathbf{C} \quad (2.15)$$

from that obtain [32]

$$\mathbf{r} \cdot (\dot{\mathbf{r}} \times \mathbf{h}) = (\mathbf{r} \times \dot{\mathbf{r}}) \cdot \mathbf{h} = \mathbf{h} \cdot \mathbf{h} = h^2 \quad (2.16)$$

Substituting this expression into the right side of Eqn (2.14) and substituting  $\mathbf{r} \cdot \mathbf{r} = r^2$  on the left gives [32]

$$r + \mathbf{r} \cdot \mathbf{e} = \frac{h^2}{\mu} \quad (2.17)$$

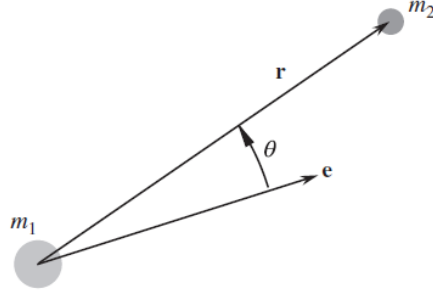


**Figure 2.4:  $\theta$  is the angle between  $e$  and  $r$  [32].**

From the definition of dot product get  $\mathbf{r} \cdot \mathbf{e} = r e \cos \theta$  that  $e$  is the eccentricity (the magnitude of the eccentricity vector  $\mathbf{e}$ ) and  $\theta$  is the true anomaly. As seen in Figure 2.4,  $\theta$  is the angle between the fixed vector  $\mathbf{e}$  and the variable position vector  $\mathbf{r}$ .

Rewrite Eqn (2.44) as  $r + r e \cos \theta = \frac{h^2}{\mu}$  or [32]

$$r = \frac{h^2}{\mu} \frac{1}{1 + e \cos \theta} \quad (2.18)$$

This is the orbit equation that defines the path of the body  $m_2$  around  $m_1$  relative to  $m_1$ . Also  $\mu$ ,  $h$ ,  $e$  are constants.  $\mathbf{h}$  is perpendicular to  $\mathbf{e}$  so  $\mathbf{r} \cdot \mathbf{e} = 0$ . There are not negative values of eccentricity,  $e \geq 0$ . It is a mathematical statement of Kepler's first law that the planets follow elliptical paths around the sun due to the orbit equation describes conic sections, including ellipses. Two body orbits are frequently referred to as Keplerian orbits [32].

The angular velocity of the position vector  $\mathbf{r}$  is  $\dot{\theta}$ , the rate of change of the true anomaly. The component of velocity normal to the position vector in terms of the angular velocity [32]

$$v_{\perp} = r \dot{\theta} \quad (2.19)$$

Substituting this into Eqn (2.4) gives the specific angular momentum in terms of the angular velocity [32]

$$h = r^2 \dot{\theta} \quad (2.20)$$

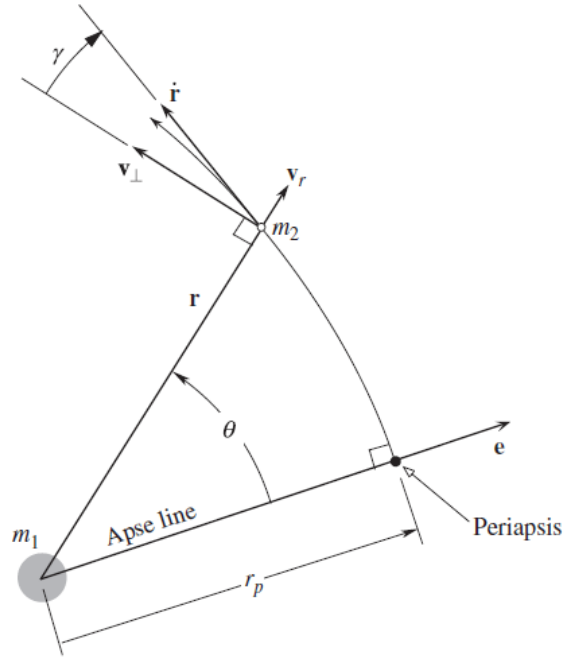


**Figure 2.5: Position and velocity of  $m_2$  in polar coordinates at  $m_1$  [32].**

As seen in Figure 2.5, it is convenient to have formulas for computing the radial and azimuthal components of velocity. From  $h = rv_{\perp}$ , obtain  $v_{\perp} = \frac{h}{r}$ . Substituting  $r$  from Eqn (2.18) readily gives [32]

$$v_{\perp} = \frac{\mu}{h}(1 + e\cos\theta) \quad (2.21)$$

For the reason that  $v_r = \dot{r}$ , take the derivative of Eqn (2.18) to get  $\dot{r} = \frac{dr}{dt} = \frac{d}{dt} \left[ \frac{h^2}{\mu} \frac{1}{1+e\cos\theta} \right] = \frac{h^2}{\mu} \left[ -\frac{e(-\dot{\theta}\sin\theta)}{(1+e\cos\theta)^2} \right] = \frac{h^2}{\mu} \frac{e\sin\theta}{(1+e\cos\theta)^2} \frac{h}{r^2}$  where use of the fact that  $\dot{\theta} = \frac{h}{r^2}$  from Eqn (2.20). Substituting Eqn (2.18) one more time and simplifying finally gives [32]

$$v_r = \frac{\mu}{h} e\sin\theta \quad (2.22)$$

As seen from Eqn (2.18),  $m_2$  comes closest to  $m_1$  ( $r$  is the smallest) when  $\theta=0$  (unless  $e=0$ , in which case the distance between  $m_1$  and  $m_2$  is constant). Periapsis is the point of closest approach lies on the apse line and as seen in Figure 2.5 the distance  $r_p$  to periapsis is obtained by setting the true anomaly equal to zero [32],

$$r_p = \frac{h^2}{\mu} \frac{1}{1+e} \quad (2.23)$$

As seen from Eqn (2.22), the radial component of velocity is zero at periapsis. For  $0 < \theta < 180^\circ$ ,  $v_r$  is positive so  $m_2$  is moving away from periapsis. Nonetheless, Eqn (2.22) shows that if  $180^\circ < \theta < 360^\circ$ , then  $v_r$  is negative so  $m_2$  is moving toward periapsis [32].

As seen in Figure 2.5, the flight path angle  $\gamma$  is the angle that the velocity vector  $\mathbf{v} = \dot{\mathbf{r}}$  makes with the normal to the position vector. Local horizon is the normal to the position vector points in the direction of  $v_\perp$ . From Figure 2.5 [32]

$$\tan\gamma = \frac{v_r}{v_\perp} \quad (2.24)$$

Substituting Eqns (2.21) and (2.22) leads at once to the expression [32]

$$\tan\gamma = \frac{e \sin\theta}{1 + e \cos\theta} \quad (2.25)$$

The flight path angle, like  $v_r$ , is positive (velocity vector directed above the local horizon) at that time the spacecraft is moving away from periapsis and is negative (velocity vector directed below the local horizon) at that time the spacecraft is moving toward periapsis [32].

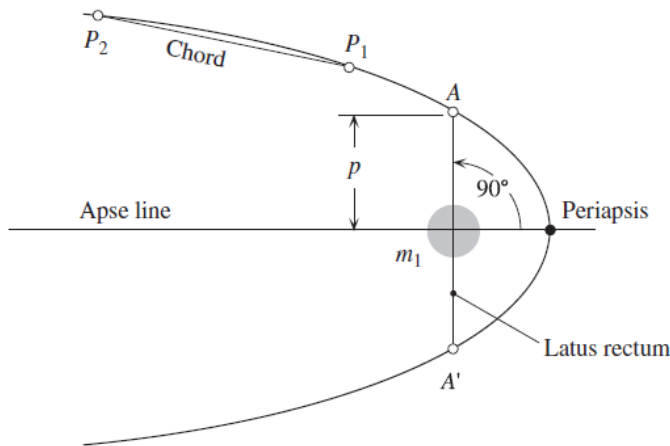


**Figure 2.6: Illustration of latus rectum, semilatus rectum  $p$ , and chord [32].**

As seen in Figure 2.6, the trajectory described by the orbit equation is symmetric about the apsis line due to  $\cos(-\theta) = \cos\theta$ , that also shows a chord, the straight line connecting any two points on the orbit. The latus rectum is the chord through the center of attraction perpendicular to the apsis line and the center of attraction divides

the latus rectum into two equal parts by symmetry, each of length  $p$  known as semilatus rectum. It is seen from Eqn (2.18) [32]

$$p = \frac{h^2}{\mu} \quad (2.26)$$

Furthermore, true anomaly is measured positive counterclockwise consistent with the usual polar coordinate sign convention [32].

### 2.3. Circular Orbits ( $e = 0$ )

If  $e = 0$  in the orbital equation  $r = \frac{h^2}{\mu} \frac{1}{1+e\cos\theta}$  gives [32]

$$r = \frac{h^2}{\mu} \quad (2.27)$$

Thus,  $r = \text{constant}$ , so the orbit of  $m_2$  around  $m_1$  is a circle. Moreover  $\dot{r} = 0$  and accordingly  $v = v_\perp$ , so angular momentum formula  $h = rv_\perp$  becomes simply  $h = rv$  for a circular orbit. Substituting this  $h$  expression into Eqn (2.62) and solving for  $v$  gives the velocity of a circular orbit [32]:

$$v_{\text{circular}} = \sqrt{\frac{\mu}{r}} \quad (2.28)$$

Period is the time  $T$  required for one orbit. The period of a circular orbit is easy to compute due to the speed is constant,  $T = \frac{\text{circumference}}{\text{speed}} = \frac{2\pi r}{\sqrt{\mu/r}}$  so [32]

$$T_{\text{circular}} = \frac{2\pi}{\sqrt{\mu}} r^{3/2} \quad (2.29)$$

The specific energy of a circular orbit,  $\varepsilon = -\frac{1}{2} \frac{\mu^2}{h^2}$ . Employing Eqn (2.27) gives [32]

$$\varepsilon_{\text{circular}} = -\frac{\mu}{2r} \quad (2.30)$$

Visibly, the energy of a circular orbit is negative. When the radius goes up, the energy becomes less negative so it increases [32].

Specific energy  $\varepsilon$  must be increased in order to launch a satellite from the surface of the earth into a circular orbit. The rocket motors of the launch vehicle supplies this energy. A propulsion system that can place a large mass in LEO can place a smaller mass in a higher earth orbit because of the energy of a satellite of mass  $m$  is  $\mathcal{E} = m\varepsilon$  [32].

Altitude of LEO lies between about 150 km and about 1000 km. Furthermore, an LEO is well above the outer limits of the drag producing atmosphere (about 80 km) and well below the hazardous Van Allen radiation belts, the innermost of that begins at about 2400 km [32].

The center of mass of the two body system lies at the center of the earth due to the earth is nearly 20 orders of magnitude more massive than the largest conceivable artificial satellite and  $\mu = G(m_{earth} + m_{satellite}) = Gm_{earth}$ . The value of the earth's gravitational parameter to be used throughout this book is [32]

$$\mu_{earth} = 398600 \text{ km}^3/\text{s}^2 \quad (2.31)$$

GEO is circular orbit that a satellite remains always above the same point on the earth's equator. The radial from the center of the earth to the satellite must have the same angular velocity as the earth itself,  $2\pi$  radians per sidereal day for GEO. The sidereal day is the time it takes the earth to complete one rotation relative to inertial space (the fixed stars) while the ordinary 24h day, or synodic day, is the time it takes the sun to apparently rotate when around the earth from high noon one day to high noon the next. The synodic and sidereal days would be identical with the condition that the earth stood still in space. Nevertheless,  $2\pi/365.26$  rad along its solar orbit is advanced during the earth makes one absolute rotation around its axis. Thus, its inertial angular velocity  $\omega_E$  is  $\left[\left(2\pi + \frac{2\pi}{365.26}\right) \text{ rad}\right]/(24h)$ , that is [32]

$$\omega_E = 72.9217 \times 10^{-6} \text{ rad/s} \quad (2.32)$$

Communication satellites and global weather satellites are located in GEO due to the large portion of the earth's surface visible from that altitude and strictly, ground stations do not have to track the satellite that appears motionless in the sky [32].

From Eqn (2.28), the speed of the satellite in its circular GEO of radius  $r_{GEO}$  is  $v_{GEO} = \sqrt{\frac{\mu}{r_{GEO}}}$ . Otherwise, the speed  $v_{GEO}$  along its circular path is related to the absolute angular velocity  $\omega_E$  of the earth by the kinematics formula  $v_{GEO} = \omega_E r_{GEO}$ . Equalize these two expressions and solve for  $r_{GEO}$  gives  $r_{GEO} = \sqrt[3]{\frac{\mu}{\omega_E^2}}$ . Substituting Eqn (2.31) and (2.32) gives [32]

$$r_{GEO} = \sqrt[3]{\frac{398600}{(72.9217 \times 10^{-6})^2}} = 42164 \text{ km} \quad (2.33)$$

Moreover, the distance of the satellite above the earth's surface is  $z_{GEO} = r_{GEO} - R_E = 42164 - 6378 = 35786 \text{ km}$ . Substituting Eqn (2.33) into  $v_{GEO} = \sqrt{\frac{\mu}{r_{GEO}}}$  gives [32]

$$v_{GEO} = \sqrt{\frac{398600}{42164}} = 3.075 \text{ km/s} \quad (2.34)$$

#### 2.4. Elliptical Orbits ( $0 < e < 1$ )

The denominator of Eqn (2.45) varies with the true anomaly  $\theta$  but it remains positive and never becomes zero in condition that  $0 < e < 1$ . Thus, the relative position vector that remains bounded has its smallest magnitude at the periapsis  $r_p$ . Once the denominator of  $r = \frac{h^2}{\mu} \frac{1}{1 + e \cos \theta}$  gets its minimum value (at  $\theta = 180^\circ$ ), the maximum value of  $r$  is reached and that point is known as the apoapsis. Radial coordinate of apoapsis  $r_a$  is [32]

$$r_a = \frac{h^2}{\mu} \frac{1}{1 - e} \quad (2.35)$$

In this case, an ellipse is defined by Eqn (2.18) [32].

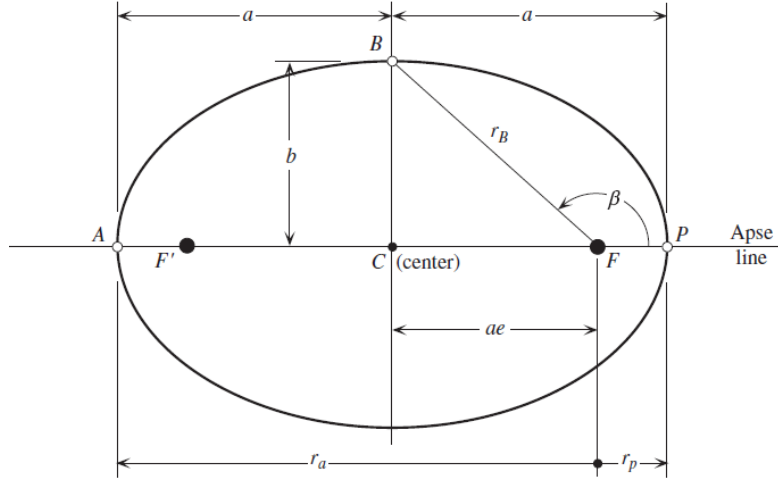


**Figure 2.7:  $m_I$  is at the focus  $F$ .  $F'$  is the unoccupied empty focus [32].**

As seen in Figure 2.7,  $2a$  is the distance measured along the apse line from periapsis  $P$  to apoapsis  $A$ . Thus,  $2a = r_p + r_a$ . Substituting Eqns (2.23) and (2.35) into this expression yields [32]

$$a = \frac{h^2}{\mu} \frac{1}{1 - e^2} \quad (2.36)$$

where  $a$  is the semimajor axis of the ellipse. An alternative form of the orbit equation is get by solving Eqn (2.36) for  $\frac{h^2}{\mu}$  and putting the result into Eqn (2.18) [32].

$$r = a \frac{1 - e^2}{1 + e \cos \theta} \quad (2.37)$$

As illustrated in Figure 2.7,  $F$  is denoting the location of the body  $m_I$  is the origin of the  $r, \theta$  polar coordinate system. The point lying midway between the apoapsis and the periapsis is the center  $C$  of the ellipse. The distance  $CF$  from the center  $C$  to the focus  $F$  is  $CF = a - FP = a - r_p$ . However, evaluated at  $\theta = 0$  from Eqn (2.37) [32]

$$r_p = a(1 - e) \quad (2.38)$$

Thus, as seen in Figure 2.7,  $CF = ae$ .  $B$  is the point on the perpendicular bisector of the major axis  $AP$  and the distance  $b$  from  $C$  to  $B$  is the semiminor axis. On the condition that the true anomaly of point  $B$  is  $\beta$ , the radial coordinate of  $B$  according to Eqn (2.37) is [32]



$$r_B = a \frac{1 - e^2}{1 + e \cos \beta} \quad (2.39)$$

The projection of  $r_B$  onto the apse line  $ae$  is  $ae = r_B \cos(180 - \beta) = -r_B \cos \beta = -\left(a \frac{1 - e^2}{1 + e \cos \beta}\right) \cos \beta$ . Solve this expression for  $e$  gives [32]

$$e = -\cos \beta \quad (2.40)$$

Substituting this result into Eqn (2.39) shows that  $r_B = a$ . According to the Pythagorean theorem,  $b^2 = r_B^2 - (ae)^2 = a^2 - a^2 e^2$ . Thus, the semiminor axis is found in terms of the semimajor axis and the eccentricity of the ellipse as [32]

$$b = a \sqrt{1 - e^2} \quad (2.41)$$

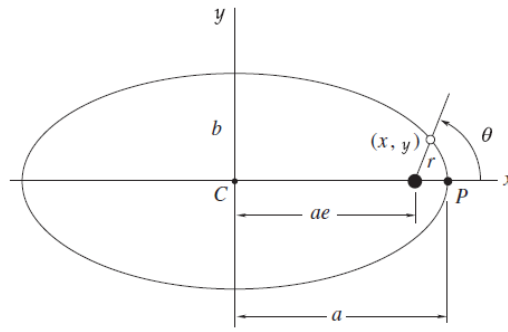


**Figure 2.8: Cartesian coordinate description of the orbit [32].**

$xy$  Cartesian coordinate system be centered at  $C$  is shown in Figure 2.8. The  $x$  coordinate of a point on the orbit in terms of  $r$  and  $\theta$  is  $x = ae + r \cos \theta = ae + \left(a \frac{1 - e^2}{1 + e \cos \theta}\right) \cos \theta = a \frac{e + \cos \theta}{1 + e \cos \theta}$ . From this expression [32]

$$\frac{x}{a} = \frac{e + \cos \theta}{1 + e \cos \theta} \quad (2.42)$$

For the  $y$  coordinate, utilize Eqn (2.41) to obtain  $y = r \sin \theta = \left(a \frac{1 - e^2}{1 + e \cos \theta}\right) \sin \theta = b \frac{\sqrt{1 - e^2}}{1 + e \cos \theta} \sin \theta$ . Thus [32]

$$\frac{y}{b} = \frac{\sqrt{1 - e^2}}{1 + e \cos \theta} \sin \theta \quad (2.43)$$

Utilize Eqns (2.42) and (2.43) to find  $\frac{x^2}{a^2} + \frac{y^2}{b^2} = \frac{1}{(1+ecos\theta)^2} [(e + cos\theta)^2 + (1 - e^2)sin^2\theta] = \frac{1}{(1+ecos\theta)^2} [e^2 + 2ecos\theta + cos^2\theta + sin^2\theta - e^2sin^2\theta] = \frac{1}{(1+ecos\theta)^2} [e^2 + 2ecos\theta + 1 - e^2sin^2\theta] = \frac{1}{(1+ecos\theta)^2} [e^2(1 - sin^2\theta) + 2ecos\theta + 1] = \frac{1}{(1+ecos\theta)^2} [e^2cos^2\theta + 2ecos\theta + 1] = \frac{1}{(1+ecos\theta)^2} (1 + ecos\theta)^2$ . That is [32]

$$\frac{x^2}{a^2} + \frac{y^2}{b^2} = 1 \quad (2.44)$$

The common Cartesian coordinate formula for an ellipse centered at the origin with  $x$ -intercepts at  $\pm a$  and  $y$ -intercepts at  $\pm b$  is the Eqn (2.44). Eqn (2.44) describes a circle that is really an ellipse whose eccentricity is zero in condition that  $a = b$ . The specific energy of an elliptical orbit that is  $\varepsilon = -\frac{1}{2} \frac{\mu^2}{h^2} (1 - e^2)$ . According to Eqn (2.36) [32]

$$\varepsilon = -\frac{\mu}{2a} \quad (2.45)$$

Therefore, the specific energy is independent of the eccentricity and depends only on the semimajor axis of the ellipse. From a different viewpoint, the conservation of energy for an elliptical orbit is [32]

$$\frac{v^2}{2} - \frac{\mu}{r} = -\frac{\mu}{2a} \quad (2.46)$$

The area of an ellipse is found using semimajor and semiminor axes,  $A = \pi ab$  (the area of a circle is  $A = \pi a^2 = \pi b^2$ ). The period of  $T$  of the elliptical orbit is found according to Kepler's second law,  $\frac{dA}{dt} = \frac{h}{2}$  to get  $\Delta A = \frac{h}{2} \Delta t$ . For one complete revolution,  $\Delta A = \pi ab$  and  $\Delta t = T$  so  $\pi ab = \frac{h}{2} T$  or  $T = \frac{2\pi ab}{h}$ . Substituting Eqns (2.36) and (2.41) yields  $T = \frac{2\pi}{h} a^2 \sqrt{1 - e^2} = \frac{2\pi}{h} \left( \frac{h^2}{\mu} \frac{1}{1 - e^2} \right)^2 \sqrt{1 - e^2}$ . Thus the period of an elliptical orbit in terms of the orbital parameters  $h$  and  $e$  turns into [32]

$$T = \frac{2\pi}{\mu^2} \left( \frac{h}{\sqrt{1 - e^2}} \right)^3 \quad (2.47)$$

Once again call Eqn (2.36) to substitute  $h = \sqrt{\mu a(1 - e^2)}$  into this equation in order to obtain an alternative expression for the period [32]

$$T = \frac{2\pi}{\sqrt{\mu}} a^{3/2} \quad (2.48)$$

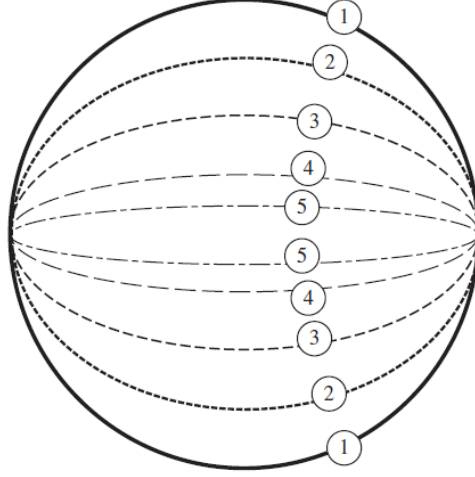


**Figure 2.9: Since same major axis, periods and energies are identical [32].**

As shown in Figure 2.9, like circular orbit, the energy and the period of an elliptical orbit is independent of the eccentricity. Eqn (2.48) represent Kepler's third law that the period of a planet is proportional to the three half power of its semimajor axis. In conclusion, dividing Eqn (2.23) by Eqn (2.35) gives  $\frac{r_p}{r_a} = \frac{1-e}{1+e}$ . Use this expression to calculate the eccentricity of an elliptical orbit [32]

$$e = \frac{r_a - r_p}{r_a + r_p} \quad (2.49)$$

$r_a - r_p = \overline{F'F}$  is the distance between the foci as seen in Figure 2.7. Eqn (2.49) has the geometrical interpretation because of  $r_a + r_p = 2a$ ,  $eccentricity = \frac{\text{distance between the foci}}{\text{length of the major axis}}$  [32].

A rectilinear ellipse is defined as having a zero angular momentum and eccentricity of 1 so the distance between the foci equals the finite length of the major axis along that the relative motion happens. Eqn (2.45) applies to rectilinear ellipses as well due to only the length of the semimajor axis determines the orbital specific energy [32].

Divide the range of the true anomaly ( $2\pi$ ) into  $n$  equal segments in order to find the average distance of  $m_2$  from  $m_1$  in the course of one complete orbit,  $n = \frac{2\pi}{\Delta\theta}$ . After that utilize  $r = \frac{h^2}{\mu} \frac{1}{1+e\cos\theta}$  to evaluate  $r(\theta)$  at the  $n$  equally spaced values of the true anomaly, starting at the periapsis:  $\theta_1 = 0, \theta_2 = \Delta\theta, \theta_3 = 2\Delta\theta, \dots, \theta_n = (n-1)\Delta\theta$ . The average of this set of  $n$  values of  $r$  is [32]

$$\bar{r}_\theta = \frac{1}{n} \sum_{i=1}^n r(\theta_i) = \frac{\Delta\theta}{2\pi} \sum_{i=1}^n r(\theta_i) = \frac{1}{2\pi} \sum_{i=1}^n r(\theta_i) \Delta\theta \quad (2.50)$$

Once  $n$  becomes very large,  $\Delta\theta$  becomes very small. Eqn (2.50) becomes in condition that  $n \rightarrow \infty$  [32]

$$\bar{r}_\theta = \frac{1}{2\pi} \int_0^{2\pi} r(\theta) d\theta \quad (2.51)$$

Substituting Eqn (2.37) into the integrand gives  $\bar{r}_\theta = \frac{1}{2\pi} a(1-e^2) \int_0^{2\pi} \frac{d\theta}{1+e\cos\theta}$ . The integral in this expression can be found using integral tables [32]

$$\bar{r}_\theta = \frac{1}{2\pi} a(1-e^2) \left( \frac{2\pi}{\sqrt{1-e^2}} \right) = a\sqrt{1-e^2} \quad (2.52)$$

When compare this result with Eqn (2.41), true anomaly averaged orbital radius equals the length of the semiminor axis  $b$  of the ellipse is seen. Therefore, the semimajor axis is not the mean distance. Eqn (2.52) also indicate that due to from Eqn (2.37),  $r_p = a(1-e)$  and  $r_a = a(1+e)$  [32]

$$\bar{r}_\theta = \sqrt{r_p r_a} \quad (2.53)$$

Consequently, the mean distance is the one-half power of the product of the maximum and minimum distances from the focus and not one-half of their sums [32].

## 2.5. Perifocal Frame

The perifocal frame that is the natural frame for an orbit is a Cartesian coordinate system fixed in space and centered at the focus of the orbit [32].

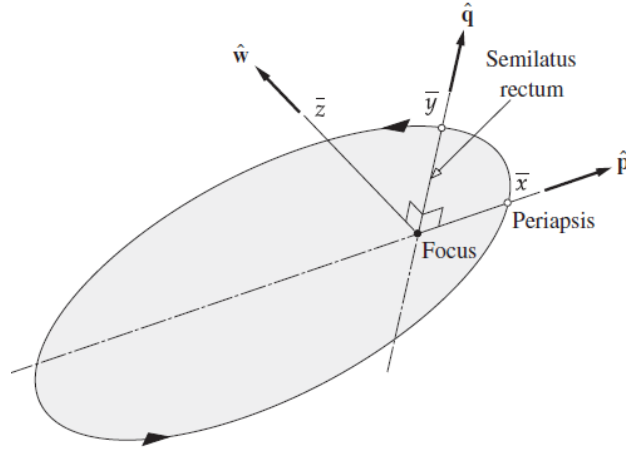


**Figure 2.10: Perifocal frame  $\hat{p}\hat{q}\hat{w}$  [32].**

As shown in Figure 2.10, the perifocal frame's  $\bar{x}\bar{y}$  plane is the plane of the orbit and its  $\bar{x}$  axis is centered from the focus through the periapsis. The unit vector along the  $\bar{x}$  axis (the apse line) is indicated  $\hat{p}$ , the  $\bar{y}$  axis with unit vector  $\hat{q}$  lies at  $90^\circ$  true anomaly to the  $\bar{x}$  axis and the  $\bar{z}$  axis is normal to the plane of the orbit in the direction of the angular momentum vector  $\mathbf{h}$ . The  $\bar{z}$  unit vector is  $\hat{w}$  [32],

$$\hat{w} = \frac{\mathbf{h}}{h} \quad (2.54)$$

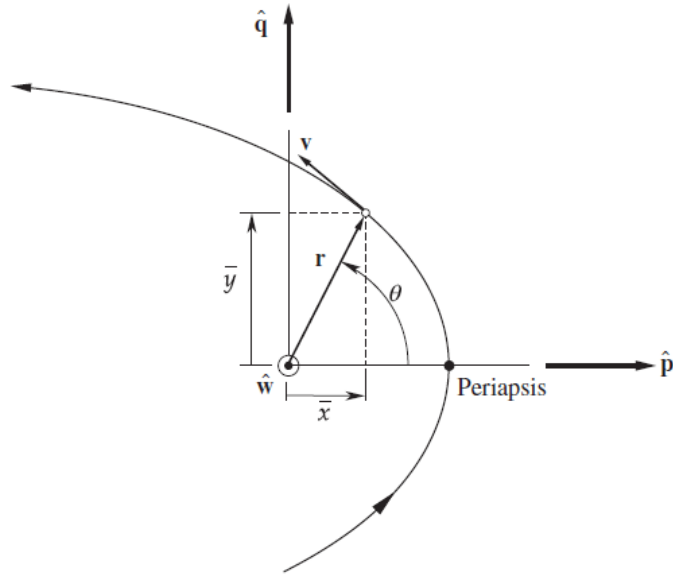


**Figure 2.11: Position and velocity relative to the perifocal frame [32].**

The position vector  $\mathbf{r}$  in the perifocal frame is shown in Figure 2.11 [32]

$$\mathbf{r} = \bar{x}\hat{p} + \bar{y}\hat{q} \quad (2.55)$$

where [32]

$$\bar{x} = r \cos \theta \quad \bar{y} = r \sin \theta \quad (2.56)$$

and the magnitude of  $\mathbf{r}$ ,  $r$  is  $r = \frac{h^2}{\mu} \frac{1}{1 + e \cos \theta}$ . So write Eqn (2.55) as [32]

$$\mathbf{r} = \frac{h^2}{\mu} \frac{1}{1 + e \cos \theta} (\cos \theta \hat{\mathbf{p}} + \sin \theta \hat{\mathbf{q}}) \quad (2.57)$$

Take the time derivative of  $\mathbf{r}$  to find the velocity [32]

$$\mathbf{v} = \dot{\mathbf{r}} = \dot{x} \hat{\mathbf{p}} + \dot{y} \hat{\mathbf{q}} \quad (2.58)$$

From Eqn (2.56) [32]

$$\dot{x} = \dot{r} \cos \theta - r \dot{\theta} \sin \theta \quad \dot{y} = \dot{r} \sin \theta + r \dot{\theta} \cos \theta \quad (2.59)$$

The radial component of velocity  $v_r$  is  $\dot{r}$ . Thus, according to Eqn (2.22) [32],

$$\dot{r} = \frac{\mu}{h} e \sin \theta \quad (2.60)$$

From Eqns (2.19) and (2.21) [32],

$$r \dot{\theta} = v_{\perp} = \frac{\mu}{h} (1 + e \cos \theta) \quad (2.61)$$

Substituting Eqns (2.60) and (2.61) into Eqn (2.58) and simplifying the results gives [32]

$$\dot{x} = -\frac{\mu}{h} \sin \theta \quad \dot{y} = \frac{\mu}{h} (e + \cos \theta) \quad (2.62)$$

Thus, Eqn (2.59) becomes [32]

$$\mathbf{v} = \frac{\mu}{h} [-\sin \theta \hat{\mathbf{p}} + (e + \cos \theta) \hat{\mathbf{q}}] \quad (2.63)$$

## 2.6. The Lagrange Coefficients

The position and velocity at any later time are found in terms of the initial values in condition that the position and velocity of an orbiting body are known at a given instant. Start with Eqns (2.56) and (2.59) [32],

$$\mathbf{r} = \bar{x}\hat{\mathbf{p}} + \bar{y}\hat{\mathbf{q}} \quad (2.64)$$

$$\mathbf{v} = \dot{\mathbf{r}} = \dot{\bar{x}}\hat{\mathbf{p}} + \dot{\bar{y}}\hat{\mathbf{q}} \quad (2.65)$$

A subscript zero to quantities evaluated at time  $t = t_0$  is attached and the expressions for  $\mathbf{r}$  and  $\mathbf{v}$  evaluated at  $t = t_0$  are [32]

$$\mathbf{r}_0 = \bar{x}_0\hat{\mathbf{p}} + \bar{y}_0\hat{\mathbf{q}} \quad (2.66)$$

$$\mathbf{v}_0 = \dot{\bar{x}}_0\hat{\mathbf{p}} + \dot{\bar{y}}_0\hat{\mathbf{q}} \quad (2.67)$$

Calculate the constant angular momentum  $\mathbf{h}$  utilizing the initial conditions. Substituting Eqns (2.66) and (2.67) into Eqn (2.1) gives [32]

$$\mathbf{h} = \mathbf{r}_0 \times \mathbf{v}_0 = \begin{vmatrix} \hat{\mathbf{p}} & \hat{\mathbf{q}} & \hat{\mathbf{w}} \\ \bar{x}_0 & \bar{y}_0 & 0 \\ \dot{\bar{x}}_0 & \dot{\bar{y}}_0 & 0 \end{vmatrix} = \hat{\mathbf{w}}(\bar{x}_0 \dot{\bar{y}}_0 - \bar{y}_0 \dot{\bar{x}}_0) \quad (2.68)$$

Thus, the coefficient of  $\hat{\mathbf{w}}$  on the right side of Eqn (2.68) must be magnitude of the angular momentum where  $\hat{\mathbf{w}}$  is the unit vector in the direction of  $\mathbf{h}$  [32].

$$h = \bar{x}_0 \dot{\bar{y}}_0 - \bar{y}_0 \dot{\bar{x}}_0 \quad (2.69)$$

Solve the two vector Eqns (2.66) and (2.67) for the unit vectors  $\hat{\mathbf{p}}$  and  $\hat{\mathbf{q}}$  in terms of  $\mathbf{r}_0$  and  $\mathbf{v}_0$ . From Eqn (2.66) [32]

$$\hat{\mathbf{q}} = \frac{1}{\bar{y}_0}\mathbf{r}_0 - \frac{\bar{x}_0}{\bar{y}_0}\hat{\mathbf{p}} \quad (2.70)$$

Substituting this into Eqn (2.67), combine terms and use Eqn (2.68) to obtain  $\mathbf{v}_0 = \dot{\bar{x}}_0\hat{\mathbf{p}} + \dot{\bar{y}}_0\left(\frac{1}{\bar{y}_0}\mathbf{r}_0 - \frac{\bar{x}_0}{\bar{y}_0}\hat{\mathbf{p}}\right) = \frac{\bar{y}_0\dot{\bar{x}}_0 - \bar{x}_0\dot{\bar{y}}_0}{\bar{y}_0}\hat{\mathbf{p}} + \frac{\dot{\bar{y}}_0}{\bar{y}_0}\mathbf{r}_0 = -\frac{h}{\bar{y}_0}\hat{\mathbf{p}} + \frac{\dot{\bar{y}}_0}{\bar{y}_0}\mathbf{r}_0$ . Solve this for  $\hat{\mathbf{p}}$  to acquire [32]

$$\hat{\mathbf{p}} = \frac{\dot{\bar{y}}_0}{h} \mathbf{r}_0 - \frac{\bar{y}_0}{h} \mathbf{v}_0 \quad (2.71)$$

Putting this result back into Eqn (2.70) yields  $\hat{\mathbf{q}} = \frac{1}{\bar{y}_0} \mathbf{r}_0 - \frac{\bar{x}_0}{\bar{y}_0} \left( \frac{\dot{\bar{y}}_0}{h} \mathbf{r}_0 - \frac{\bar{y}_0}{h} \mathbf{v}_0 \right) = \frac{h - \bar{x}_0 \dot{\bar{y}}_0}{\bar{y}_0} \mathbf{r}_0 + \frac{\bar{x}_0}{h} \mathbf{v}_0$ . Upon replacing h with the right side of Eqn (2.69) to get [32]

$$\hat{\mathbf{q}} = -\frac{\dot{\bar{x}}_0}{h} \mathbf{r}_0 + \frac{\bar{x}_0}{h} \mathbf{v}_0 \quad (2.72)$$

Eqns (2.71) and (2.72) yield  $\hat{\mathbf{p}}$  and  $\hat{\mathbf{q}}$  in reference to the initial position and velocity.

Substituting those expressions into Eqns (2.64) and (2.65) gives severally  $\mathbf{r} =$

$$\bar{x} \left( \frac{\dot{\bar{y}}_0}{h} \mathbf{r}_0 - \frac{\bar{y}_0}{h} \mathbf{v}_0 \right) + \bar{y} \left( -\frac{\dot{\bar{x}}_0}{h} \mathbf{r}_0 + \frac{\bar{x}_0}{h} \mathbf{v}_0 \right) = \frac{\bar{x} \dot{\bar{y}}_0 - \bar{y} \dot{\bar{x}}_0}{h} \mathbf{r}_0 + \frac{-\bar{x} \bar{y}_0 + \bar{y} \bar{x}_0}{h} \mathbf{v}_0$$

$$\mathbf{v} = \dot{\bar{x}} \left( \frac{\dot{\bar{y}}_0}{h} \mathbf{r}_0 - \frac{\bar{y}_0}{h} \mathbf{v}_0 \right) + \dot{\bar{y}} \left( -\frac{\dot{\bar{x}}_0}{h} \mathbf{r}_0 + \frac{\bar{x}_0}{h} \mathbf{v}_0 \right) = \frac{\dot{\bar{x}} \dot{\bar{y}}_0 - \dot{\bar{y}} \dot{\bar{x}}_0}{h} \mathbf{r}_0 + \frac{-\dot{\bar{x}} \bar{y}_0 + \dot{\bar{y}} \bar{x}_0}{h} \mathbf{v}_0 \quad \text{.Thus [32],}$$

$$\mathbf{r} = f \mathbf{r}_0 + g \mathbf{v}_0 \quad (2.73)$$

$$\mathbf{v} = \dot{f} \mathbf{r}_0 + \dot{g} \mathbf{v}_0 \quad (2.74)$$

where  $f$  and  $g$  are [32]

$$f = \frac{\bar{x} \dot{\bar{y}}_0 - \bar{y} \dot{\bar{x}}_0}{h} \quad (2.75a)$$

$$g = \frac{-\bar{x} \bar{y}_0 + \bar{y} \bar{x}_0}{h} \quad (2.75b)$$

And their time derivatives [32]

$$\dot{f} = \frac{\dot{\bar{x}} \dot{\bar{y}}_0 - \dot{\bar{y}} \dot{\bar{x}}_0}{h} \quad (2.76a)$$

$$\dot{g} = \frac{-\dot{\bar{x}} \bar{y}_0 + \dot{\bar{y}} \bar{x}_0}{h} \quad (2.76b)$$

The  $f$  and  $g$  functions are known as the Lagrange coefficients. As seen from Eqns (2.73) and (2.74), the position and velocity vectors  $\mathbf{r}$  and  $\mathbf{v}$  are indeed linear combinations of the initial position and velocity vectors while the Lagrange



coefficients and their time derivatives in these expressions are themselves functions of time and the initial conditions [32].

The conservation of angular momentum  $h$  forces upon a condition on  $f$ ,  $g$  and their time derivatives  $\dot{f}$  and  $\dot{g}$  is shown by calculating  $h$  using Eqns (2.73) and (2.74),  $\mathbf{h} = \mathbf{r} \times \mathbf{v} = (f\mathbf{r}_0 + g\mathbf{v}_0) \times (\dot{f}\mathbf{r}_0 + \dot{g}\mathbf{v}_0)$ . Expanding the right side gives  $\mathbf{h} = (f\mathbf{r}_0 \times \dot{f}\mathbf{r}_0) + (f\mathbf{r}_0 \times \dot{g}\mathbf{v}_0) + (g\mathbf{v}_0 \times \dot{f}\mathbf{r}_0) + (g\mathbf{v}_0 \times \dot{g}\mathbf{v}_0)$ . Factor out the scalars  $f$ ,  $g$ ,  $\dot{f}$  and  $\dot{g}$  to get  $\mathbf{h} = f\dot{f}(\mathbf{r}_0 \times \mathbf{r}_0) + f\dot{g}(\mathbf{r}_0 \times \mathbf{v}_0) + \dot{f}g(\mathbf{v}_0 \times \mathbf{r}_0) + g\dot{g}(\mathbf{v}_0 \times \mathbf{v}_0)$ . However,  $\mathbf{r}_0 \times \mathbf{r}_0 = \mathbf{v}_0 \times \mathbf{v}_0 = 0$ . Thus,  $\mathbf{h} = f\dot{g}(\mathbf{r}_0 \times \mathbf{v}_0) + \dot{f}g(\mathbf{v}_0 \times \mathbf{r}_0)$ . For the reason that  $\mathbf{v}_0 \times \mathbf{r}_0 = -(\mathbf{r}_0 \times \mathbf{v}_0)$ , this reduce to  $\mathbf{h} = (f\dot{g} - \dot{f}g)(\mathbf{r}_0 \times \mathbf{v}_0)$  or  $\mathbf{h} = (f\dot{g} - \dot{f}g)\mathbf{h}_0$  where  $\mathbf{h}_0 = \mathbf{r}_0 \times \mathbf{v}_0$  that is the angular momentum at  $t = t_0$ .  $\mathbf{h} = \mathbf{h}_0$  due to the angular momentum is constant, so  $\mathbf{h} = (f\dot{g} - \dot{f}g)\mathbf{h}$ . Seeing that  $\mathbf{h}$  cannot be zero (unless the body is traveling in a straight line toward the center of attraction), it gives [32]

$$f\dot{g} - \dot{f}g = 1 \quad (\text{Conservation of angular momentum}) \quad (2.77)$$

Utilize Eqns (2.75) and (2.76) to decide the Lagrange coefficients and their time derivative in terms of the true anomaly. Firstly, at time  $t = t_0$  [32]

$$\begin{aligned} \bar{x}_0 &= r_0 \cos \theta_0 \\ \bar{y}_0 &= r_0 \sin \theta_0 \end{aligned} \quad (2.78)$$

Moreover, get that from Eqn (2.62) [32]

$$\begin{aligned} \dot{\bar{x}}_0 &= -\frac{\mu}{h} \sin \theta_0 \\ \dot{\bar{y}}_0 &= \frac{\mu}{h} (e + \cos \theta_0) \end{aligned} \quad (2.79)$$

Substitute Eqns (2.57) and (2.79) into Eqn (2.75a) to evaluate the function  $f$  [32]

$$\begin{aligned} f &= \frac{\bar{x} \dot{\bar{y}}_0 - \bar{y} \dot{\bar{x}}_0}{h} = \frac{1}{h} \left\{ [r \cos \theta] \left[ \frac{\mu}{h} (e + \cos \theta_0) \right] - [r \sin \theta] \left[ -\frac{\mu}{h} \sin \theta_0 \right] \right\} \\ &= \frac{\mu r}{h^2} [e \cos \theta + (\cos \theta \cos \theta_0 + \sin \theta \sin \theta_0)] \end{aligned} \quad (2.80)$$

If call upon the trig identity to get [32]

$$\cos(\theta - \theta_0) = \cos\theta\cos\theta_0 + \sin\theta\sin\theta_0 \quad (2.81)$$

$\Delta\theta$  signifies the difference between the current and initial true anomalies [32]

$$\Delta\theta = \theta - \theta_0 \quad (2.82)$$

So Eqn (2.80) becomes [32]

$$f = \frac{\mu r}{h^2} (e\cos\theta + \cos\Delta\theta) \quad (2.83)$$

Consequently, get that from Eqn (2.18) [32]

$$e\cos\theta = \frac{h^2}{\mu r} - 1 \quad (2.84)$$

Substituting this into Eqn (2.83) yields [32]

$$f = 1 - \frac{\mu r}{h^2} (1 - \cos\Delta\theta) \quad (2.85)$$

Indicate the orbit equation in terms of the difference in true anomalies [32]

$$r = \frac{h^2}{\mu} \frac{1}{1 + e\cos(\theta_0 + \Delta\theta)} \quad (2.86)$$

Eqn (2.86) becomes that by replacing  $\theta_0$  with  $-\Delta\theta$  in Eqn (2.81) [32]

$$r = \frac{h^2}{\mu} \frac{1}{1 + e\cos\theta_0\cos\Delta\theta - e\sin\theta_0\sin\Delta\theta} \quad (2.87)$$

Imply Eqn (2.84) at  $t = t_0$  to remove  $\theta_0$  from this expression [32]

$$e\cos\theta_0 = \frac{h^2}{\mu r_0} - 1 \quad (2.88)$$

Moreover, obtain that from Eqn (2.22) for the radial velocity [32]

$$e\sin\theta_0 = \frac{h v_{r0}}{\mu} \quad (2.89)$$

Substituting Eqns (2.88) and (2.89) into Eqn (2.87) gives [32]

$$r = \frac{h^2}{\mu} \frac{1}{1 + \left(\frac{h^2}{\mu r_0} - 1\right) \cos \Delta\theta - \frac{h v_{r_0}}{\mu} \sin \Delta\theta} \quad (2.90)$$

$r$  in terms of the initial conditions and the change in the true anomaly can be found by using this form of the orbit equation. Therefore,  $f$  in Eqn (2.85) is undecided without  $\Delta\theta$  [32].

Substitute Eqns (2.83) and (2.78) into Eqn (2.75b) to find the Lagrange coefficient  $g$  [32]

$$\begin{aligned} \dot{g} &= \frac{-\bar{x} \bar{y}_0 + \bar{y} \bar{x}_0}{h} = \frac{1}{h} [(-r \cos \theta)(r_0 \sin \theta_0) + (r \sin \theta)(r \cos \theta_0)] \\ &= \frac{r r_0}{h} (\sin \theta \cos \theta_0 - \cos \theta \sin \theta_0) \end{aligned} \quad (2.91)$$

Use the trig identity,  $\sin(\theta - \theta_0) = \sin \theta \cos \theta_0 - \cos \theta \sin \theta_0$ . Find that with Eqn (2.82) [32]

$$g = \frac{r r_0}{h} \sin(\Delta\theta) \quad (2.92)$$

Substitute Eqns (2.89) and (2.78) into Eqn (2.138b) to obtain  $\dot{g}$ ,  $\dot{g} = \frac{-\dot{\bar{x}} \bar{y}_0 + \dot{\bar{y}} \bar{x}_0}{h} = \frac{1}{h} \left\{ -\left[ -\frac{\mu}{h} \sin \theta \right] (r_0 \sin \theta_0) + \left[ \frac{\mu}{h} (e + \cos \theta) \right] (r_0 \cos \theta_0) \right\} = \frac{\mu r_0}{h^2} [e \cos \theta_0 + (\cos \theta \cos \theta_0 + \sin \theta \sin \theta_0)]$ . Reduce it using Eqns (2.81) and (2.88) [32]

$$\dot{g} = 1 - \frac{\mu r_0}{h^2} (1 - \cos \Delta\theta) \quad (2.93)$$

Also find  $\dot{f}$  with Eqn (2.77) [32]

$$\dot{f} = \frac{1}{g} (f \dot{g} - 1) \quad (2.94)$$

Substitute Eqns (2.85), (2.91) and (2.93) yields  $\dot{f} = \frac{1}{\frac{r r_0}{h} \sin \Delta\theta} \left\{ \left[ 1 - \frac{\mu r}{h^2} (1 - \cos \Delta\theta) \right] \left[ 1 - \frac{\mu r_0}{h^2} (1 - \cos \Delta\theta) \right] - 1 \right\} = \frac{1}{\frac{r r_0}{h} \sin \Delta\theta} \frac{h^2 \mu r r_0}{h^4} \left[ (1 - \cos \Delta\theta)^2 \frac{\mu}{h^2} - (1 - \cos \Delta\theta) \left( \frac{1}{r_0} + \frac{1}{r} \right) \right]$  or [32]

$$\dot{f} = \frac{\mu}{h} \frac{1 - \cos \Delta \theta}{\sin \Delta \theta} \left[ \frac{\mu}{h^2} (1 - \cos \Delta \theta) - \frac{1}{r_0} - \frac{1}{r} \right] \quad (2.95)$$

Briefly, the Lagrange coefficients in terms of the change in true anomaly where Eqn (2.90) gives  $r$  [32]

$$f = 1 - \frac{\mu r}{h^2} (1 - \cos \Delta \theta) \quad (2.96a)$$

$$g = \frac{r r_0}{h} \sin(\Delta \theta) \quad (2.96b)$$

$$\dot{f} = \frac{\mu}{h} \frac{1 - \cos \Delta \theta}{\sin \Delta \theta} \left[ \frac{\mu}{h^2} (1 - \cos \Delta \theta) - \frac{1}{r_0} - \frac{1}{r} \right] \quad (2.96c)$$

$$\dot{g} = 1 - \frac{\mu r_0}{h^2} (1 - \cos \Delta \theta) \quad (2.96d)$$

There is no need knowing the type of orbit (ellipse, parabola and hyperbola) to determine the position and velocity from the initial conditions using the Lagrange coefficients. Thus, eccentricity is not in Eqns (2.90) and (2.96). Nevertheless, the angular momentum  $h = \|\mathbf{r}_0 \times \mathbf{v}_0\|$  gives that information. The initial radial velocity  $v_{r0}$  is the projection of  $\mathbf{v}_0$  onto the direction of  $\mathbf{r}_0$ ,  $v_{r0} = \mathbf{v}_0 \cdot \frac{\mathbf{r}_0}{r_0}$  and from Eqns (2.18) and (2.22)  $r_0 = \frac{h^2}{\mu} \frac{1}{1 + e \cos \theta_0}$  and  $v_{r0} = \frac{\mu}{h} e \sin \theta_0$ . Thus, eccentricity  $e$  and true anomaly of the initial point  $\theta_0$  can solve with these two equations [32].

Utilizing a relation between  $\Delta \theta$  and time to use the Lagrange coefficients to find the position and velocity as a function of time instead of true anomaly is needed. Obtain polynomial expressions for  $f$  and  $g$  in which the variable  $\Delta \theta$  is recovered by the time interval  $\Delta t = t - t_0$  for times  $t$  that are close to the initial time  $t_0$ . Expand the position vector  $\mathbf{r}(t)$  as a function of time in a Taylor series about  $t - t_0$  [32]

$$\mathbf{r}(t) = \sum_{n=0}^{\infty} \frac{1}{n!} \mathbf{r}^{(n)}(t_0) (t - t_0)^n \quad (2.97)$$

where  $\mathbf{r}^{(n)}(t_0)$  is the  $n$ th time derivative of  $\mathbf{r}(t)$  evaluated at  $t_0$  [32]

$$\mathbf{r}^{(n)}(t_0) = \left( \frac{d^n \mathbf{r}}{dt^n} \right)_{t=t_0} \quad (2.98)$$

Trim this infinite series at four terms [32]

$$\begin{aligned} \mathbf{r}(t) = \mathbf{r}(t_0) + \left(\frac{d\mathbf{r}}{dt}\right)_{t=t_0} \Delta t + \frac{1}{2} \left(\frac{d^2\mathbf{r}}{dt^2}\right)_{t=t_0} \Delta t^2 + \frac{1}{6} \left(\frac{d^3\mathbf{r}}{dt^3}\right)_{t=t_0} \Delta t^3 \\ + \frac{1}{24} \left(\frac{d^4\mathbf{r}}{dt^4}\right)_{t=t_0} \Delta t^4 \end{aligned} \quad (2.99)$$

where  $\Delta t = t - t_0$ . Firstly, evaluate the four derivatives [32]

$$\left(\frac{d\mathbf{r}}{dt}\right)_{t=t_0} = \mathbf{v}_0 \quad (2.100)$$

Then evaluate  $\left(\frac{d^2\mathbf{r}}{dt^2}\right)_{t=t_0}$  [32]

$$\ddot{\mathbf{r}} = -\frac{\mu}{r^3} \mathbf{r} \quad (2.101)$$

Therefore [32],

$$\left(\frac{d^2\mathbf{r}}{dt^2}\right)_{t=t_0} = -\frac{\mu}{r_0^3} \mathbf{r}_0 \quad (2.102)$$

Evaluate  $\left(\frac{d^3\mathbf{r}}{dt^3}\right)_{t=t_0}$  by differentiating Eqn (2.101) [32]

$$\left(\frac{d^3\mathbf{r}}{dt^3}\right)_{t=t_0} = -\mu \frac{d}{dt} \left(\frac{\mathbf{r}}{r^3}\right) = -\mu \left(\frac{r^3 \mathbf{v} - 3\mathbf{r}r^2 \dot{r}}{r^6}\right) = -\mu \frac{\mathbf{v}}{r^3} + 3\mu \frac{\dot{r}\mathbf{r}}{r^4} \quad (2.103)$$

From Eqn (2.8a) [32]

$$\dot{r} = \frac{\mathbf{r} \cdot \mathbf{v}}{r} \quad (2.104)$$

Thus, Eqn (2.103) is evaluated at  $t = t_0$  [32]

$$\left(\frac{d^3\mathbf{r}}{dt^3}\right)_{t=t_0} = -\mu \frac{\mathbf{v}_0}{r_0^3} + 3\mu \frac{\mathbf{r}_0 \cdot \mathbf{v}_0}{r_0^5} \mathbf{r}_0 \quad (2.105)$$

Conclusively  $\left(\frac{d^4\mathbf{r}}{dt^4}\right)_{t=t_0}$  is detected by first differentiating Eqn (2.103) [32],

$$\begin{aligned}
\left(\frac{d^4 \mathbf{r}}{dt^4}\right)_{t=t_0} &= \frac{d}{dt} \left( -\mu \frac{\dot{\mathbf{r}}}{r^3} + 3\mu \frac{\dot{\mathbf{r}} \mathbf{r}}{r^4} \right) \\
&= -\mu \left( \frac{r^3 \ddot{\mathbf{r}} - 3r^2 \dot{\mathbf{r}} \dot{\mathbf{r}}}{r^6} \right) + 3\mu \left( \frac{r^4 (\ddot{\mathbf{r}} \mathbf{r} + \dot{\mathbf{r}} \dot{\mathbf{r}}) - 4r^3 r^2 \dot{\mathbf{r}}}{r^8} \right)
\end{aligned} \tag{2.106}$$

Find  $\ddot{\mathbf{r}}$  in terms of  $r$  and  $v$  by differentiating Eqn (2.166) and making use of Eqn (2.101) [32]

$$\ddot{\mathbf{r}} = \frac{d}{dt} \left( \frac{\mathbf{r} \cdot \dot{\mathbf{r}}}{r} \right) = \frac{v^2}{r} - \frac{\mu}{r^2} - \frac{(\mathbf{r} \cdot \mathbf{v})^2}{r^3} \tag{2.107}$$

Substitute Eqns (2.1601), (2.104) and (2.107) into Eqn (2.106), combine terms and evaluate the result at  $t = t_0$  gives [32]

$$\left(\frac{d^4 \mathbf{r}}{dt^4}\right)_{t=t_0} = \left[ -2 \frac{\mu^2}{r_0^6} + 3\mu \frac{v_0^2}{r_0^5} - 15\mu \frac{(\mathbf{r}_0 \cdot \mathbf{v}_0)^2}{r_0^7} \right] \mathbf{r}_0 + 6\mu \frac{(\mathbf{r}_0 \cdot \mathbf{v}_0)}{r_0^5} \mathbf{v}_0 \tag{2.108}$$

Substitute Eqns (2.102), (2.102), (2.105) and (2.108) into Eqn (2.99) and rearrange and collect terms to obtain [32]

$$\begin{aligned}
\mathbf{r}(t) &= \left\{ 1 - \frac{\mu}{2r_0^3} \Delta t^2 + \frac{\mu \mathbf{r}_0 \cdot \mathbf{v}_0}{2 r_0^5} \Delta t^3 \right. \\
&\quad \left. + \frac{\mu}{24} \left[ -2 \frac{\mu}{r_0^6} + 3 \frac{v_0^2}{r_0^5} - 15 \frac{(\mathbf{r}_0 \cdot \mathbf{v}_0)^2}{r_0^7} \right] \Delta t^4 \right\} \mathbf{r}_0 \\
&\quad + \left[ \Delta t - \frac{1}{6} \frac{\mu}{r_0^3} \Delta t^3 + \frac{\mu (\mathbf{r}_0 \cdot \mathbf{v}_0)}{4 r_0^5} \Delta t^4 \right] \mathbf{v}_0
\end{aligned} \tag{2.109}$$

Compare this expression [32]

$$\begin{aligned}
f &= 1 - \frac{\mu}{2r_0^3} \Delta t^2 + \frac{\mu \mathbf{r}_0 \cdot \mathbf{v}_0}{2 r_0^5} \Delta t^3 \\
&\quad + \frac{\mu}{24} \left[ -2 \frac{\mu}{r_0^6} + 3 \frac{v_0^2}{r_0^5} - 15 \frac{(\mathbf{r}_0 \cdot \mathbf{v}_0)^2}{r_0^7} \right] \Delta t^4 \\
g &= \Delta t - \frac{1}{6} \frac{\mu}{r_0^3} \Delta t^3 + \frac{\mu (\mathbf{r}_0 \cdot \mathbf{v}_0)}{4 r_0^5} \Delta t^4
\end{aligned} \tag{2.172}$$

These  $f$  and  $g$  series shall be utilized for small values of elapsed time  $\Delta t$  in order to calculate the position of an orbiting body from the initial conditions [32].





### 3. ORBITS IN THREE DIMENSIONS

#### 3.1. Introduction

In this chapter, orbits in three-dimensional space that is for real missions and orbital maneuvers of earth satellites are described. Using of right ascension (RA) and declination (Dec) to explain the location of stars, planets and other celestial objects on the sphere, and inertial geocentric equatorial frame of reference and the concept of state vector are also defined. Moreover, the instantaneous position and velocity of an object relative to the inertial frame and the characteristics of the orbit are given by the six components of state vector are described. Transforming the state vector into orbital elements that uniquely explain the shape and orientation of an orbit and location of a body on it, and two of the major perturbations of earth orbits due to the earth's nonspherical shape are also defined [32].

#### 3.2. Geocentric Right Ascension Declination Frame

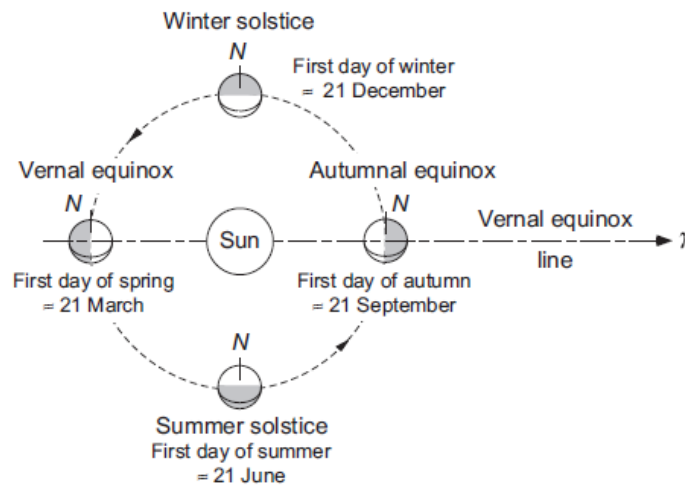


**Figure 3.1: The earth's orbit around the sun [32].**

Earth orbits in three dimensions is described in terms of earth's equatorial plane, the ecliptic plane and the earth's axis of rotation are defined by the coordinate system. Figure 3.1 shows the ecliptic that is the plane of the earth's orbit around the sun. The earth's axis of rotation that moving through the north and south poles is not perpendicular to the ecliptic and is tilted away by an angle called as the obliquity of the ecliptic,  $\varepsilon$  (approximately  $23.4^\circ$  for earth). Vernal equinox line is defined by  $\gamma$  is intersected the earth's equatorial plane and the ecliptic. Vernal equinox, that is the

day which number of hours of daylight and darkness are equal, is the first day of spring in the northern hemisphere on the calendar once the noontime sun crosses the equator from south to north. The autumnal equinox that happens precisely one half year later once the sun crosses back over the equator from north to south is the first day of autumn [32].

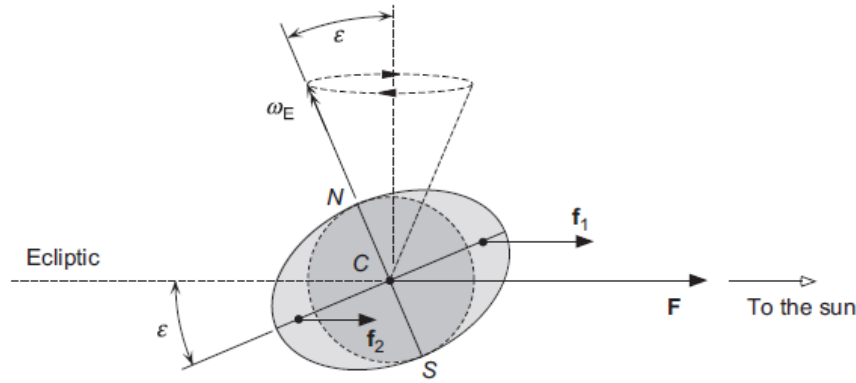


**Figure 3.2: Secondary (perturbing) gravitational forces on the earth [32].**

The vernal equinox line rotates bit by bit for the reason that the earth's tilted spin axis processes westward around the normal to the ecliptic at the rate of about  $1.4^\circ$  per century but assume that the it is fixed in the space for many practical purposes. Action of the sun and the moon on the nonspherical distribution of mass within the earth causes this slow precision and the centrifugal force of rotation about its own axis causes that he earth rounds out very slightly outward at its equator as shown in Figure 3.2. The force of the sun's gravity  $f_1$  on its mass is slightly larger than the force  $f_2$  on opposite side farthest from the sun due to one of the bulging sides is closer to the sun than the other. The forces  $f_1$ ,  $f_2$  and the dominant force  $F$  on the spherical mass contain the total force of the sun on the earth that is holding it in its solar orbit. A net clockwise moment (a vector into the page) that is produced by  $f_1$  and  $f_2$  about the center of the earth would rotate the earth's equator into alignment with the ecliptic because not the earth has an angular momentum directed along its south to north polar axis by reason of its spin around that axis at an angular velocity  $\omega_E$  of about  $360^\circ$  per day. The moment causes rotating the angular momentum vector in the direction of the moment (into the page). Thus, as shown in Figure 3.2 the spin axis is forced to precess in a counterclockwise direction around the normal to the ecliptic, sweeping out a cone. Samely, the moon also applies a torque on the earth. Combined effect of the sun and the moon causes a precession of the spin axis, so  $\gamma$

that has a period of 26000 years. Moreover, the moon's action superimposes a small nutation on the precession generates the obliquity  $\varepsilon$  differing with a maximum amplitude of  $0.0025^\circ$  over a period of 18.6 years [32].

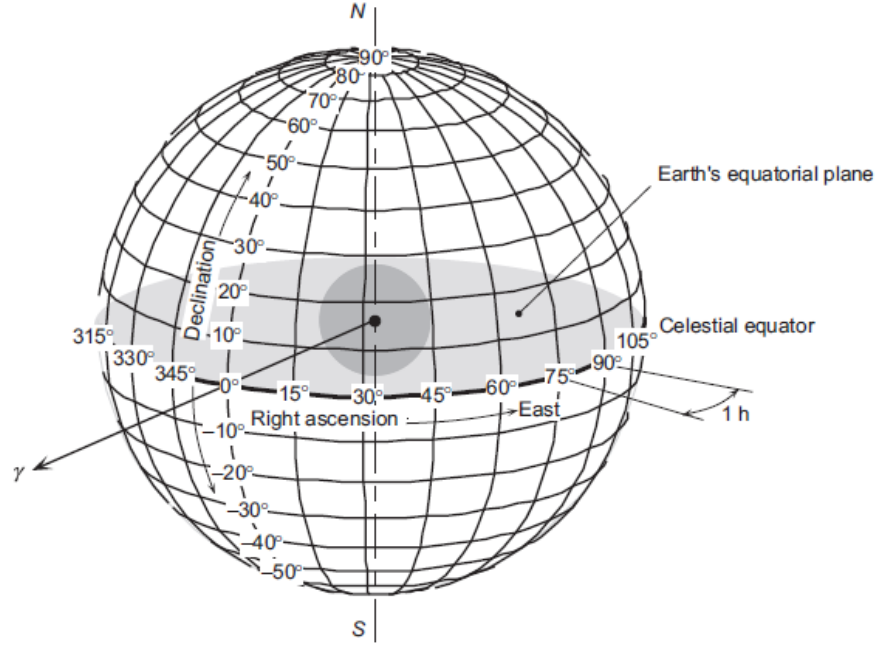


**Figure 3.3: Grid lines of right ascension and declination [32].**

Figure 3.3 shows objects in the night sky appear as points on a celestial sphere surrounding the earth. Those north and south poles of this fixed sphere correspond to those of the earth rotating within it while coordinates of latitude and longitude are utilized for locating points on the celestial sphere in much the same way as on the surface of the earth. The celestial equator is defined by the projection of the earth's equatorial plane outward onto the celestial sphere. The vernal equinox  $\gamma$  is located on the celestial equator is the origin for measurement of longitude that is known as right ascension while declination is known as latitude in astronomical parlance. Right ascension (RA or  $\alpha$ ) is estimated along the celestial equator in degrees east from the vernal equinox (astronomers estimate right ascension in hours instead of degrees where 24 hours equals  $360^\circ$ ) whilst declination (Dec or  $\delta$ ) is estimated along a meridian in degrees, positive to north of the equator and negative to the south [8].

Planets, comets, satellite, etc. pass on the fixed surface of the stars and stars are so far away from the earth whose positions relative to each other appear stationary on the celestial sphere. However, positions of stars relative to equinox vary bit by bit with time [32].

### 3.3. State Vector and the Geocentric Equatorial Frame

Velocity  $\mathbf{v}$  and orbital acceleration  $\mathbf{a}$  are comprised by state vector of a satellite at any given time. The equation governing the state vector of a satellite travelling around the earth for two body problem is [32]

$$\ddot{\mathbf{r}} = -\frac{\mu}{r^3}\mathbf{r} \quad (3.1)$$

where  $\mathbf{r}$  is the position vector of the satellite relative to the center of the earth. The components of  $\mathbf{r}$  and its time derivatives  $\dot{\mathbf{r}} = \mathbf{v}$  and  $\ddot{\mathbf{r}} = \mathbf{a}$  are be obliged to calculate in a nonrotating frame attached to the earth [32].

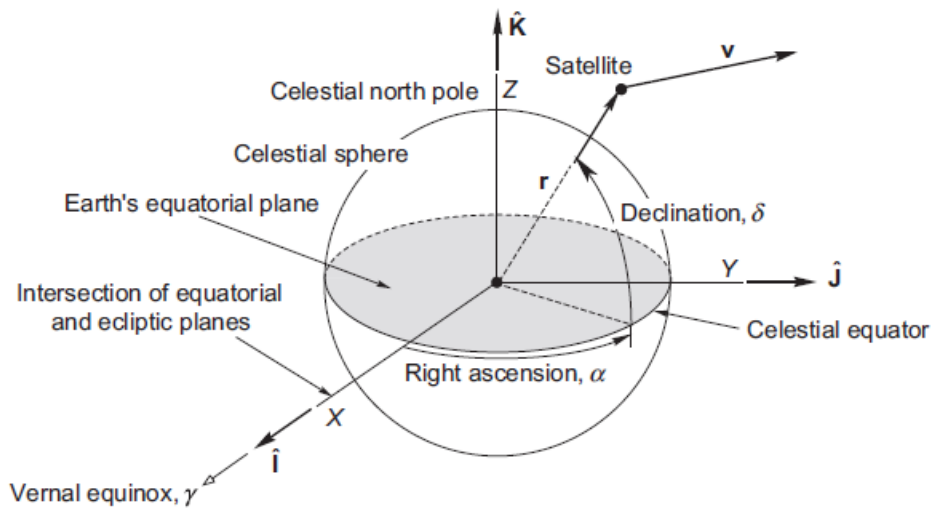


**Figure 3.4: The geocentric equatorial frame [32].**

Figure 3.4 shows the geocentric equatorial frame that is commonly used nonrotating right handed Cartesian coordinate system. The X-axis directs in the vernal equinox direction and XY plane is the earth's equatorial plane while Z-axis intersects with the earth's axis of rotation and directs northward. A right handed triad is formed by the unit vectors  $\hat{\mathbf{i}}, \hat{\mathbf{j}}$  and  $\hat{\mathbf{k}}$ . Eqn (4.1) is for the nonrotating geocentric equatorial frame performed as an inertial frame for the two body earth satellite problem. Ignore the two body problem because the center of the earth is always accelerating toward a third body, the sun (to say nothing of the moon) [32].

The state vector in the geocentric equatorial frame in component form is [32]

$$\mathbf{r} = X\hat{\mathbf{i}} + Y\hat{\mathbf{j}} + Z\hat{\mathbf{k}} \quad (3.2)$$

$$\mathbf{v} = v_x \hat{\mathbf{I}} + v_y \hat{\mathbf{J}} + v_z \hat{\mathbf{K}} \quad (3.3)$$

In condition that  $r$  is the magnitude of the position vector [32]

$$\mathbf{r} = r \hat{\mathbf{u}}_r \quad (3.4)$$

The components of  $\hat{\mathbf{u}}_r$  (the direction cosines  $l$ ,  $m$  and  $n$  of  $\hat{\mathbf{u}}_r$ ) are obtained in terms of the RA  $\alpha$  and Dec  $\delta$  as shown in Figure 3.4 [32]:

$$\hat{\mathbf{u}}_r = l \hat{\mathbf{I}} + m \hat{\mathbf{J}} + n \hat{\mathbf{K}} = \cos \delta \cos \alpha \hat{\mathbf{I}} + \cos \delta \sin \alpha \hat{\mathbf{J}} + \sin \delta \hat{\mathbf{K}} \quad (3.5)$$

As shown in Figure 3.4 and Eqn (3.5), magnitude of  $\mathbf{r}$  is  $r = \sqrt{X^2 + Y^2 + Z^2}$ , direction cosines of  $\mathbf{r}$  are  $l = \frac{X}{r}$ ,  $m = \frac{Y}{r}$  and  $n = \frac{Z}{r}$ . Dec is found as  $\delta = \sin^{-1} n$ , Dec lies between  $-90^\circ$  and  $+90^\circ$  so that means it is precisely the range of the principal values of the arcsine function due to no quadrant ambiguity, and  $\cos \delta$  cannot be negative. Moreover, RA is found as  $\alpha = \cos^{-1}(\frac{l}{\cos \delta})$  due to  $l = \cos \delta \cos \alpha$ , so two values of  $\alpha$  between  $0^\circ$  and  $360^\circ$ . Sign of the direction cosine  $m = \cos \delta \sin \alpha$ , is the same as the sign of  $\sin \alpha$  because  $\cos \delta$  cannot be negative, gives the correct quadrant for  $\alpha$ .  $\alpha$  lies in the range  $0^\circ - 180^\circ$  when  $\sin \alpha > 0$  whilst  $\alpha$  lies in the range  $180^\circ - 360^\circ$  when  $\sin \alpha < 0$ . RA and Dec can be found by using the position vector, but  $r$  cannot be found by using just RA and Dec. Thus, the distance  $r$  is essential to yield the position vector from Eqn (3.4) [32].

The state vector  $(\mathbf{r}_0, \mathbf{v}_0)$  at any other time in terms of the initial vector in terms of Lagrange coefficients can be determined in condition that state vector at a given instant is provided, so [32]

$$\begin{aligned} \mathbf{r} &= f \mathbf{r}_0 + g \mathbf{v}_0 \\ \mathbf{v} &= \dot{f} \mathbf{r}_0 + \dot{g} \mathbf{v}_0 \end{aligned} \quad (3.6)$$

Thus the size, shape and orientation of the orbit are completely determined by specifying the total of six components of  $\mathbf{r}_0$  and  $\mathbf{v}_0$  [32].

### 3.4. Orbital Elements and the State Vector

Eccentricity and angular momentum are required to define an orbit in the plane are used to obtain other parameters such as the semimajor axis, the specific energy and the period (for an ellipse). The third parameter, the true anomaly leads the time since perigee is required locates a point on the orbit [32].

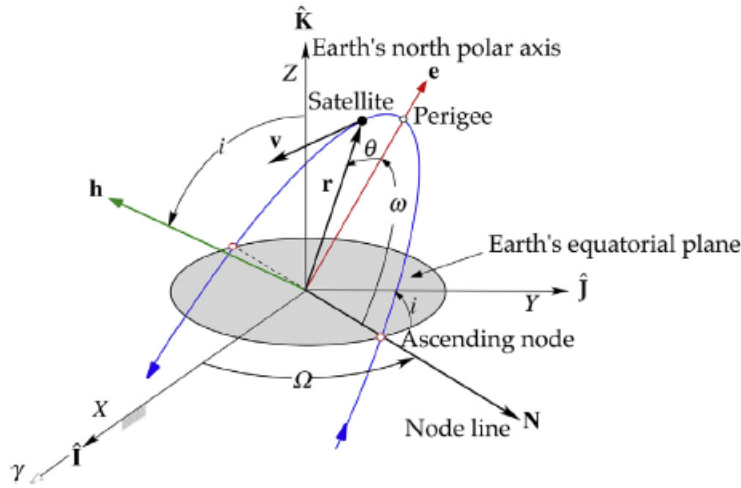


**Figure 3.5: Geocentric equatorial frame and the orbital elements [32].**

Figure 3.5 shows the Euler angles that are required three additional parameters to describe the orientation of an orbit in three dimensions. When locating the intersection of the orbital plane with the equatorial (XY) plane that is known as the node line, the point on the node line where the orbit passes above the equatorial plane from below is known as the ascending node. The node line vector  $\mathbf{N}$  draws out outward from the origin through the ascending node and descending node is pointed at the other end of the node line where the orbit dives below the equatorial plane. The first Euler angle  $\Omega$ , RA of the ascending node, is the angle between the positive X-axis and the node line where RA is a positive number lying  $0^\circ$  and  $360^\circ$ . The inclination  $i$  is the dihedral angle between the orbital plane and the equatorial plane is measured according to the right hand rule that is counterclockwise around the node line vector from the equator to the orbit and also is the angle between the positive Z-axis and the normal to the plane of the orbit. As mentioned before the angular momentum vector  $\mathbf{h}$  is normal to the plane of the orbit, so the inclination  $i$  is the angle between the positive Z-axis and  $\mathbf{h}$  is a positive number between  $0^\circ$  and  $180^\circ$ . The perigee of the orbit located at the intersection of the eccentricity vector  $\mathbf{e}$  with the orbital path whilst the third angle  $\omega$ , the argument of perigee that is the angle

between the node line vector  $\mathbf{N}$  and the eccentricity vector  $\mathbf{e}$  measured in the plane of the orbit is a positive number between  $0^\circ$  and  $360^\circ$  [32].

As briefly, the six orbital elements are [32]

- $h$ : Specific angular momentum
- $i$ : Inclination
- $\Omega$ : Right ascension of the ascending node
- $e$ : Eccentricity
- $\omega$ : Argument of perigee
- $\theta$ : True anomaly

The semimajor axis  $a$  and the mean anomaly  $M$  commonly replace with the angular momentum  $h$  and true anomaly  $\theta$  [32].

Obtaining the orbital elements for given the position  $\mathbf{r}$  and velocity  $\mathbf{v}$  of a spacecraft in the geocentric equatorial frame step by step is starting by calculating the distance

$r = \sqrt{\mathbf{r} \cdot \mathbf{r}} = \sqrt{X^2 + Y^2 + Z^2}$  and calculating the speed  $v = \sqrt{\mathbf{v} \cdot \mathbf{v}} = \sqrt{v_X^2 + v_Y^2 + v_Z^2}$ . Then calculate the radial velocity  $v_r = \frac{\mathbf{r} \cdot \mathbf{v}}{r} = \frac{Xv_X + Yv_Y + Zv_Z}{r}$  in

condition that when  $v_r > 0$ , the satellite is flying away from perigee and when  $v_r < 0$ , it is flying toward perigee. Calculate the specific angular momentum  $\mathbf{h} = \mathbf{r} \times \mathbf{v} =$

$\begin{vmatrix} \hat{\mathbf{i}} & \hat{\mathbf{j}} & \hat{\mathbf{k}} \\ X & Y & Z \\ v_X & v_Y & v_Z \end{vmatrix}$  and the magnitude of the specific angular momentum  $h = \sqrt{\mathbf{h} \cdot \mathbf{h}}$  that

is the first orbital element. After that, calculate the inclination [32]

$$i = \cos^{-1} \left( \frac{h_Z}{h} \right) \quad (3.7)$$

The inclination  $i$  which is the second orbital element must lie between  $0^\circ$  and  $180^\circ$  that is precisely the range (principle values) of the arccosine function, so there is not quadrant ambiguity to contend with here. On the other hand, in condition that  $90^\circ < i \leq 180^\circ$ , the angular momentum  $\mathbf{h}$  points in a southerly direction and it causes the orbit is retrograde that means the motion of the satellite around the earth is opposite to earth's rotation. The calculate the node line vector [32]

$$\mathbf{N} = \hat{\mathbf{K}} \times \mathbf{h} = \begin{vmatrix} \hat{\mathbf{I}} & \hat{\mathbf{J}} & \hat{\mathbf{K}} \\ 0 & 0 & 0 \\ h_x & h_y & h_z \end{vmatrix} \quad (3.8)$$

Thus, the magnitude of  $\mathbf{N}$  is  $N = \sqrt{\mathbf{N} \cdot \mathbf{N}}$ . Calculate the third orbital element, the right ascension of the ascending node  $\Omega = \cos^{-1}\left(\frac{N_x}{N}\right)$ .  $\Omega$  locates in either the first or fourth quadrant when  $\left(\frac{N_x}{N}\right) > 0$  while  $\Omega$  locates in either the second or third quadrant when  $\left(\frac{N_x}{N}\right) < 0$ . Moreover, the ascending node locates in the positive side of the vertical  $XZ$  plane ( $0 \leq \Omega < 180^\circ$ ) when  $N_y > 0$  whilst the ascending node locates in the negative side of the vertical  $XZ$  plane ( $180^\circ \leq \Omega < 360^\circ$ ) when  $N_y < 0$ . Thus,  $N_y > 0$  suggests that  $0 < \Omega < 180^\circ$ , on the other hand  $N_y < 0$  suggests that  $180^\circ < \Omega < 360^\circ$ . In briefly [32],

$$\Omega = \begin{cases} \cos^{-1}\left(\frac{N_x}{N}\right) & (N_y \geq 0) \\ 360^\circ - \cos^{-1}\left(\frac{N_x}{N}\right) & (N_y < 0) \end{cases} \quad (3.9)$$

Calculate the fourth orbital element, the eccentricity vector recalling Eqn (2.40) [32]:

$$\mathbf{e} = \frac{1}{\mu} \left[ \left( v^2 - \frac{\mu}{r} \right) \mathbf{r} - r v_r \mathbf{v} \right] \quad (3.10)$$

Thus, the magnitude of eccentricity is  $= \sqrt{\mathbf{e} \cdot \mathbf{e}}$ . Substitute Eqn (3.10) to lead for forming depending only on the scalars gained so far [32]:

$$e = \sqrt{1 + \frac{h^2}{\mu^2} \left( v^2 - \frac{2\mu}{r} \right)} \quad (3.11)$$

Then calculate the fifth orbital element, the argument of perigee  $\omega = \cos^{-1}\left(\frac{\mathbf{N} \cdot \mathbf{e}}{N e}\right)$ .  $\omega$  locates in either first or fourth quadrant when  $\mathbf{N} \cdot \mathbf{e} > 0$  whilst  $\omega$  locates in either second or third quadrant when  $\mathbf{N} \cdot \mathbf{e} < 0$ . The perigee locates above the equatorial plane ( $0 \leq \omega < 180^\circ$ ) when  $\mathbf{e}$  points up (in the positive  $Z$  direction) while the perigee locates below the plane ( $180^\circ \leq \omega < 360^\circ$ ) when  $\mathbf{e}$  points down. Thus,  $e_z \geq 0$  suggests that  $0 < \omega < 180^\circ$ , on the other hand  $e_z < 0$  suggests that  $180^\circ < \omega < 360^\circ$ . In briefly [32],



$$\omega = \begin{cases} \cos^{-1}\left(\frac{\mathbf{N} \cdot \mathbf{e}}{N} \cdot \frac{\mathbf{e}}{e}\right) & (e_z \geq 0) \\ 360^\circ - \cos^{-1}\left(\frac{\mathbf{N} \cdot \mathbf{e}}{N} \cdot \frac{\mathbf{e}}{e}\right) & (e_z < 0) \end{cases} \quad (3.12)$$

After that, calculate the sixth and final orbital element, the true anomaly  $\theta = \cos^{-1}\left(\frac{\mathbf{e} \cdot \mathbf{r}}{e} \cdot \frac{\mathbf{r}}{r}\right)$ .  $\theta$  locates in either first or fourth quadrant when  $\mathbf{e} \cdot \mathbf{r} > 0$  whilst  $\theta$  locates in either second or third quadrant when  $\mathbf{e} \cdot \mathbf{r} < 0$ . The satellite is flying away from perigee ( $\mathbf{r} \cdot \mathbf{v} \geq 0$ ) when ( $0 \leq \omega < 180^\circ$ ) while the satellite is flying toward perigee ( $\mathbf{r} \cdot \mathbf{v} < 0$ ) when ( $180^\circ \leq \omega < 360^\circ$ ). In briefly [32],

$$\theta = \begin{cases} \cos^{-1}\left(\frac{\mathbf{e}}{e} \cdot \frac{\mathbf{r}}{r}\right) & (v_r \geq 0) \\ 360^\circ - \cos^{-1}\left(\frac{\mathbf{e}}{e} \cdot \frac{\mathbf{r}}{r}\right) & (v_r < 0) \end{cases} \quad (3.13a)$$

For an alternative form, substitute Eqn (3.10) [32]

$$\theta = \begin{cases} \cos^{-1}\left[\frac{1}{e}\left(\frac{h^2}{\mu r} - 1\right)\right] & (v_r \geq 0) \\ 360^\circ - \cos^{-1}\left[\frac{1}{e}\left(\frac{h^2}{\mu r} - 1\right)\right] & (v_r < 0) \end{cases} \quad (3.13b)$$

### 3.5. Effects of The Earth's Oblateness

Centrifugal force causes to distend at the equator for the earth like all planets with comparable or higher rotational rates. The earth's equatorial radius is 21 km larger than the polar radius and this flattening at the poles are known as oblateness,  $Oblateness = \frac{Equatorial\ radius - Polar\ radius}{Equatorial\ radius}$ . The earth is an oblate spheroid and the force of gravity on an orbiting body is not directed toward the center of the earth due to lack of symmetry. The gravitational field of a perfectly spherical planet depends only on the distance from its distance, on the other hand oblateness creates a variation also with latitude that is known as a zonal variation [32].

**Table 3.1: Oblateness and second zonal harmonics [32].**

Planet	Oblateness	$J_2$
Mercury	0.000	$60 \times 10^{-6}$
Venus	0.000	$4.458 \times 10^{-6}$

Earth	0.003353	$1.08263 \times 10^{-3}$
Mars	0.00648	$1.96045 \times 10^{-3}$
Jupiter	0.06487	$14.736 \times 10^{-3}$
Saturn	0.09796	$16.298 \times 10^{-3}$
Uranus	0.02293	$3.34343 \times 10^{-3}$
Neptune	0.01708	$3.411 \times 10^{-3}$
(Moon)	0.0012	$202.7 \times 10^{-3}$

The second zonal harmonic  $J_2$  is dimensionless parameter quantifies the major effects of oblateness on orbits. Table 3.1 shows  $J_2$  and oblateness values of each planet [32].

The right ascension  $\Omega$  and the argument of periapsis  $\omega$  vary significantly with time due to oblateness. The average rates of change of these two angles are [32]

$$\dot{\Omega} = - \left[ \frac{3}{2} \frac{\sqrt{\mu} J_2 R^2}{(1 - e^2)^2 a^{7/2}} \right] \cos i \quad (3.14)$$

$$\dot{\omega} = - \left[ \frac{3}{2} \frac{\sqrt{\mu} J_2 R^2}{(1 - e^2)^2 a^{7/2}} \right] \left( \frac{5}{2} \sin^2 i - 2 \right) \quad (3.15)$$

where  $R$  is the radius of the planet [32].

In the condition that  $0 \leq i < 90^\circ$ , so  $\dot{\Omega} < 0$  and the node line drifts westward for prograde orbits. This event is known as regression of the nodes because the RA of the node continuously decreases. On the other hand, in the condition that  $90^\circ < i \leq 180^\circ$ , so  $\dot{\Omega} > 0$  and the node line of retrograde orbits moves eastward. Moreover, the node line is stationary for polar orbits ( $i = 90^\circ$ ) [32].

Likewise, in the condition that  $0 \leq i < 63.4^\circ$  or  $116.6^\circ < i \leq 180^\circ$ ,  $\dot{\omega}$  is positive so the perigee moves in the direction of the motion of the satellite (“advance of perigee” event). On the other hand, in the condition that  $63.4^\circ < i \leq 116.6^\circ$ , the perigee regresses so perigee moves opposite to the direction of motion. Furthermore,  $i = 63.4^\circ$  and  $i = 116.6^\circ$  are the critical inclinations at that the apse line does not move [32].

The coefficient of the trigonometric terms in Eqns (3.14) and (3.15) are identical, thus [32]

$$\dot{\omega} = \dot{\Omega} \frac{\left(\frac{5}{2}\right) \sin^2 i - 2}{\cos i} \quad (3.16)$$

Additionally, zero time-averaged variations of the inclination, eccentricity, angular momentum and semimajor axis are produced by  $J_2$  effect. Sun-synchronous and Molniya orbits take advantage the effect of orbit inclination on node regression and advance of perigee [32].



## 4. PRELIMINARY ORBIT DETERMINATION

### 4.1. Introduction

Some of the classical methods to determine the satellite orbit from earth-bound observations are described in this chapter based on the two-body equations of motion. These methods are used for preliminary orbit determination that does not include perturbations [32].

Firstly the details of Gibbs method using three position vectors and time are given. Then, Lambert's problem using two position vectors and time is explained. Two-body orbits lie in a plane based on the Gibbs and Lambert procedure while Lambert problem is more complex and requires utilizing the Lagrange  $f$  and  $g$  functions and the universal variable formulation [32].

After that, sidereal time, JD, topocentric coordinate systems and the relationships between topocentric right ascension/ declination angles and azimuth/ elevation angles, how orbits are estimated from measuring the range and angular orientation of the line of sight together with their rates are described. Finally, angles-only orbit determination methods are explained [32].

### 4.2. Three Position Vectors and Time - Gibbs Method

J.W.Gibbs (1839-1903) find a solution for the observations of a space object obtained the geocentric position vectors  $\mathbf{r}_1$ ,  $\mathbf{r}_2$  and  $\mathbf{r}_3$  at the three successive times  $t_1$ ,  $t_2$  and  $t_3$  ( $t_1 < t_2 < t_3$ ) to determine the velocities  $\mathbf{v}_1$ ,  $\mathbf{v}_2$  and  $\mathbf{v}_3$  at  $t_1$ ,  $t_2$  and  $t_3$  assuming that the object is in a two-body orbit [32].

The position vectors of an orbiting body must lie in the same plane based on the conservation of angular momentum, so the unit vector normal to the plane of  $\mathbf{r}_2$  and  $\mathbf{r}_3$  must be perpendicular to the unit vector in the direction of  $\mathbf{r}_1$ . Therefore, when  $\widehat{\mathbf{u}}_{r_1} = \mathbf{r}_1/r_1$  and  $\widehat{\mathbf{C}}_{23} = (\mathbf{r}_2 \times \mathbf{r}_3)/\|\mathbf{r}_2 \times \mathbf{r}_3\|$ ,  $\widehat{\mathbf{u}}_{r_1} \cdot \widehat{\mathbf{C}}_{23} = 0$  [32].

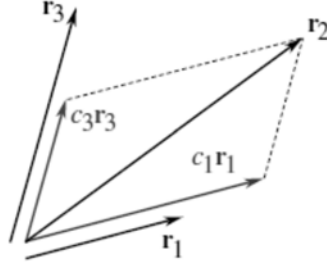


**Figure 4.1: Any one of a set of three coplanar vectors ( $r_1, r_2, r_3$ ) [32].**

Scalar factors  $c_1$  and  $c_3$  can be applied to  $r_2$  and  $r_3$ , because  $r_1, r_2$  and  $r_3$  lie in the same plane, so [32]

$$r_2 = c_1 r_1 + c_3 r_3 \quad (4.1)$$

Recall Eqn (2.40) in order to find the velocity  $\mathbf{v}$  corresponding to any of the three given position vector  $\mathbf{r}$ ,  $\mathbf{v} \times \mathbf{h} = \mu \left( \frac{\mathbf{r}}{r} + \mathbf{e} \right)$  where  $\mathbf{h}$  is the angular momentum and  $\mathbf{e}$  is the eccentricity vector. Taking the crossproduct of this equation with the angular momentum yields isolating the velocity [32],

$$\mathbf{h} \times (\mathbf{v} \times \mathbf{h}) = \mu \left( \frac{\mathbf{h} \times \mathbf{r}}{r} + \mathbf{h} \times \mathbf{e} \right) \quad (4.2)$$

The left side changes into based on bac-cab rule,  $\mathbf{h} \times (\mathbf{v} \times \mathbf{h}) = \mathbf{v}(\mathbf{h}\mathbf{h}) - \mathbf{h}(\mathbf{h}\mathbf{v})$ .  $\mathbf{h}\mathbf{h} = h^2$  and  $\mathbf{h}\mathbf{v} = 0$  because  $\mathbf{v}$  is perpendicular to  $\mathbf{h}$ . Thus,  $\mathbf{h} \times (\mathbf{v} \times \mathbf{h}) = h^2 \mathbf{v}$ , so [32]

$$\mathbf{v} = \frac{\mu}{h^2} \left( \frac{\mathbf{h} \times \mathbf{r}}{r} + \mathbf{h} \times \mathbf{e} \right) \quad (4.3)$$

The unit vector  $\hat{\mathbf{p}}$  lies in the direction of the eccentricity vector  $\mathbf{e}$  and  $\hat{\mathbf{w}}$  is the unit vector normal to the orbital plane in the direction of the angular momentum vector  $\mathbf{h}$  in the perifocal coordinate system as mentioned before. Therefore [32],

$$\mathbf{e} = e \hat{\mathbf{p}} \quad (4.4a)$$

$$\mathbf{h} = h \hat{\mathbf{w}} \quad (4.4b)$$

So [32],

$$\mathbf{v} = \frac{\mu}{h^2} \left( \frac{h\hat{\mathbf{w}} \times \mathbf{r}}{r} + h\hat{\mathbf{w}} \times e\hat{\mathbf{p}} \right) \quad (4.5)$$

$\hat{\mathbf{p}} \times \hat{\mathbf{q}} = \hat{\mathbf{w}}$  and  $\hat{\mathbf{q}} \times \hat{\mathbf{w}} = \hat{\mathbf{p}}$  because right hand rule and also [32]

$$\hat{\mathbf{w}} \times \hat{\mathbf{p}} = \hat{\mathbf{q}} \quad (4.6)$$

Thus [32],

$$\mathbf{v} = \frac{\mu}{h} \left( \frac{\hat{\mathbf{w}} \times \mathbf{r}}{r} + e\hat{\mathbf{q}} \right) \quad (4.7)$$

Taking the dot product of Eqn (4.1) with the eccentricity vector  $\mathbf{e}$  yields the scalar equation [32]

$$\mathbf{r}_2 \mathbf{e} = \mathbf{c}_1 \mathbf{r}_1 \mathbf{e} + \mathbf{c}_3 \mathbf{r}_3 \mathbf{e} \quad (4.8)$$

According to the orbit equation (Eqn (2.44)) [32],

$$\mathbf{r}_1 \mathbf{e} = \frac{h^2}{\mu} - r_1 \quad \mathbf{r}_2 \mathbf{e} = \frac{h^2}{\mu} - r_2 \quad \mathbf{r}_3 \mathbf{e} = \frac{h^2}{\mu} - r_3 \quad (4.9)$$

Substitute these equations into Eqn (4.8) to obtain [32]

$$\frac{h^2}{\mu} - r_2 = \mathbf{c}_1 \left( \frac{h^2}{\mu} - r_1 \right) + \mathbf{c}_3 \left( \frac{h^2}{\mu} - r_3 \right) \quad (4.10)$$

Taking the crossproduct of Eqn (4.1) first  $\mathbf{r}_1$  and then with  $\mathbf{r}_3$  will eliminate the unknown coefficients  $\mathbf{c}_1$  and  $\mathbf{c}_2$  from this expression [32],

$$\mathbf{r}_2 \times \mathbf{r}_1 = \mathbf{c}_3 (\mathbf{r}_3 \times \mathbf{r}_1) \quad \mathbf{r}_2 \times \mathbf{r}_3 = -\mathbf{c}_1 (\mathbf{r}_3 \times \mathbf{r}_1) \quad (4.11)$$

Multiplying Eqn (4.10) through by the vector  $\mathbf{r}_3 \times \mathbf{r}_1$  yields  $\frac{h^2}{\mu} (\mathbf{r}_3 \times \mathbf{r}_1) - r_2 (\mathbf{r}_3 \times \mathbf{r}_1) = \mathbf{c}_1 (\mathbf{r}_3 \times \mathbf{r}_1) \left( \frac{h^2}{\mu} - r_1 \right) + \mathbf{c}_3 (\mathbf{r}_3 \times \mathbf{r}_1) \left( \frac{h^2}{\mu} - r_3 \right)$ . This change into that utilizing Eqn (4.11),  $\frac{h^2}{\mu} (\mathbf{r}_3 \times \mathbf{r}_1) - r_2 (\mathbf{r}_3 \times \mathbf{r}_1) = -(\mathbf{r}_2 \times \mathbf{r}_3) \left( \frac{h^2}{\mu} - r_1 \right) + (\mathbf{r}_2 \times \mathbf{r}_1) \left( \frac{h^2}{\mu} - r_3 \right)$ . Rearrange terms to obtain [32]

$$\begin{aligned} \frac{h^2}{\mu} (\mathbf{r}_1 \times \mathbf{r}_2 + \mathbf{r}_2 \times \mathbf{r}_3 + \mathbf{r}_3 \times \mathbf{r}_1) \\ = r_1(\mathbf{r}_2 \times \mathbf{r}_3) + r_2(\mathbf{r}_3 \times \mathbf{r}_1) + r_3(\mathbf{r}_1 \times \mathbf{r}_2) \end{aligned} \quad (4.12)$$

Allow using the following notation for the vectors on each side of Eqn (4.12) [32]

$$\mathbf{N} = r_1(\mathbf{r}_2 \times \mathbf{r}_3) + r_2(\mathbf{r}_3 \times \mathbf{r}_1) + r_3(\mathbf{r}_1 \times \mathbf{r}_2) \quad (4.13)$$

and [32]

$$\mathbf{D} = \mathbf{r}_1 \times \mathbf{r}_2 + \mathbf{r}_2 \times \mathbf{r}_3 + \mathbf{r}_3 \times \mathbf{r}_1 \quad (4.14)$$

Therefore, Eqn (4.12) becomes  $\mathbf{N} = \frac{h^2}{\mu} \mathbf{D}$  and from that [32]

$$N = \frac{h^2}{\mu} D \quad (4.15)$$

where  $N = \|\mathbf{N}\|$  and  $D = \|\mathbf{D}\|$ . Thus, the angular momentum  $h$  is [32]

$$h = \sqrt{\mu \frac{N}{D}} \quad (4.16)$$

$\mathbf{D}$  must be normal to the orbital plane because  $\mathbf{r}_1$ ,  $\mathbf{r}_2$  and  $\mathbf{r}_3$  are coplanar and all of the crossproduct lie in the same direction, normal to the orbital plane. As mentioned in the perifocal frame,  $\hat{\mathbf{w}}$  denotes the orbit unit normal, so [32]

$$\hat{\mathbf{w}} = \frac{\mathbf{D}}{D} \quad (4.17)$$

From Eqns (4.4a), (4.6) and (4.17) [32],

$$\hat{\mathbf{q}} = \hat{\mathbf{w}} \times \hat{\mathbf{p}} = \frac{1}{De} (\mathbf{D} \times \mathbf{e}) \quad (4.18)$$

Substitute Eqn (4.14) to obtain [32]

$$\hat{\mathbf{q}} = \frac{1}{De} [(\mathbf{r}_1 \times \mathbf{r}_2) \times \mathbf{e} + (\mathbf{r}_2 \times \mathbf{r}_3) \times \mathbf{e} + (\mathbf{r}_3 \times \mathbf{r}_1) \times \mathbf{e}] \quad (4.19)$$



Apply the bac-cab rule to the right side,  $(\mathbf{A} \times \mathbf{B}) \times \mathbf{C} = -\mathbf{C} \times (\mathbf{A} \times \mathbf{B}) = \mathbf{B}(\mathbf{A} \cdot \mathbf{C}) - \mathbf{A}(\mathbf{B} \cdot \mathbf{C})$ . Use this vector identity yields  $(\mathbf{r}_2 \times \mathbf{r}_3) \times \mathbf{e} = \mathbf{r}_3(\mathbf{r}_2 \cdot \mathbf{e}) - \mathbf{r}_2(\mathbf{r}_3 \cdot \mathbf{e})$ ,  $(\mathbf{r}_3 \times \mathbf{r}_1) \times \mathbf{e} = \mathbf{r}_1(\mathbf{r}_3 \cdot \mathbf{e}) - \mathbf{r}_3(\mathbf{r}_1 \cdot \mathbf{e})$  and  $(\mathbf{r}_1 \times \mathbf{r}_2) \times \mathbf{e} = \mathbf{r}_2(\mathbf{r}_1 \cdot \mathbf{e}) - \mathbf{r}_1(\mathbf{r}_2 \cdot \mathbf{e})$ . Moreover, apply Eqn (4.9) to get  $(\mathbf{r}_2 \times \mathbf{r}_3) \times \mathbf{e} = \mathbf{r}_3 \left( \frac{h^2}{\mu} - r_2 \right) - \mathbf{r}_2 \left( \frac{h^2}{\mu} - r_3 \right) = \frac{h^2}{\mu}(\mathbf{r}_3 - \mathbf{r}_2) + r_3\mathbf{r}_2 - r_2\mathbf{r}_3$ ,  $(\mathbf{r}_3 \times \mathbf{r}_1) \times \mathbf{e} = \mathbf{r}_1 \left( \frac{h^2}{\mu} - r_3 \right) - \mathbf{r}_3 \left( \frac{h^2}{\mu} - r_1 \right) = \frac{h^2}{\mu}(\mathbf{r}_1 - \mathbf{r}_3) + r_1\mathbf{r}_3 - r_3\mathbf{r}_1$  and  $(\mathbf{r}_1 \times \mathbf{r}_2) \times \mathbf{e} = \mathbf{r}_2 \left( \frac{h^2}{\mu} - r_1 \right) - \mathbf{r}_1 \left( \frac{h^2}{\mu} - r_2 \right) = \frac{h^2}{\mu}(\mathbf{r}_2 - \mathbf{r}_1) + r_2\mathbf{r}_1 - r_1\mathbf{r}_2$ . Sum up these three equations, collect the terms and substitute the result into Eqn (4.19) to obtain [32]

$$\hat{\mathbf{q}} = \frac{1}{De} \mathbf{S} \quad (4.20)$$

where [32]

$$\mathbf{S} = \mathbf{r}_1(r_2 - r_3) + \mathbf{r}_2(r_3 - r_1) + \mathbf{r}_3(r_1 - r_2) \quad (4.21)$$

Substituting Eqns (4.16), (4.17) and (4.20) into Eqn (4.7) yields  $\mathbf{v} = \frac{\mu}{h} \left( \frac{\hat{\mathbf{w}} \times \mathbf{r}}{r} + e \hat{\mathbf{q}} \right) = \frac{\mu}{\sqrt{\mu^N D}} \left[ \frac{\mathbf{D} \times \mathbf{r}}{r} + e \left( \frac{1}{De} \mathbf{S} \right) \right]$ . Simplify this expression for the velocity to obtain [32]

$$\mathbf{v} = \sqrt{\frac{\mu}{ND}} \left( \frac{\mathbf{D} \times \mathbf{r}}{r} + \mathbf{S} \right) \quad (4.22)$$

As shown, the expression depends only on the given position vectors  $\mathbf{r}_1$ ,  $\mathbf{r}_2$  and  $\mathbf{r}_3$  [32].

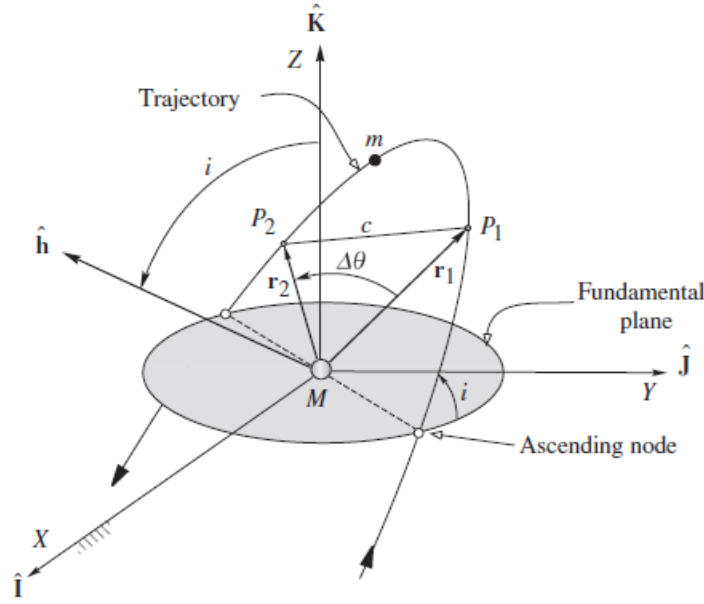
### 4.3. Two Position Vectors and Time - Lambert's Problem

Figure 4.2 shows the position vectors  $\mathbf{r}_1$  and  $\mathbf{r}_2$  of two points  $P_1$  and  $P_2$  on the path of mass  $m$  around mass  $M$ . The change in the true anomaly  $\Delta\theta$  is determined by  $\mathbf{r}_1$  and  $\mathbf{r}_2$  [32],

$$\cos\Delta\theta = \frac{\mathbf{r}_1 \cdot \mathbf{r}_2}{r_1 r_2} \quad (4.23)$$

where [32]

$$r_1 = \sqrt{\mathbf{r}_1 \mathbf{r}_1} \quad r_2 = \sqrt{\mathbf{r}_2 \mathbf{r}_2} \quad (4.24)$$



**Figure 4.2: Lambert's problem [32].**

Nevertheless,  $\Delta\theta$  lies in either the first or forth quadrant when  $\cos\Delta\theta > 0$  while  $\Delta\theta$  lies in either the second or third quadrant when  $\cos\Delta\theta < 0$ . Calculate the  $Z$  component of  $\mathbf{r}_1 \times \mathbf{r}_2$  to resolve this quadrant ambiguity,  $(\mathbf{r}_1 \times \mathbf{r}_2)_Z = \hat{\mathbf{K}}(\mathbf{r}_1 \times \mathbf{r}_2) = \hat{\mathbf{K}}(r_1 r_2 \sin\Delta\theta \hat{\mathbf{h}}) = r_1 r_2 \sin\Delta\theta (\hat{\mathbf{K}} \hat{\mathbf{w}})$  where  $\hat{\mathbf{w}}$  is the unit normal to the orbital plane. Thus,  $\hat{\mathbf{K}} \hat{\mathbf{w}} = \cos i$  where  $i$  is the inclination of the orbit [32]

$$(\mathbf{r}_1 \times \mathbf{r}_2)_Z = r_1 r_2 \sin\Delta\theta \cos i \quad (4.25)$$

The sign of the scalar  $(\mathbf{r}_1 \times \mathbf{r}_2)_Z$  is utilized to determine the correct quadrant for  $\Delta\theta$  that for two cases: prograde trajectories ( $0 < i < 90^\circ$ ) and retrograde trajectories ( $90^\circ < i < 180^\circ$ ). Figure 4.2 shows the prograde trajectory  $\cos i > 0$ ,  $\sin\Delta\theta > 0$  when  $(\mathbf{r}_1 \times \mathbf{r}_2)_Z > 0$  so  $0 < \Delta\theta < 180^\circ$ .  $\Delta\theta = \cos^{-1}\left(\frac{r_1 r_2}{r_1 r_2}\right)$  when  $\Delta\theta$  lies in the first or second quadrant. Otherwise,  $\sin\Delta\theta < 0$  when  $(\mathbf{r}_1 \times \mathbf{r}_2)_Z < 0$  so  $180^\circ < \Delta\theta < 360^\circ$ .  $\Delta\theta = 360^\circ - \cos^{-1}\left(\frac{r_1 r_2}{r_1 r_2}\right)$  when  $\Delta\theta$  lies in the third or fourth quadrant. Moreover, for the retrograde trajectories  $\cos i < 0$ ,  $\sin\Delta\theta < 0$  when  $(\mathbf{r}_1 \times \mathbf{r}_2)_Z > 0$  so  $\Delta\theta$  lies in the third or fourth quadrant. Likewise,  $\Delta\theta$  lies in the first or second quadrant when  $(\mathbf{r}_1 \times \mathbf{r}_2)_Z < 0$ . In shortly [32],

$$\Delta\theta = \begin{cases} \cos^{-1}\left(\frac{\mathbf{r}_1\mathbf{r}_2}{r_1r_2}\right) & \text{when } (\mathbf{r}_1 \times \mathbf{r}_2)_Z < 0 \\ 360^\circ - \cos^{-1}\left(\frac{\mathbf{r}_1\mathbf{r}_2}{r_1r_2}\right) & \text{when } (\mathbf{r}_1 \times \mathbf{r}_2)_Z < 0 \end{cases} \begin{matrix} \text{prograde} \\ \text{retrograde} \end{matrix} \quad (4.26)$$

J.H. Lambert (1728-1777) suggested the situation shown in Figure 4.2 that the transfer time  $\Delta t$  from  $P_1$  and  $P_2$  is independent of the orbit's eccentricity and depends only on the sum  $r_1 + r_2$  of the magnitudes of the position vectors, the semimajor axis  $a$  and the length  $c$  of the chord joining  $P_1$  and  $P_2$ . In addition, the period (of an ellipse) and the specific mechanical energy are independent of the eccentricity, too.

Lambert's problem finds the trajectory joining  $P_1$  and  $P_2$  when the time of flight  $\Delta t$  is known.  $\mathbf{r}_1$  and  $\mathbf{v}_1$  are used to determine the position and velocity of any point on the path as shown in Figure 4.2 [32],

$$\mathbf{r}_2 = f\mathbf{r}_1 + g\mathbf{v}_1 \quad (4.27a)$$

$$\mathbf{v}_2 = \dot{f}\mathbf{r}_1 + \dot{g}\mathbf{v}_1 \quad (4.27b)$$

Solve the first of these for  $\mathbf{v}_1$  to obtain [32]

$$\mathbf{v}_1 = \frac{1}{g}(\mathbf{r}_2 - f\mathbf{r}_1) \quad (4.28)$$

Substituting this result into Eqn (4.27b) yields  $\mathbf{v}_2 = \dot{f}\mathbf{r}_1 + \frac{\dot{g}}{g}(\mathbf{r}_2 - f\mathbf{r}_1) = \frac{\dot{g}}{g}\mathbf{r}_2 - \frac{f\dot{g} - \dot{f}g}{g}\mathbf{r}_1$ . Nevertheless,  $f\dot{g} - \dot{f}g = 1$  according to Eqn (2.139), so [32]

$$\mathbf{v}_2 = \frac{1}{g}(\dot{g}\mathbf{r}_2 - \mathbf{r}_1) \quad (4.29)$$

Orbital elements can be found from either  $\mathbf{r}_1$  and  $\mathbf{v}_1$  or  $\mathbf{r}_2$  and  $\mathbf{v}_2$ . Determine the Lagrange coefficients  $f$ ,  $g$ ,  $\dot{f}$  and  $\dot{g}$  to Lambert's problem. Lagrange coefficients  $f$ ,  $g$ ,  $\dot{f}$  and  $\dot{g}$  in terms of  $\Delta\theta$  [32],

$$f = 1 - \frac{\mu r_2}{h^2} (1 - \cos \Delta \theta) \quad g = \frac{r_1 r_2}{h} \sin \Delta \theta \quad (4.30a)$$

$$\dot{f} = \frac{\mu}{h} \frac{1 - \cos \Delta \theta}{\sin \Delta \theta} \left[ \frac{\mu}{h^2} (1 - \cos \Delta \theta) - \frac{1}{r_0} - \frac{1}{r} \right] \quad \dot{g} = 1 - \frac{\mu r_1}{h^2} (1 - \cos \Delta \theta) \quad (4.30b)$$

Moreover, in terms of the universal anomaly  $\chi$  [32],

$$f = 1 - \frac{\chi^2}{r_1} C(z) \quad g = \Delta t - \frac{1}{\sqrt{\mu}} \chi^3 S(z) \quad (4.31a)$$

$$\dot{f} = \frac{\sqrt{\mu}}{r_1 r_2} \chi [z S(z) - 1] \quad \dot{g} = 1 - \frac{\chi^2}{r_2} C(z) \quad (4.31b)$$

where  $z = \alpha \chi^2$ . The Lagrange coefficients are an obvious choice for the solution of Lambert's problem due to no depending on the eccentricity [32].

Eqns (4.30) and (4.31) gives four equations in three unknowns  $h$ ,  $\chi$  and  $z$ , but only three of these equations are independent due to  $f \dot{g} - \dot{f} g = 1$  [32].

Relationship between  $\Delta \theta$  and  $\Delta t$  is found using  $g$  expression of Eqns (4.30) and (4.31) [32],

$$\frac{r_1 r_2}{h} \sin \Delta \theta = \Delta t - \frac{1}{\sqrt{\mu}} \chi^3 S(z) \quad (4.32)$$

Equating the expressions for  $f$  in Eqns (4.30) and (4.31) yields chance to eliminate the unknown angular momentum  $h$ ,  $1 - \frac{\mu r_2}{h^2} (1 - \cos \Delta \theta) = 1 - \frac{\chi^2}{r_1} C(z)$ . Thus [32],

$$h = \sqrt{\frac{\mu r_1 r_2 (1 - \cos \Delta \theta)}{\chi^2 C(z)}} \quad (4.33)$$

Substitute Eqn (4.33) into Eqn (4.32), simplify and rearrange the terms to obtain [32]

$$\sqrt{\mu} \Delta t = \chi^3 S(z) + \chi \sqrt{C(z)} \left( \sin \Delta \theta \sqrt{\frac{r_1 r_2}{1 - \cos \Delta \theta}} \right) \quad (4.34)$$

Allow assign the term in parentheses on the right the symbol  $A$  due to constancy [32],

$$A = \sin\Delta\theta \sqrt{\frac{r_1 r_2}{1 - \cos\Delta\theta}} \quad (4.35)$$

Thus, Eqn (4.34) becomes [32]

$$\sqrt{\mu}\Delta t = \chi^3 S(z) + A\chi\sqrt{C(z)} \quad (4.36)$$

Equate the expressions for  $\dot{f}$  finding a relationship among  $z$  and  $\chi$  that does not contain orbital parameters like  $z = \alpha\chi^2$ ,  $\frac{\mu}{h} \frac{1 - \cos\Delta\theta}{\sin\Delta\theta} \left[ \frac{\mu}{h^2} (1 - \cos\Delta\theta) - \frac{1}{r_1} - \frac{1}{r_2} \right] = \frac{\sqrt{\mu}}{r_1 r_2} \chi [zS(z) - 1]$ . Multiply through by  $r_1 r_2$  and substitute for the angular momentum

utilizing Eqn (4.33) to obtain  $\frac{\mu}{\sqrt{\frac{\mu r_1 r_2 (1 - \cos\Delta\theta)}{\chi^2 C(z)}}} \frac{1 - \cos\Delta\theta}{\sin\Delta\theta} \left[ \frac{\mu}{\frac{\mu r_1 r_2 (1 - \cos\Delta\theta)}{\chi^2 C(z)}} (1 - \cos\Delta\theta) - r_1 - r_2 \right] = \sqrt{\mu}\chi [zS(z) - 1]$ . Simplify and divide out the common factors to obtain  $\frac{\sqrt{1 - \cos\Delta\theta}}{\sqrt{r_1 r_2 \sin\Delta\theta}} \sqrt{C(z)} [\chi^2 C(z) - r_1 - r_2] = zS(z) - 1$ . Rearranging it leads to  $\chi^2 C(z) = r_1 + r_2 + A \frac{zS(z) - 1}{\sqrt{C(z)}}$ . Allow calling the right hand side  $y(z)$  that depends only  $z$  [32],

$$\chi = \sqrt{\frac{y(z)}{C(z)}} \quad (4.37)$$

where [32]

$$y(z) = r_1 + r_2 + A \frac{zS(z) - 1}{\sqrt{C(z)}} \quad (4.38)$$

Substitute Eqn (4.37) back into Eqn (4.36) to obtain [32]

$$\sqrt{\mu}\Delta t = \left[ \frac{y(z)}{C(z)} \right]^{3/2} S(z) + A\sqrt{y(z)} \quad (4.39)$$

Eqn (4.39) can be used to solve for  $z$ , given the time interval  $\Delta t$  iteratively. Use Newton's method to form the function [32]

$$F(z) = \left[ \frac{y(z)}{C(z)} \right]^{\frac{3}{2}} S(z) + A\sqrt{y(z)} - \sqrt{\mu}\Delta t \quad (4.40)$$

and [32]

$$F'(z) = \frac{1}{2\sqrt{y(z)C^5(z)}} \{ [2C(z)S'(z) - 3C'(z)S(z)]y^2(z) + [AC^{5/2}(z) + 3C(z)S(z)y(z)]y'(z) \} \quad (4.41)$$

where  $C'(z)$  and  $S'(z)$  are the derivative of the Stumpff functions. Find  $y'(z)$  by differentiating Eqn (4.38),  $y'(z) = \frac{A}{2C(z)^{3/2}} \{ [1 - zS(z)]C'(z) + 2[S(z) + zS'(z)]C(z) \}$ . A much simpler form [32],

$$y'(z) = \frac{A}{4}\sqrt{C} \quad (4.42)$$

trig functions in terms of  $C(z)$  and  $S(z)$  [32]

$F'(z)$

$$= \begin{cases} \left[ \frac{y(z)}{C(z)} \right]^{\frac{3}{2}} \left\{ \frac{1}{2z} \left[ C(z) - \frac{3}{2} \frac{S(z)}{C(z)} \right] + \frac{3}{4} \frac{S(z)^2}{C(z)} \right\} + \frac{A}{8} \left[ 3 \frac{S(z)}{C(z)} \sqrt{y(z)} + A \sqrt{\frac{C(z)}{y(z)}} \right] & \text{for } z \neq 0 \\ \frac{\sqrt{2}}{40} y(0)^{3/2} + \frac{A}{8} \left[ \sqrt{y(0)} + A \sqrt{\frac{1}{2y(0)}} \right] & \text{for } z = 0 \end{cases} \quad (4.43)$$

Evaluate  $F'(z)$  at  $z = 0$  carefully due to the  $z$  in the denominator within the curly brackets. Let  $z$  is very small but not quite zero for handling  $z = 0$ , so retain just the first two terms in the series expansions of  $C(z)$  and  $S(z)$ ,  $C(z) = \frac{1}{2} - \frac{z}{24} + \dots$  and  $S(z) = \frac{1}{6} - \frac{z}{120} + \dots$  [32].

Evaluating the term within the curly brackets to obtain  $\frac{1}{2z} \left[ C(z) - \frac{3}{2} \frac{S(z)}{C(z)} \right] \approx$

$$\begin{aligned} \frac{1}{2z} \left[ \left( \frac{1}{2} - \frac{z}{24} \right) - \frac{3}{2} \left( \frac{\frac{1}{6} - \frac{z}{120}}{\frac{1}{2} - \frac{z}{24}} \right) \right] &= \frac{1}{2z} \left[ \left( \frac{1}{2} - \frac{z}{24} \right) - 3 \left( \frac{1}{6} - \frac{z}{120} \right) \left( 1 - \frac{z}{12} \right)^{-1} \right] \approx \frac{1}{2z} \left[ \left( \frac{1}{2} - \frac{z}{24} \right) - \right. \\ 3 \left( \frac{1}{6} - \frac{z}{120} \right) \left( 1 + \frac{z}{12} \right) \Big] &= \frac{1}{2z} \left( -\frac{7}{120} + \frac{z^2}{480} \right) = -\frac{7}{240} + \frac{z}{960} \quad [32]. \end{aligned}$$

The following familiar binomial theorem is utilized in the third step [32],

$$\begin{aligned} (a + b)^n &= a^n + na^{n-1}b + \frac{n(n-1)}{2!} a^{n-2}b^2 \\ &+ \frac{n(n-1)(n-2)}{3!} a^{n-3}b^3 + \dots \end{aligned} \quad (4.44)$$

For setting  $(1 - z/12)^{-1} \approx 1 + z/12$  that is true when  $z$  is close to zero. Therefore, is  $z$  is really zero,  $\frac{1}{2z} \left[ C(z) - \frac{3}{2} \frac{S(z)}{C(z)} \right] = -\frac{7}{240}$  and evaluating the other terms in  $F'(z)$  does not present difficulties. Use  $F(z)$  in Eqn (4.40) and  $F'(z)$  in Eqn (4.43) for Newton's formula to iterate [32],

$$z_{i+1} = z_i - \frac{F(z_i)}{F'(z_i)} \quad (4.45)$$

$z = (1/\alpha)\chi^2$  for choice of a starting value.  $z = E^2$  for an ellipse and  $z = -F^2$  for an hyperbola, but what the orbit do not know so set  $z_0 = 0$  for simple choice or plot or tabulate  $F(z)$  and choose  $z_0$  to be a point near where  $F(z)$  changes sign [32].

Substitute Eqns (4.37) and (4.39) into Eqn (4.31) to obtain the Lagrange coefficients as functions of  $z$  alone [32],

$$f = 1 - \frac{\left[ \frac{y(z)}{C(z)} \right]^2}{r_1} C(z) = 1 - \frac{y(z)}{r_1} \quad (4.46a)$$

$$g = \frac{1}{\sqrt{\mu}} \left\{ \left[ \frac{y(z)}{C(z)} \right]^{3/2} S(z) + A\sqrt{y(z)} \right\} - \frac{1}{\sqrt{\mu}} \left[ \frac{y(z)}{C(z)} \right]^{3/2} S(z) = A\sqrt{\frac{y(z)}{\mu}} \quad (4.46b)$$

$$\dot{f} = \frac{\sqrt{\mu}}{r_1 r_2} \sqrt{\frac{y(z)}{C(z)}} [zS(z) - 1] \quad (4.46c)$$

$$\dot{g} = 1 - \frac{\left[ \frac{y(z)}{\sqrt{C(z)}} \right]^2}{r_2} C(z) = 1 - \frac{y(z)}{r_2} \quad (4.46d)$$

Then calculate  $\mathbf{v}_1$  and  $\mathbf{v}_2$  from Eqns (4.28) and (4.29). After that utilize  $\mathbf{r}_1$  and  $\mathbf{v}_1$  (or  $\mathbf{r}_2$  and  $\mathbf{v}_2$ ) to obtain the orbital elements [32].

#### 4.4. Sidereal Time

Recording the time of each observation is important for determining the orbit of a satellite or celestial body from observations. Solar time that is reckoned by the motion of the sun across the sky is utilized in everyday life. The time required for the sun to return to the same position overhead to lie on the same meridian comprises from high noon to high noon is solar day. On the other hand, Universal Time (UT) is the time required for the sun's passage across the Greenwich meridian, that is zero degrees terrestrial longitude. The sun lies on the Greenwich meridian at noon UT and local standard time or civil time is estimated from the UT by adding 1 h for each time zone between Greenwich and the site, measured westward [32].

Moreover, the time for a distant star to return to its same position overhead to lie on the same meridian takes 24 sidereal hours is called as sidereal time. Sidereal day is shorter than the solar day takes 23 hours and 56 minutes. In other words, the earth rotates  $360^\circ$  in one sidereal day while rotating takes  $360.986^\circ$  in a solar day [32].

The time elapsed since the local meridian of the site passed through the vernal equinox is local sidereal time  $\theta$  of a site is required to know the location of a point on the earth at any given instant relative to the geocentric equatorial frame. The number of degrees (measured eastward) between the vernal equinox and the local meridian is the sidereal time multiplied by 15, the Greenwich sidereal time  $\theta_G$  (the sidereal time of the Greenwich meridian) is firstly determined to find the local sidereal time of a site, after that the east longitude (or subtracting the west longitude) of the site is added. Notion of Julian day is used to estimate sidereal time [32].

The number of days since noon UT on January 1, 4713 Before Christ (BC) is the JD number. Simply subtract the Julian day of one from that of the other to find the number of days between two events. Astronomers observe the heavens at night



would not have to deal with a change of date while their watch because the JD begins at noon rather than at midnight [32].

$J_0$  is the symbol for the Julian day number at 0 h UT that is halfway into the Julian day and the Julian day at any other UT is estimated by [32]

$$JD = J_0 + \frac{UT}{24} \quad (4.47)$$

$J_0$  is obtained by [32]

$$J_0 = 367y - INT \left\{ \frac{7 \left[ y + INT \left( \frac{m+9}{12} \right) \right]}{4} \right\} + INT \left( \frac{275m}{9} \right) + d + 1721013.5 \quad (4.48)$$

where year ( $y$ ), month ( $m$ ) and day ( $d$ ) are integers lying in the coming ranges  $1901 \leq y \leq 2099$ ,  $1 \leq m \leq 12$  and  $1 \leq d \leq 31$ . Meaning of  $INT(x)$  is retaining only the integer portion of  $x$  without rounding. For instance,  $INT(-3.9) = -3$  and  $INT(3.9) = 3$  [32].

Noon on January 1, 2000 is the current Julian epoch is denoted J2000, which has exact Julian day number 2451545.0. A Julian century has 36525 days because there are 365.25 days in a Julian year. The time in Julian centuries between the Julian day  $J_0$  and J2000 is [32]

$$T_0 = \frac{J_0 - 2451545}{36525} \quad (4.49)$$

The Greenwich sidereal time  $\theta_{G0}$  at 0 h UT in degrees in terms of this dimensionless time is [32]

$$\theta_{G0} = 100.4606184 + 36000.77004T_0 + 0.000387933T_0^2 - 2.583(10^{-8})T_0^3 \quad (4.50)$$

where  $0 \leq \theta_{G0} \leq 360^\circ$ . Appropriate integer multiple of  $360^\circ$  must be added or subtracted to bring  $\theta_{G0}$  into that range when there is a value outside the range. The Greenwich sidereal time  $\theta_G$  at any other UT is [32]

$$\theta_G = \theta_{G0} + 360.98564724 \frac{UT}{24} \quad (4.51)$$

where UT is in hours and the coefficient of the second term on the right is the number of degrees the earth rotates in 24 h (solar time) [32].

Consequently, add its east longitude  $\Lambda$  to the Greenwich sidereal time to find the local sidereal time  $\theta$  of a site [32]

$$\theta = \theta_G + \Lambda \quad (4.52)$$

Similarly appropriate integer multiple of  $360^\circ$  must be added or subtracted to bring  $\theta$  into that range when there is a value outside the range [32].

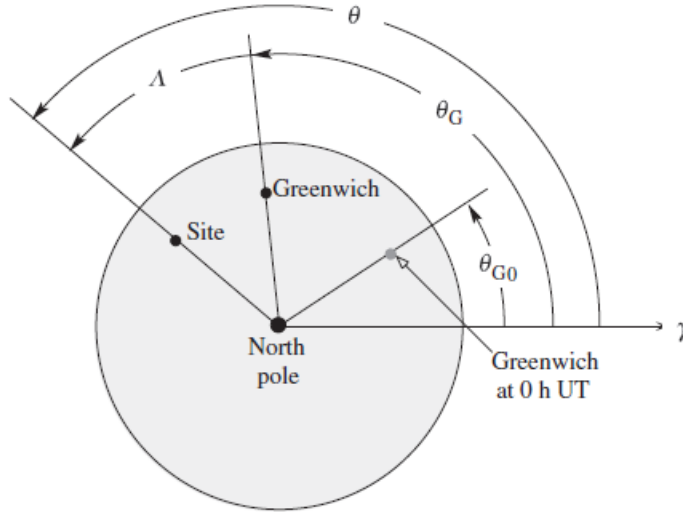


**Figure 4.3: Schematic of the relationship among  $\theta_{G0}$ ,  $\theta_G$ ,  $\Lambda$  and  $\theta$  [32].**

Relationship between  $\theta_{G0}$ ,  $\theta_G$ ,  $\Lambda$  and  $\theta$  is shown in Figure 4.3 [32].

#### 4.5. Topocentric Coordinate System

Figure 4.4 shows a topocentric coordinate system that is centered at the observer's location on the surface of the earth displays an object  $B$  (a satellite or celestial body) and an observer  $O$  on the earth's surface. The relationship between the position  $\mathbf{r}$  of the body  $B$  relative to the center of attraction  $C$ , the position vector  $\mathbf{R}$  of the observer relative to  $C$  and the position  $\rho$  of the body  $B$  relative to the observer is [32]

$$\mathbf{r} = \mathbf{R} + \rho \quad (4.53)$$

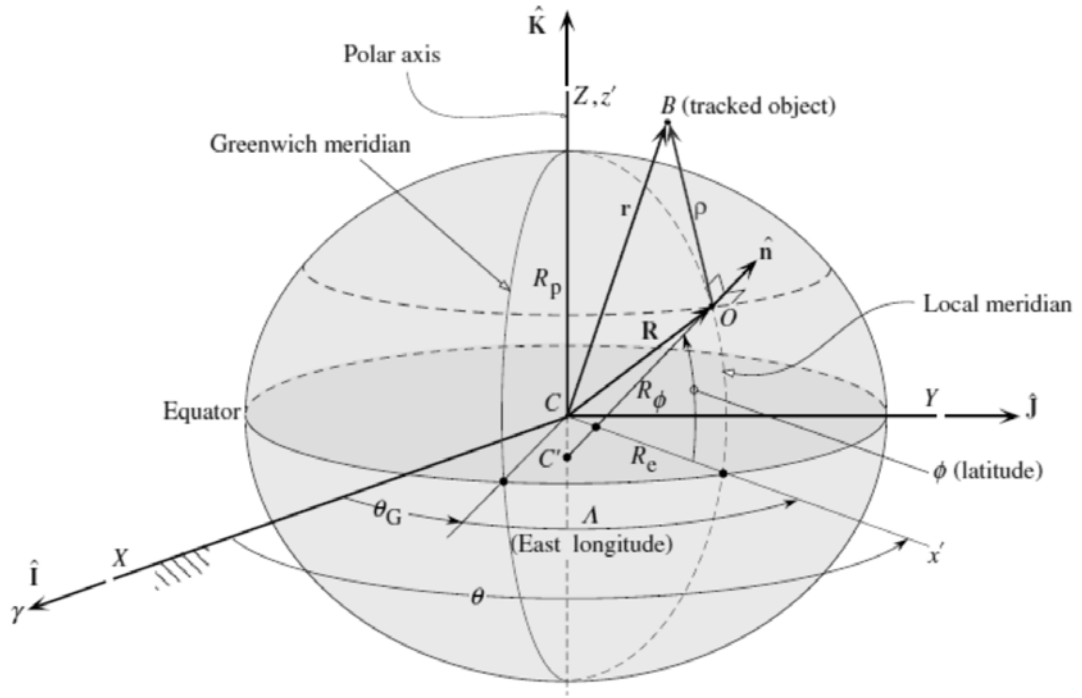


**Figure 4.4: Oblate spheroidal earth (exaggerated) [32].**

The ellipsoidal shape of earth because it is not a sphere is exaggerated in Figure 4.4 where the location of observation site  $O$  is determined by specifying its east longitude  $\Lambda$  and latitude  $\phi$ . East longitude  $\Lambda$  is determined positive eastward from the Greenwich meridian to the meridian through  $O$  whilst the angle between the vernal equinox direction ( $XZ$  plane) and the meridian of  $O$  is the local sidereal time  $\theta$  and the Greenwich sidereal time is  $\theta_G$ . Moreover, the angle among the equator and the normal  $\hat{n}$  to the earth's surface at  $O$  is latitude  $\phi$  [32].

The earth is not a perfect sphere, so the position vector  $\mathbf{R}$  does not point in the direction of the normal except at the equator and the poles [32].

The oblateness or flattening  $f$  is  $f = \frac{R_e - R_p}{R_e}$  in which  $R_e$  is the equatorial radius,  $R_p$  is the polar radius and  $f = 0.00335$  for the earth [32].

The ellipse of the meridian through  $O$  is illustrated in Figure 4.5 where  $R_e$  and  $R_p$  are, respectively, the semimajor and semiminor axes of the ellipse. Accordingly Eqn (2.76),  $R_p = R_e \sqrt{1 - e^2}$ . Thus,  $e = \sqrt{2f - f^2}$  and  $f = 1 - \sqrt{1 - e^2}$  [32].

Point  $C'$  lies below the center  $C$  of the earth (when  $O$  is in the northern hemisphere) shows intersection of the normal to the earth's surface at  $O$  and the polar axis. The

geodetic latitude is the angle  $\varphi$  between the normal and the equator while the geocentric latitude  $\varphi'$  is the angle between the equatorial plane and the line joining  $O$  to the center of the earth [32].

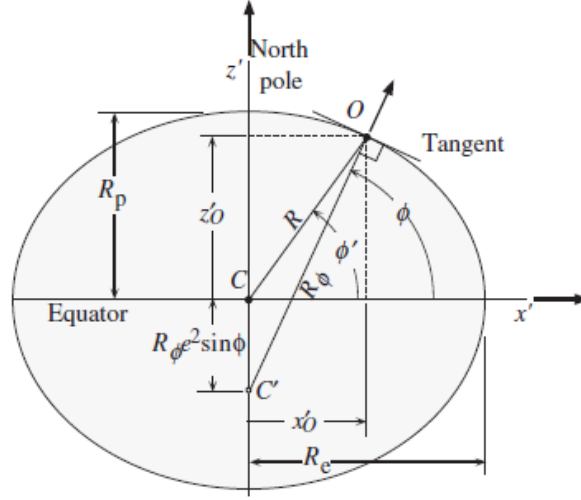


**Figure 4.5: Geocentric latitude ( $\varphi'$ ) and geodetic latitude ( $\varphi$ ) [32].**

The distance from  $C$  to  $C'$  is  $R_\varphi e^2 \sin^2 \varphi$  in which  $R_\varphi$  that is the distance from  $C'$  to  $O$  is a function of latitude [32]

$$R_\varphi = \frac{R_e}{\sqrt{1 - e^2 \sin^2 \varphi}} = \frac{R_e}{\sqrt{1 - (2f - f^2) \sin^2 \varphi}} \quad (4.54)$$

Therefore, the meridional coordinates of  $O$  are  $x'_O = R_\varphi \cos \varphi$  and  $z'_O = (1 - e^2) R_\varphi \sin \varphi = (1 - f)^2 R_\varphi \sin \varphi$ . In the condition that the observation point  $O$  is at an elevation  $H$  above the ellipsoidal surface,  $H \cos \varphi$  must be added to  $x'_O$  while  $H \sin \varphi$  must be added to  $z'_O$  [32],

$$x'_O = R_c \cos \varphi \quad z'_O = R_s \sin \varphi \quad (4.55a)$$

in which [32]

$$R_c = R_\varphi + H \quad R_s = (1 - f)^2 R_\varphi + H \quad (4.55b)$$

where  $R_c$  is the distance of  $O$  from point  $C'$  on the earth's axis and  $R_s$  is the distance from  $O$  to the intersection of the line  $OC'$  with the equatorial plane [32].

The geocentric equatorial coordinates of  $O$  are  $X = x'_0 \cos \theta$ ,  $Y = y'_0 \sin \theta$  and  $Z = z'_0$  in which  $\theta$  is the local sidereal time (Eqn (4.52)). Thus, the position vector  $\mathbf{R}$  is  $\mathbf{R} = R_c \cos \varphi \cos \theta \hat{\mathbf{I}} + R_c \cos \varphi \sin \theta \hat{\mathbf{J}} + R_s \sin \varphi \hat{\mathbf{K}}$  [32].

Substitute Eqns (4.54) and (4.55b) to obtain [32]

$$\begin{aligned} \mathbf{R} = & \left[ \frac{R_e}{\sqrt{1 - (2f - f^2) \sin^2 \varphi}} + H \right] \cos \varphi (\cos \theta \hat{\mathbf{I}} + \sin \theta \hat{\mathbf{J}}) \\ & + \left[ \frac{R_e(1 - f)^2}{\sqrt{1 - (2f - f^2) \sin^2 \varphi}} + H \right] \sin \varphi \hat{\mathbf{K}} \end{aligned} \quad (4.56)$$

In terms of the geocentric latitude  $\varphi'$ ,  $\mathbf{R} = R_e \cos \varphi' \cos \theta \hat{\mathbf{I}} + R_e \cos \varphi' \sin \theta \hat{\mathbf{J}} + R_e \sin \varphi' \hat{\mathbf{K}}$ . Equate these two expressions for  $\mathbf{R}$  and set  $H = 0$  to present that the geodetic latitude is related to geocentric latitude  $\varphi'$  at sea level,  $\tan \varphi' = (1 - f)^2 \tan \varphi$  [32].

#### 4.6. Topocentric Equatorial Coordinate System

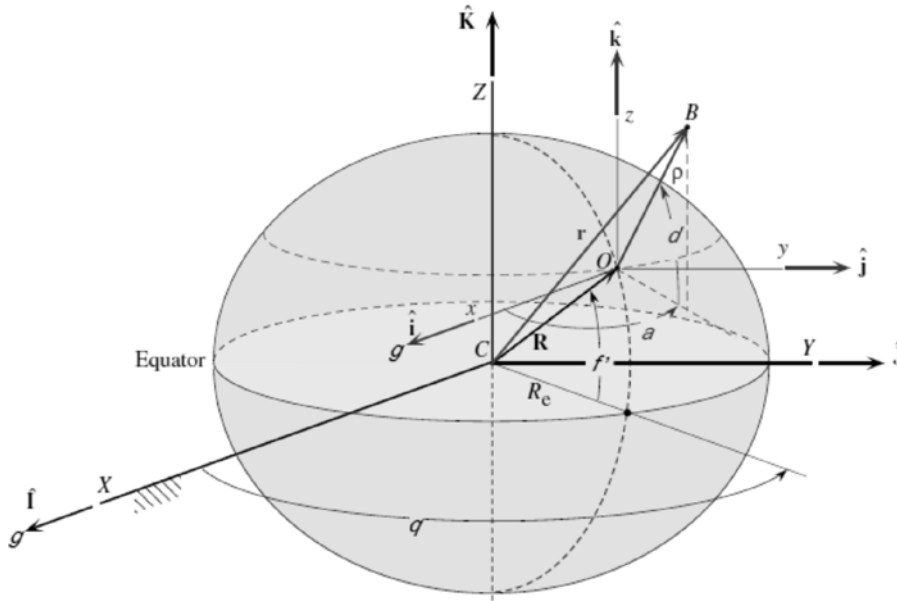


**Figure 4.6 Topocentric equatorial coordinate system [32].**

Figure 4.6 shows the topocentric equatorial coordinate system with the origin at point  $O$  on the surface of the earth utilizes a nonrotating set of  $xyz$  axes through  $O$  that coincide with the  $XYZ$  axes of the geocentric equatorial frame. The relative position vector  $\rho$  in terms of the topocentric right ascension and declination is  $\rho = \rho \cos \delta \cos \alpha \hat{\mathbf{i}} + \rho \cos \delta \sin \alpha \hat{\mathbf{j}} + \rho \sin \delta \hat{\mathbf{k}}$ .  $\hat{\mathbf{i}} = \hat{\mathbf{I}}$ ,  $\hat{\mathbf{j}} = \hat{\mathbf{J}}$  and  $\hat{\mathbf{k}} = \hat{\mathbf{K}}$ , then  $\rho = \rho \hat{\rho}$  in

which  $\rho$  is the slant range and  $\hat{\rho}$  is the unit vector in the direction of the position vector  $\rho$  [32],

$$\hat{\rho} = \cos\delta\cos\alpha\hat{\mathbf{I}} + \cos\delta\sin\alpha\hat{\mathbf{J}} + \sin\delta\hat{\mathbf{K}} \quad (4.57)$$

The origins of the geocentric and topocentric systems do not coincide, so the direction cosines of the position vectors  $\mathbf{r}$  and  $\rho$  will in general differ. Especially, the topocentric right ascension and declination of an earth-orbiting body B will not be same as the geocentric right ascension and declination; this is just an example of parallax. Otherwise, the difference between the geocentric and topocentric position vectors, for this reason the right ascension and declination is negligible for the distant planets and stars when  $\|\mathbf{r}\| \gg \|\mathbf{R}\|$  [32].

#### 4.7. Topocentric Horizon Coordinate System

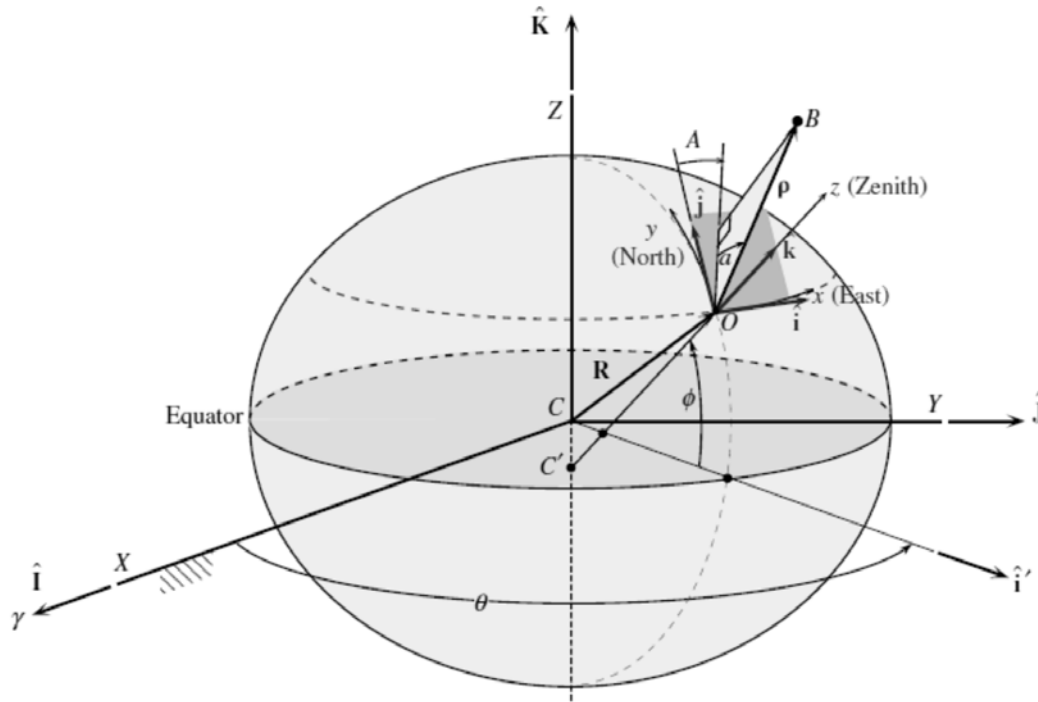


**Figure 4.7: Topocentric horizon (xyz) coordinate system [32].**

Figure 4.7 shows the topocentric coordinate system, which is centered at the observation point  $O$  whose position vector is  $\mathbf{R}$ , where the  $xy$  plane is the local horizon that is the plane tangent to the ellipsoid at point  $O$ . The  $z$ -axis is normal to this plane directed outward toward the zenith whilst the  $x$ -axis is directed eastward and  $y$ -axis points north. This frame may be called as an *ENZ* (East-North-Zenith) frame for the reason that the  $x$ -axis points east. The *SEZ* (South-East-Zenith) frame

which in the  $x$ -axis points toward the south and the  $y$ -axis toward east is obtained from  $ENZ$  by a  $90^\circ$  clockwise rotation around the zenith. Thus,  $[\mathbf{R}_3(-90^\circ)]$  is the matrix of the transformation from  $NEZ$  (North-East-Zenith) to  $SEZ$  [32].

Figure 4.7 illustrates the position vector  $\boldsymbol{\rho}$  of a body  $B$  relative to the topocentric horizon system is  $\boldsymbol{\rho} = \rho \cos a \sin A \hat{\mathbf{i}} + \rho \cos a \cos A \hat{\mathbf{j}} + \rho \sin a \hat{\mathbf{k}}$  where  $\rho$  is the range,  $A$  is the azimuth measured positive clockwise from due north ( $0 \leq A \leq 360^\circ$ ) and  $a$  is the elevation angle or altitude measured from the horizontal to the line of sight of the body  $B$  ( $-90^\circ \leq a \leq 90^\circ$ ). The unit vector  $\hat{\boldsymbol{\rho}}$  in the line of sight direction is [32]

$$\hat{\boldsymbol{\rho}} = \cos a \sin A \hat{\mathbf{i}} + \cos a \cos A \hat{\mathbf{j}} + \sin a \hat{\mathbf{k}} \quad (4.58)$$

Firstly, determine the projections of the topocentric base vectors  $\hat{\mathbf{i}}\hat{\mathbf{j}}\hat{\mathbf{k}}$  onto those of the geocentric equatorial frame to find the transformation between geocentric equatorial and topocentric horizon systems. As shown in Figure 4.7,  $\hat{\mathbf{k}} = \cos \varphi \hat{\mathbf{i}}' + \sin \varphi \hat{\mathbf{K}}$  and  $\hat{\mathbf{i}}' = \cos \theta \hat{\mathbf{I}} + \sin \theta \hat{\mathbf{J}}$ , in which  $\hat{\mathbf{i}}'$  lies in the local meridional plane and is normal to the  $Z$ -axis. Thus [32],

$$\hat{\mathbf{k}} = \cos \varphi \cos \theta \hat{\mathbf{I}} + \cos \varphi \sin \theta \hat{\mathbf{J}} + \sin \varphi \hat{\mathbf{K}} \quad (4.59)$$

Take the cross product of  $\hat{\mathbf{K}}$  into the unit normal  $\hat{\mathbf{k}}$  to find the eastward-directed unit vector  $\hat{\mathbf{i}}$  [32],

$$\hat{\mathbf{i}} = \frac{\hat{\mathbf{K}} \times \hat{\mathbf{k}}}{\|\hat{\mathbf{K}} \times \hat{\mathbf{k}}\|} = \frac{-\cos \varphi \sin \theta \hat{\mathbf{I}} + \cos \varphi \cos \theta \hat{\mathbf{J}}}{\sqrt{\cos^2 \varphi (\sin^2 \theta + \cos^2 \theta)}} = -\sin \theta \hat{\mathbf{I}} + \cos \theta \hat{\mathbf{J}} \quad (4.60)$$

In the end, cross  $\hat{\mathbf{k}}$  into  $\hat{\mathbf{i}}$  to obtain  $\hat{\mathbf{j}}$  [32],

$$\begin{aligned} \hat{\mathbf{j}} = \hat{\mathbf{k}} \times \hat{\mathbf{i}} &= \begin{vmatrix} \hat{\mathbf{i}} & \hat{\mathbf{j}} & \hat{\mathbf{K}} \\ \cos \varphi \cos \theta & \cos \varphi \sin \theta & \sin \varphi \\ -\sin \theta & \cos \theta & 0 \end{vmatrix} \\ &= -\sin \varphi \cos \theta \hat{\mathbf{I}} - \sin \varphi \sin \theta \hat{\mathbf{J}} + \cos \varphi \hat{\mathbf{K}} \end{aligned} \quad (4.61)$$

Denote the matrix of the transformation from the geocentric equatorial to the topocentric horizon as  $[\mathbf{Q}]_{xx}$  whose rows comprise the direction cosines of  $\hat{\mathbf{i}}$ ,  $\hat{\mathbf{j}}$  and  $\hat{\mathbf{k}}$ , respectively. From Eqns (4.59)-(4.61) [32]

$$[\mathbf{Q}]_{xx} = \begin{bmatrix} -\sin\theta & \cos\theta & 0 \\ -\sin\varphi\cos\theta & -\sin\varphi\sin\theta & \cos\varphi \\ \cos\varphi\cos\theta & \cos\varphi\sin\theta & \sin\varphi \end{bmatrix} \quad (4.62a)$$

Transpose of this matrix that is the from the topocentric horizon to the geocentric equatorial [32],

$$[\mathbf{Q}]_{xx} = \begin{bmatrix} -\sin\theta & -\sin\varphi\cos\theta & \cos\varphi\cos\theta \\ \cos\theta & -\sin\varphi\sin\theta & \cos\varphi\sin\theta \\ 0 & \cos\varphi & \sin\varphi \end{bmatrix} \quad (4.62b)$$

The unit basis vectors of the latter coincide with those of the geocentric equatorial coordinate system, so these matrices also signify the transformation between the topocentric horizon and the topocentric equatorial frames [32].

#### 4.8. Orbit Determination from Angle and Range Measurements

When the state vectors  $\mathbf{r}$  and  $\mathbf{v}$  in the inertial geocentric equatorial frame are known at a given instant of time (epoch), an orbit around the earth is defined [32].

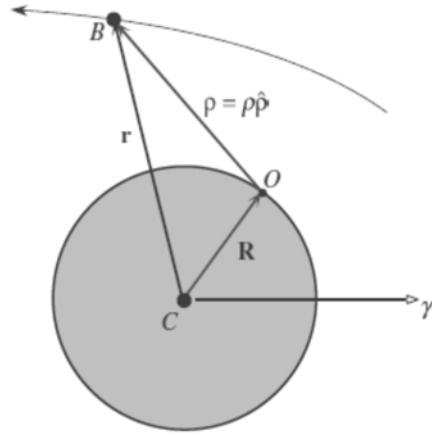


**Figure 4.8: Earth-orbiting body  $B$  tracked by an observer  $O$  [32].**

Figure 4.4 and Figure 4.8 shows the fundamental vector triangle formed by the topocentric position vector  $\rho$  of a satellite relative to a tracking station, the position vector  $\mathbf{R}$  of the station relative to the center of attraction  $C$  and the geocentric position vector  $\mathbf{r}$ . The relationship between these three vectors is [32]

$$\mathbf{r} = \mathbf{R} + \rho\hat{\rho} \quad (4.63)$$



where the range  $\rho$  is the distance of the body  $B$  from the tracking site and  $\hat{\boldsymbol{\rho}}$  is the unit vector including the directional information about  $B$ . Differentiate Eqn (4.63) with respect to time to obtain the velocity  $\boldsymbol{v}$  and acceleration  $\boldsymbol{a}$  [32],

$$\boldsymbol{v} = \dot{\boldsymbol{r}} = \dot{\boldsymbol{R}} + \rho\dot{\hat{\boldsymbol{\rho}}} + \dot{\rho}\hat{\boldsymbol{\rho}} \quad (4.64)$$

$$\boldsymbol{a} = \ddot{\boldsymbol{r}} = \ddot{\boldsymbol{R}} + \ddot{\rho}\hat{\boldsymbol{\rho}} + 2\dot{\rho}\dot{\hat{\boldsymbol{\rho}}} + \rho\ddot{\hat{\boldsymbol{\rho}}} \quad (4.65)$$

Express all these equations in the common basis  $(\hat{\boldsymbol{I}}\hat{\boldsymbol{J}}\hat{\boldsymbol{K}})$  of the inertial (nonrotating) geocentric equatorial frame [32].

Constant angular velocity of earth is  $\boldsymbol{\Omega} = \omega_E \hat{\boldsymbol{K}}$  because  $\boldsymbol{R}$  is a vector fixed in the earth. Using  $\boldsymbol{r} = \boldsymbol{r}_o + \boldsymbol{r}_{rel}$  and  $\boldsymbol{r}_{rel} = x\hat{\boldsymbol{i}} + y\hat{\boldsymbol{j}} + z\hat{\boldsymbol{k}}$  [32],

$$\dot{\boldsymbol{R}} = \boldsymbol{\Omega} \times \boldsymbol{R} \quad (4.66)$$

$$\ddot{\boldsymbol{R}} = \boldsymbol{\Omega} \times (\boldsymbol{\Omega} \times \boldsymbol{R}) \quad (4.67)$$

The direction cosine vector  $\hat{\boldsymbol{\rho}}$  when  $L_X$ ,  $L_Y$  and  $L_Z$  are the topocentric equatorial direction cosines [32],

$$\hat{\boldsymbol{\rho}} = L_X \hat{\boldsymbol{I}} + L_Y \hat{\boldsymbol{J}} + L_Z \hat{\boldsymbol{K}} \quad (4.68)$$

and its first and second derivatives are [32]

$$\dot{\hat{\boldsymbol{\rho}}} = \dot{L}_X \hat{\boldsymbol{I}} + \dot{L}_Y \hat{\boldsymbol{J}} + \dot{L}_Z \hat{\boldsymbol{K}} \quad (4.69)$$

and [32]

$$\ddot{\hat{\boldsymbol{\rho}}} = \ddot{L}_X \hat{\boldsymbol{I}} + \ddot{L}_Y \hat{\boldsymbol{J}} + \ddot{L}_Z \hat{\boldsymbol{K}} \quad (4.70)$$

Thus the topocentric equatorial direction cosines in terms of the topocentric right ascension  $\alpha$  and declination  $\delta$  are [32]

$$\begin{Bmatrix} L_X \\ L_Y \\ L_Z \end{Bmatrix} = \begin{Bmatrix} \cos\alpha\cos\delta \\ \sin\alpha\cos\delta \\ \sin\delta \end{Bmatrix} \quad (4.71)$$

Differentiate this equation twice to obtain [32]

$$\begin{pmatrix} \dot{L}_X \\ \dot{L}_Y \\ \dot{L}_Z \end{pmatrix} = \begin{pmatrix} -\dot{\alpha}\sin\alpha\cos\delta - \dot{\delta}\cos\alpha\sin\delta \\ \dot{\alpha}\cos\alpha\cos\delta - \dot{\delta}\sin\alpha\sin\delta \\ \dot{\delta}\cos\delta \end{pmatrix} \quad (4.72)$$

and [32]

$$\begin{pmatrix} \ddot{L}_X \\ \ddot{L}_Y \\ \ddot{L}_Z \end{pmatrix} = \begin{pmatrix} -\ddot{\alpha}\sin\alpha\cos\delta - \ddot{\delta}\cos\alpha\sin\delta - (\dot{\alpha}^2 + \dot{\delta}^2)\cos\alpha\cos\delta + 2\dot{\alpha}\dot{\delta}\sin\alpha\sin\delta \\ \ddot{\alpha}\cos\alpha\cos\delta - \ddot{\delta}\sin\alpha\sin\delta - (\dot{\alpha}^2 + \dot{\delta}^2)\sin\alpha\cos\delta - 2\dot{\alpha}\dot{\delta}\cos\alpha\sin\delta \\ \ddot{\delta}\cos\delta - \dot{\delta}^2\sin\delta \end{pmatrix} \quad (4.73)$$

Relationship between the direction cosines and their rates with the right ascension, declination and their rates are shown in Eqns (4.71)-(4.73) [32].

The relative position vector in the topocentric horizon system is [32]

$$\hat{\rho} = l_X \hat{i} + l_Y \hat{j} + l_Z \hat{k} \quad (4.74)$$

in which the direction cosines  $l_X$ ,  $l_Y$  and  $l_Z$  are found in terms of the azimuth  $A$  and elevation  $a$  according to Eqn (4.58) [32]

$$\begin{pmatrix} l_X \\ l_Y \\ l_Z \end{pmatrix} = \begin{pmatrix} \sin A \cos a \\ \cos A \cos a \\ \sin a \end{pmatrix} \quad (4.75)$$

$L_X$ ,  $L_Y$  and  $L_Z$  are found from  $l_X$ ,  $l_Y$  and  $l_Z$  by the coordinate transformation [32],

$$\begin{pmatrix} L_X \\ L_Y \\ L_Z \end{pmatrix} = [\mathbf{Q}]_{XX} \begin{pmatrix} l_X \\ l_Y \\ l_Z \end{pmatrix} \quad (4.76)$$

Therefore [32],

$$\begin{pmatrix} L_X \\ L_Y \\ L_Z \end{pmatrix} = \begin{bmatrix} -\sin\theta & -\sin\varphi\cos\theta & \cos\varphi\cos\theta \\ \cos\theta & -\sin\varphi\sin\theta & \cos\varphi\sin\theta \\ 0 & \cos\varphi & \sin\varphi \end{bmatrix} \begin{pmatrix} \sin A \cos a \\ \cos A \cos a \\ \sin a \end{pmatrix} \quad (4.77)$$

Substitute Eqn (4.71) to find relationship between the topocentric right ascension/ declination and azimuth/ elevation [32],

$$\begin{pmatrix} \cos\alpha\cos\delta \\ \sin\alpha\cos\delta \\ \sin\delta \end{pmatrix} = \begin{bmatrix} -\sin\theta & -\sin\varphi\cos\theta & \cos\varphi\cos\theta \\ \cos\theta & -\sin\varphi\sin\theta & \cos\varphi\sin\theta \\ 0 & \cos\varphi & \sin\varphi \end{bmatrix} \begin{pmatrix} \sin A\cos\alpha \\ \cos A\cos\alpha \\ \sin\alpha \end{pmatrix}.$$
 Expand the right-hand side and solve for  $\sin\delta$ ,  $\sin\alpha$  and  $\cos\alpha$  to obtain [32]

$$\sin\delta = \cos\varphi\cos A\cos\alpha + \sin\varphi\sin\alpha \quad (4.78a)$$

$$\sin\alpha = \frac{(\cos\varphi\sin\alpha - \cos A\cos\alpha\sin\varphi)\sin\theta + \cos\theta\sin A\cos\alpha}{\cos\delta} \quad (4.78b)$$

$$\cos\alpha = \frac{(\cos\varphi\sin\alpha - \cos A\cos\alpha\sin\varphi)\cos\theta - \sin\theta\sin A\cos\alpha}{\cos\delta} \quad (4.78c)$$

Use notation of the hour angle  $h$  to simplify Eqns (4.78b) and (4.78c) [32],

$$h = \theta - \alpha \quad (4.79)$$

where  $h$  is the angular distance between the object and the local meridian. The object is west of meridian when  $h$  is positive whilst the object is east of the meridian when  $h$  is negative. Use following trig-identities [32],

$$\sin(\theta - \alpha) = \sin\theta\cos\alpha - \cos\theta\sin\alpha \quad (4.80a)$$

$$\cos(\theta - \alpha) = \cos\theta\cos\alpha + \sin\theta\sin\alpha \quad (4.80b)$$

Substitute Eqns (4.78b) and (4.78c) on the right of Eqn (4.80a) and simplify to obtain [32]

$$\sinh = -\frac{\sin A\cos\alpha}{\cos\delta} \quad (4.81)$$

Moreover, from Eqn (4.80b) [32]

$$\cosh = \frac{\cos\varphi\sin\alpha - \sin\varphi\cos A\cos\alpha}{\cos\delta} \quad (4.82)$$

Calculate  $h$  while resolve quadrant ambiguity by checking the sign of  $\sinh$ ,  $h = \cos^{-1}\left(\frac{\cos\varphi\sin\alpha - \sin\varphi\cos A\cos\alpha}{\cos\delta}\right)$  when  $\sinh$  is positive. On the other hand, subtract  $h$  from  $360^\circ$ . Neither  $\cos\alpha$  nor  $\cos\delta$  can be negative because both the elevation angle  $\alpha$  and the declination  $\delta$  lie between  $-90^\circ$  and  $90^\circ$ . Thus, the sign of  $\sinh$  depends just on that of  $\sin A$  [32].

The topocentric declination  $\delta$  and right ascension  $\alpha$  in terms of the topocentric azimuth  $A$  and altitude  $a$  of the target together with the sidereal time  $\theta$  and latitude  $\varphi$  of the tracking station [32],

$$\delta = \sin^{-1}(\cos\varphi\cos A\cos a + \sin\varphi\sin a) \quad (4.83a)$$

$$h = \begin{cases} 360^\circ - \cos^{-1}\left(\frac{\cos\varphi\sin a - \sin\varphi\cos A\cos a}{\cos\delta}\right) & 0^\circ < A < 180^\circ \\ \cos^{-1}\left(\frac{\cos\varphi\sin a - \sin\varphi\cos A\cos a}{\cos\delta}\right) & 180^\circ \leq A \leq 360^\circ \end{cases} \quad (4.83b)$$

$$\alpha = \theta - h \quad (4.83c)$$

$\alpha$  and  $\delta$  can be found as functions of time from Eqn (4.83) when  $A$  and  $a$  are known as functions of time. Furthermore,  $\dot{\alpha}$  and  $\dot{\delta}$  can be found in terms of  $\dot{A}$  and  $\dot{a}$  as following explanations. Differentiate Eqn (4.78a) with respect to time to obtain [32]

$$\dot{\delta} = \frac{1}{\cos\delta} [-\dot{A}\cos\varphi\sin A\cos a + \dot{a}(\sin\varphi\cos a - \cos\varphi\cos A\sin a)] \quad (4.84)$$

Differentiate Eqn (6.81) to obtain,  $\dot{h}\cosh = -\frac{1}{\cos^2\delta} [(\dot{A}\cos A\cos a - \dot{a}\sin A\sin a)\cos\delta + \dot{\delta}\sin A\cos a\sin\delta]$ . Substitute Eqn (4.82) and simplify to obtain  $\dot{h} = -\frac{\dot{A}\cos A\cos a - \dot{a}\sin A\sin a + \dot{\delta}\sin A\cos a\sin\delta}{\cos\varphi\sin a - \sin\varphi\cos A\cos a}$ . However  $\dot{h} = \dot{\theta} - \dot{\alpha} = \omega_E - \dot{\alpha}$ , so [32]

$$\dot{\alpha} = \omega_E + \frac{\dot{A}\cos A\cos a - \dot{a}\sin A\sin a + \dot{\delta}\sin A\cos a\sin\delta}{\cos\varphi\sin a - \sin\varphi\cos A\cos a} \quad (4.85)$$

#### 4.9. Angles-only Observations

Orbit determination requires specifying six independent quantities that are six classical orbital elements or the total of six components of the state vectors  $\mathbf{r}$  and  $\mathbf{v}$  at a given instant. Measurements of only the two angles, azimuth and elevation with a telescope are needed to determine the orbit in the absence of range and range rate measuring capability. The six quantities are accumulated with a minimum of three observations of azimuth and elevation, and then convert the angular measurements to topocentric right ascension  $\alpha$  and declination  $\delta$  as mentioned before [8].

Optical sensors, which must be utilized for angle-only measurements, basically take pictures of regions of the sky. After that, once a satellite streaks across the picture, its location is brought into consideration to known stars in the picture and the angular directions are decided without range information [1].

Gauss's, Laplace's and double r-iteration will be explained as three techniques for angles-only orbit determination. Laplace's method applies merely the middle point, nonetheless it is usually close to the other data points and it is unsuccessfully for near earth satellites while Gauss's method applies data to all three points is trustworthy for all data. Moreover, it is more suitable for near earth satellites, however the spread of data (usually less than  $60^\circ$  apart) is limited by formulation. Furthermore, the double r-iteration is efficient for large spreads in the data in a condition of multiple observing locations [1].

#### 4.9.1. Gauss method

German mathematician Carl Friedrich Gauss (1777-1855) invented the classical method of angles-only orbit determination, Gauss method that needs to gather angular information over closely spaced intervals of time and gives a preliminary orbit determination based on those initial observations [32].

Gauss method is the best for interplanetary studies. The method is best when the angular separation between observations is less than about  $60^\circ$  whilst it is notably well once data is separated by  $10^\circ$  or less. Determining the  $f$  and  $g$  series is also important process. As a result, Gauss is humility dependable method for determining a satellite's position with angles-only data [1].

Figure 4.9 shows three observations of an orbiting body at times  $t_1$ ,  $t_2$  and  $t_3$  in which the geocentric position vector  $\mathbf{r}$  is related to the observer's position vector  $\mathbf{R}$ , the slant range  $\rho$  and the topocentric direction cosine vector  $\hat{\mathbf{p}}$  at each time [32].

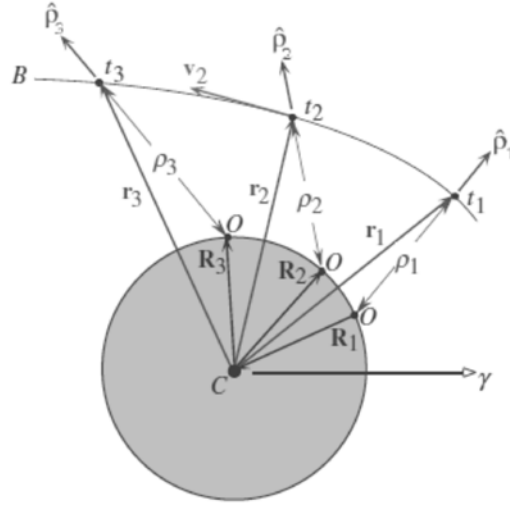


**Figure 4.9: Center of attraction  $C$ , observer  $O$  and tracked body  $B$  [32].**

$$\mathbf{r}_1 = \mathbf{R}_1 + \rho_1 \hat{\mathbf{p}}_1 \quad (4.86a)$$

$$\mathbf{r}_2 = \mathbf{R}_2 + \rho_2 \hat{\mathbf{p}}_2 \quad (4.86b)$$

$$\mathbf{r}_3 = \mathbf{R}_3 + \rho_3 \hat{\mathbf{p}}_3 \quad (4.86c)$$

The location of the tracking station and the time of the observations gives the positions  $\mathbf{R}_1$ ,  $\mathbf{R}_2$  and  $\mathbf{R}_3$ . Moreover, measuring the right ascension  $\alpha$  and declination  $\delta$  of the body at each of the three times gives  $\rho_1$ ,  $\rho_2$  and  $\rho_3$ . Eqns (4.86) shows three vector equations, and so nine scalar equations in 12 unknowns in which the three components of each of the three vectors  $\mathbf{r}_1$ ,  $\mathbf{r}_2$  and  $\mathbf{r}_3$  and the three slant ranges  $\rho_1$ ,  $\rho_2$  and  $\rho_3$  [32].

The conservation of angular momentum needs the vectors  $\mathbf{r}_1$ ,  $\mathbf{r}_2$  and  $\mathbf{r}_3$  to lie in the same plane add an additional three equations.  $\mathbf{r}_2$  is a linear combination of  $\mathbf{r}_1$  and  $\mathbf{r}_3$  as mentioned Gibbs method [32],

$$\mathbf{r}_2 = c_1 \mathbf{r}_1 + c_3 \mathbf{r}_3 \quad (4.87)$$

Two new unknowns,  $c_1$  and  $c_3$  are added with this equation, so there are 12 scalar equations in 14 unknowns [32].

The state vectors  $\mathbf{r}$  and  $\mathbf{v}$  of the orbiting body can be written in terms of the state vectors at any given time via the Lagrange coefficients. Thus, the position vectors  $\mathbf{r}_1$  and  $\mathbf{r}_3$  can be written in terms of the position  $\mathbf{r}_2$  and velocity  $\mathbf{v}_2$  at the intermediate time  $t_2$  [32],

$$\mathbf{r}_1 = f_1 \mathbf{r}_2 + g_1 \mathbf{v}_2 \quad (4.88a)$$

$$\mathbf{r}_3 = f_3 \mathbf{r}_2 + g_3 \mathbf{v}_2 \quad (4.88b)$$

in which  $f_1$  and  $g_1$  are the Lagrange coefficients evaluated at  $t_1$  whilst  $f_3$  and  $g_3$  are the Lagrange coefficients evaluated at  $t_3$ .  $f$  and  $g$  depend virtually only on the distance from the center of attraction at the initial time according to Eqns (2.172) when the time intervals between the three observations are enough small. Therefore, the coefficients in Eqn (4.88) depend only on  $\mathbf{r}_2$ . Six scalar equations (the three components of  $\mathbf{v}_2$  and  $\mathbf{r}_2$ ) are added via Eqns (4.88), so there are 18 equations in 18 unknowns and solution can be obtained when  $\mathbf{v}_2$  and  $\mathbf{r}_2$  are known [32].

Firstly, take crossproduct of each term in Eqn (4.87) to find  $c_1$  and  $c_3$ ,  $\mathbf{r}_2 \times \mathbf{r}_3 = c_1(\mathbf{r}_1 \times \mathbf{r}_3) + c_3(\mathbf{r}_3 \times \mathbf{r}_3)$ . Then,  $\mathbf{r}_2 \times \mathbf{r}_3 = c_1(\mathbf{r}_1 \times \mathbf{r}_3)$  due to  $\mathbf{r}_3 \times \mathbf{r}_3 = 0$ . Take dot product of this result with  $\mathbf{r}_1 \times \mathbf{r}_3$  to find  $c_1$  [32]

$$c_1 = \frac{(\mathbf{r}_2 \times \mathbf{r}_3) \cdot (\mathbf{r}_1 \times \mathbf{r}_3)}{\|\mathbf{r}_1 \times \mathbf{r}_3\|^2} \quad (4.89)$$

Similarly, take dot product of Eqn (4.87) with  $\mathbf{r}_1$  to find  $c_3$  [32]

$$c_3 = \frac{(\mathbf{r}_2 \times \mathbf{r}_1) \cdot (\mathbf{r}_3 \times \mathbf{r}_1)}{\|\mathbf{r}_1 \times \mathbf{r}_3\|^2} \quad (4.90)$$

Using Eqn (4.88) to reduce  $\mathbf{r}_1$  and  $\mathbf{r}_3$  from the expressions for  $c_1$  and  $c_3$  gives  $\mathbf{r}_1 \times \mathbf{r}_3 = (f_1 \mathbf{r}_2 + g_1 \mathbf{v}_2) \times (f_3 \mathbf{r}_2 + g_3 \mathbf{v}_2) = f_1 g_3 (\mathbf{r}_2 \times \mathbf{v}_2) + f_3 g_1 (\mathbf{v}_2 \times \mathbf{r}_2)$ .  $\mathbf{r}_2 \times \mathbf{v}_2 = \mathbf{h}$  in which  $\mathbf{h}$  is the constant angular momentum of the orbit (Eqn (2.28)), so [32]

$$\mathbf{r}_1 \times \mathbf{r}_3 = (f_1 g_3 - f_3 g_1) \mathbf{h} \quad (4.91)$$

and [32]

$$\mathbf{r}_3 \times \mathbf{r}_1 = -(f_1 g_3 - f_3 g_1) \mathbf{h} \quad (4.92)$$

Thus [32],

$$\|\mathbf{r}_1 \times \mathbf{r}_3\|^2 = (f_1 g_3 - f_3 g_1)^2 h^2 \quad (4.93)$$

Likewise [32],

$$\mathbf{r}_2 \times \mathbf{r}_3 = \mathbf{r}_2 \times (f_3 \mathbf{r}_2 + g_3 \mathbf{v}_2) = g_3 \mathbf{h} \quad (4.94)$$

and [32]

$$\mathbf{r}_2 \times \mathbf{r}_1 = \mathbf{r}_2 \times (f_1 \mathbf{r}_2 + g_1 \mathbf{v}_2) = g_1 \mathbf{h} \quad (4.95)$$

Substitute Eqns (4.91), (4.93) and (4.94) into Eqn (4.89) to obtain  $c_1 =$

$$\frac{g_3 \mathbf{h} \cdot (f_1 g_3 - f_3 g_1) \mathbf{h}}{(f_1 g_3 - f_3 g_1)^2 h^2} = \frac{g_3 (f_1 g_3 - f_3 g_1) h^2}{(f_1 g_3 - f_3 g_1)^2 h^2} \text{ or [32]}$$

$$c_1 = \frac{g_3}{f_1 g_3 - f_3 g_1} \quad (4.96)$$

Similarly, substitute Eqns (4.92), (4.93) and (4.95) into (4.90) to obtain [32]

$$c_3 = -\frac{g_1}{f_1 g_3 - f_3 g_1} \quad (4.97)$$

Eqns (4.96) and (4.97) gives  $c_1$  and  $c_3$  in terms of the Lagrange functions. Introduce time notation to approximate  $c_1$  and  $c_2$  for the assumption that the times between observations of the orbiting body are small [32],

$$\tau_1 = t_1 - t_2 \quad (4.98)$$

$$\tau_3 = t_3 - t_2$$

where  $\tau_1$  and  $\tau_3$  are the time intervals between the successive measurements of  $\hat{\rho}_1$ ,  $\hat{\rho}_2$  and  $\hat{\rho}_3$ . Just the first two terms of the series expressions for the Lagrange coefficients  $f$  and  $g$  in Eqn (2.172) are retained when the time intervals  $\tau_1$  and  $\tau_3$  are small enough, so approximations are [32]

$$f_1 \approx 1 - \frac{1}{2} \frac{\mu}{r_2^3} \tau_1^2 \quad (4.99a)$$

$$f_3 \approx 1 - \frac{1}{2} \frac{\mu}{r_2^3} \tau_3^2 \quad (4.99b)$$

and [32]



$$g_1 \approx \tau_1 - \frac{1}{6} \frac{\mu}{r_2^3} \tau_1^3 \quad (4.100a)$$

$$g_3 \approx \tau_3 - \frac{1}{6} \frac{\mu}{r_2^3} \tau_3^3 \quad (4.100b)$$

Use Eqns (4.99) and (4.100) to calculate the denominator in Eqns (4.96) and (4.97),  $f_1 g_3 - f_3 g_1 = \left(1 - \frac{1}{2} \frac{\mu}{r_2^3} \tau_1^2\right) \left(\tau_3 - \frac{1}{6} \frac{\mu}{r_2^3} \tau_3^3\right) - \left(1 - \frac{1}{2} \frac{\mu}{r_2^3} \tau_3^2\right) \left(\tau_1 - \frac{1}{6} \frac{\mu}{r_2^3} \tau_1^3\right)$ . Retain terms of at most the third order in the time intervals  $\tau_1$  and  $\tau_3$  and set [32]

$$\tau = \tau_3 - \tau_1 \quad (4.101)$$

to reduce this expression to [32]

$$f_1 g_3 - f_3 g_1 \approx \tau - \frac{1}{6} \frac{\mu}{r_2^3} \tau^3 \quad (4.102)$$

where  $\tau$  is the time interval between the first and last observations. Substitute Eqns (4.100b) and (4.102) into Eqn (4.96) to obtain [32]

$$c_1 \approx \frac{\tau_3 - \frac{1}{6} \frac{\mu}{r_2^3} \tau_3^3}{\tau - \frac{1}{6} \frac{\mu}{r_2^3} \tau^3} = \frac{\tau^3}{\tau} \left(1 - \frac{1}{2} \frac{\mu}{r_2^3} \tau_3^2\right) \left(\frac{1}{1 - \frac{1}{6} \frac{\mu}{r_2^3} \tau^2}\right)^{-1} \quad (4.103)$$

The binomial theorem is used to linearize the last term on the right. Set  $a = 1$ ,  $b = -\frac{1}{6} \frac{\mu}{r_2^3} \tau^2$  and  $n = -1$  in Eqn (4.44) and neglect terms of higher order than 2 in  $\tau$  to get  $\left(1 - \frac{1}{6} \frac{\mu}{r_2^3} \tau^2\right)^{-1} \approx 1 + \frac{1}{6} \frac{\mu}{r_2^3} \tau^2$ . Thus, Eqn (4.103) changes into [32]

$$c_1 \approx \frac{\tau_3}{\tau} \left[1 + \frac{1}{6} \frac{\mu}{r_2^3} (\tau^2 - \tau_3^2)\right] \quad (4.104)$$

In which merely second-order terms in the time have been retained. Similarly [32],

$$c_3 \approx -\frac{\tau_1}{\tau} \left[1 + \frac{1}{6} \frac{\mu}{r_2^3} (\tau^2 - \tau_1^2)\right] \quad (4.105)$$

Approximate formulas for the coefficients in Eqn (4.87) are obtained finally in terms of just the time intervals between observations and the unknown distance  $r_2$  from the center of attraction at the central time  $t_2$  [32].

Then, substitute Eqn (4.86) into (4.87) to obtain slant ranges  $\rho_1$ ,  $\rho_2$  and  $\rho_3$  in terms of  $c_1$  and  $c_2$ ,  $\mathbf{R}_2 + \rho_2 \hat{\boldsymbol{\rho}}_2 = c_1(\mathbf{R}_1 + \rho_1 \hat{\boldsymbol{\rho}}_1) + c_3(\mathbf{R}_3 + \rho_3 \hat{\boldsymbol{\rho}}_3)$ . Rearrange it [32]

$$c_1 \rho_1 \hat{\boldsymbol{\rho}}_1 - \rho_2 \hat{\boldsymbol{\rho}}_2 + c_3 \rho_3 \hat{\boldsymbol{\rho}}_3 = -c_1 \mathbf{R}_1 + \mathbf{R}_2 - c_3 \mathbf{R}_3 \quad (4.106)$$

Take the dot product of this equation with appropriate vectors to isolate the slant ranges  $\rho_1$ ,  $\rho_2$  and  $\rho_3$ . Thus, taking the dot product of each term in this equation with  $\hat{\boldsymbol{\rho}}_2 \times \hat{\boldsymbol{\rho}}_3$  to isolate  $\rho_1$  yields  $c_1 \rho_1 \hat{\boldsymbol{\rho}}_1 \cdot (\hat{\boldsymbol{\rho}}_2 \times \hat{\boldsymbol{\rho}}_3) - \rho_2 \hat{\boldsymbol{\rho}}_2 \cdot (\hat{\boldsymbol{\rho}}_2 \times \hat{\boldsymbol{\rho}}_3) + c_3 \rho_3 \hat{\boldsymbol{\rho}}_3 \cdot (\hat{\boldsymbol{\rho}}_2 \times \hat{\boldsymbol{\rho}}_3) = -c_1 \mathbf{R}_1 \cdot (\hat{\boldsymbol{\rho}}_2 \times \hat{\boldsymbol{\rho}}_3) + \mathbf{R}_2 \cdot (\hat{\boldsymbol{\rho}}_2 \times \hat{\boldsymbol{\rho}}_3) - c_3 \mathbf{R}_3 \cdot (\hat{\boldsymbol{\rho}}_2 \times \hat{\boldsymbol{\rho}}_3)$ .

$\hat{\boldsymbol{\rho}}_2 \cdot (\hat{\boldsymbol{\rho}}_2 \times \hat{\boldsymbol{\rho}}_3) = \hat{\boldsymbol{\rho}}_3 \cdot (\hat{\boldsymbol{\rho}}_2 \times \hat{\boldsymbol{\rho}}_3) = 0$ , so [32]

$$c_1 \rho_1 \hat{\boldsymbol{\rho}}_1 \cdot (\hat{\boldsymbol{\rho}}_2 \times \hat{\boldsymbol{\rho}}_3) = (-c_1 \mathbf{R}_1 + \mathbf{R}_2 - c_3 \mathbf{R}_3) \cdot (\hat{\boldsymbol{\rho}}_2 \times \hat{\boldsymbol{\rho}}_3) \quad (4.107)$$

Use notation  $D_0$  to represent the scalar triple product of  $\hat{\boldsymbol{\rho}}_1$ ,  $\hat{\boldsymbol{\rho}}_2$  and  $\hat{\boldsymbol{\rho}}_3$  [32],

$$D_0 = \hat{\boldsymbol{\rho}}_1 \cdot (\hat{\boldsymbol{\rho}}_2 \times \hat{\boldsymbol{\rho}}_3) \quad (4.108)$$

Assuming that  $D_0$  is not zero means that  $\hat{\boldsymbol{\rho}}_1$ ,  $\hat{\boldsymbol{\rho}}_2$  and  $\hat{\boldsymbol{\rho}}_3$  do not lie in the same plane. Thus, solving Eqn (4.107) for  $\rho_1$  yields [32]

$$\rho_1 = \frac{1}{D_0} \left( -D_{11} + \frac{1}{c_1} D_{21} - \frac{c_3}{c_1} D_{31} \right) \quad (4.109a)$$

where the D's stand for the scalar triple products [32]

$$D_{11} = \mathbf{R}_1 \cdot (\hat{\boldsymbol{\rho}}_2 \times \hat{\boldsymbol{\rho}}_3) \quad D_{21} = \mathbf{R}_2 \cdot (\hat{\boldsymbol{\rho}}_2 \times \hat{\boldsymbol{\rho}}_3) \quad D_{31} = \mathbf{R}_3 \cdot (\hat{\boldsymbol{\rho}}_2 \times \hat{\boldsymbol{\rho}}_3) \quad (4.109b)$$

Similarly, take the dot product of Eqn (4.106) with  $\hat{\boldsymbol{\rho}}_1 \times \hat{\boldsymbol{\rho}}_3$  and then  $\hat{\boldsymbol{\rho}}_1 \times \hat{\boldsymbol{\rho}}_2$  to get  $\rho_2$  and  $\rho_3$  [32],

$$\rho_2 = \frac{1}{D_0} (-c_1 D_{12} + D_{22} - c_3 D_{32}) \quad (4.110a)$$

in which [32]

$$D_{12} = \mathbf{R}_1 \cdot (\hat{\boldsymbol{\rho}}_1 \times \hat{\boldsymbol{\rho}}_3) \quad D_{22} = \mathbf{R}_2 \cdot (\hat{\boldsymbol{\rho}}_1 \times \hat{\boldsymbol{\rho}}_3) \quad D_{32} = \mathbf{R}_3 \cdot (\hat{\boldsymbol{\rho}}_1 \times \hat{\boldsymbol{\rho}}_3) \quad (4.110b)$$

and [32]

$$\rho_3 = \frac{1}{D_0} \left( -\frac{c_1}{c_3} D_{13} + \frac{1}{c_3} D_{23} - D_{33} \right) \quad (4.111a)$$

in which [32]

$$D_{13} = \mathbf{R}_1 \cdot (\hat{\boldsymbol{\rho}}_1 \times \hat{\boldsymbol{\rho}}_2) \quad D_{23} = \mathbf{R}_2 \cdot (\hat{\boldsymbol{\rho}}_1 \times \hat{\boldsymbol{\rho}}_2) \quad D_{33} = \mathbf{R}_3 \cdot (\hat{\boldsymbol{\rho}}_1 \times \hat{\boldsymbol{\rho}}_2) \quad (4.111b)$$

Utilizing the fact that  $\hat{\boldsymbol{\rho}}_2 \cdot (\hat{\boldsymbol{\rho}}_1 \times \hat{\boldsymbol{\rho}}_3) = -D_0$  and  $\hat{\boldsymbol{\rho}}_3 \cdot (\hat{\boldsymbol{\rho}}_1 \times \hat{\boldsymbol{\rho}}_2) = D_0$  gives these results [32].

Substitute Eqns (4.104) and (4.105) into Eqn (4.110a) to obtain the slant range  $\rho_2$  [32],

$$\rho_2 = A + \frac{\mu B}{r_2^3} \quad (4.112a)$$

where [32]

$$A = \frac{1}{D_0} \left( -D_{12} \frac{\tau_3}{\tau} + D_{22} + D_{32} \frac{\tau_1}{\tau} \right) \quad (4.112b)$$

$$B = \frac{1}{6D_0} \left[ D_{12}(\tau_3^2 - \tau^2) \frac{\tau_3}{\tau} + D_{32}(\tau^2 - \tau_1^2) \frac{\tau_1}{\tau} \right] \quad (4.112c)$$

Otherwise, substitute same equations into Eqns (4.109) and (4.111) gives the slant ranges  $\rho_1$  and  $\rho_3$  [32],

$$\rho_1 = \frac{1}{D_0} \left[ \frac{6 \left( D_{31} \frac{\tau_1}{\tau_3} + D_{21} \frac{\tau}{\tau_3} \right) r_2^3 + \mu D_{31} (\tau^2 - \tau_1^2) \frac{\tau_1}{\tau_3}}{6r_2^3 + \mu(\tau^2 - \tau_3^2)} - D_{11} \right] \quad (4.113)$$

$$\rho_3 = \frac{1}{D_0} \left[ \frac{6 \left( D_{13} \frac{\tau_3}{\tau_1} - D_{23} \frac{\tau}{\tau_1} \right) r_2^3 + \mu D_{13} (\tau^2 - \tau_3^2) \frac{\tau_3}{\tau_1}}{6r_2^3 + \mu(\tau^2 - \tau_1^2)} - D_{33} \right] \quad (4.114)$$

A relation between the slant range  $\rho_2$  and the geocentric radius  $r_2$  is shown in Eqn (4.112a) and also Eqn (4.86b), which  $\mathbf{r}_2 \cdot \mathbf{r}_2 = (\mathbf{R}_2 + \rho_2 \hat{\boldsymbol{\rho}}_2) \cdot (\mathbf{R}_2 + \rho_2 \hat{\boldsymbol{\rho}}_2)$  or [32]

$$r_2^2 = \rho_2^2 + 2E\rho_2 + R_2^2 \quad (4.115a)$$

where [32]

$$E = \mathbf{R}_2 \cdot \hat{\mathbf{p}}_2 \quad (4.115b)$$

Substitute Eqn (4.112a) into Eqn (4.115a) to obtain  $r_2^2 = \left(A + \frac{\mu B}{r_2^3}\right)^2 + 2C\left(A + \frac{\mu B}{r_2^3}\right) + R_2^2$  [32].

Finally, an eight-order polynomial is obtained by expanding and rearranging terms [32],

$$x^8 + ax^6 + bx^3 + c = 0 \quad (4.116)$$

in which  $x = r_2$  and the coefficients are [32]

$$a = -(A^2 + 2AE + R_2^2) \quad b = -2\mu B(A + E) \quad c = -\mu^2 B^2 \quad (4.117)$$

Solving Eqn (4.116) for  $r_2$  and substituting the result into Eqns (4.112)-(4.114) yields the slant ranges  $\rho_1$ ,  $\rho_2$  and  $\rho_3$ , and so Eqns (4.86) give the position vectors  $\mathbf{r}_1$ ,  $\mathbf{r}_2$  and  $\mathbf{r}_3$ . Find  $\mathbf{r}_2$  to determine the orbit. Then, find  $\mathbf{v}_2$  solving Eqn (4.88a) for  $\mathbf{r}_2$ ,  $\mathbf{r}_2 = \frac{1}{f_1}\mathbf{r}_1 - \frac{g_1}{f_1}\mathbf{v}_2$ . Substituting this result into Eqn (4.88b) yields  $\mathbf{r}_3 = \frac{f_3}{f_1}\mathbf{r}_1 + \left(\frac{f_1 g_3 - f_3 g_1}{f_1}\right)\mathbf{v}_2$ . Solve this to obtain  $\mathbf{v}_2$  [32],

$$\mathbf{v}_2 = \frac{1}{f_1 g_3 - f_3 g_1} (-f_3 \mathbf{r}_1 + f_1 \mathbf{r}_3) \quad (4.118)$$

where the approximate Lagrange functions are shown in Eqns (4.99) and (4.100).

Utilize the approximate values for  $\mathbf{r}_2$  and  $\mathbf{v}_2$  like the starting point for iteratively improving the accuracy of the computed  $\mathbf{r}_2$  and  $\mathbf{v}_2$  until convergence is reached [8].

Iterative improvement of the orbit get starts calculating the magnitude of  $\mathbf{r}_2$  ( $r_2 = \sqrt{\mathbf{r}_2 \cdot \mathbf{r}_2}$ ) and  $\mathbf{v}_2$  ( $v_2 = \sqrt{\mathbf{v}_2 \cdot \mathbf{v}_2}$ ). Then, calculate the reciprocal of the semimajor axis,  $\alpha = \frac{2}{r_2} - \frac{v_2^2}{\mu}$  and the radial components of  $\mathbf{v}_2$ ,  $v_{r2} = \mathbf{v}_2 \cdot \mathbf{r}_2 / r_2$ . Solve the universal Kepler's equation for the universal variables  $\chi_1$  and  $\chi_3$  at times  $t_1$  and  $t_3$ ,

respectively:  $\sqrt{\mu}\tau_1 = \frac{r_2 v_{r2}}{\sqrt{\mu}} \chi_1^2 C(\alpha \chi_1^2) + (1 - \alpha r_2) \chi_1^3 S(\alpha \chi_1^2) + r_2 \chi_1$  and  $\sqrt{\mu}\tau_3 = \frac{r_2 v_{r2}}{\sqrt{\mu}} \chi_3^2 C(\alpha \chi_3^2) + (1 - \alpha r_2) \chi_3^3 S(\alpha \chi_3^2) + r_2 \chi_3$ . Thus,

$f_1 = 1 - \frac{\chi_1^2}{r_2} C(\alpha \chi_1^2)$ ,  $g_1 = \tau_1 - \frac{1}{\sqrt{\mu}} \chi_1^3 S(\alpha \chi_1^2)$ ,  $f_3 = 1 - \frac{\chi_3^2}{r_2} C(\alpha \chi_3^2)$  and  $g_3 = \tau_3 - \frac{1}{\sqrt{\mu}} \chi_3^3 S(\alpha \chi_3^2)$ . Calculate  $c_1$  and  $c_3$  from Eqns (4.96) and (4.97) using these values. After that, calculate updated values of  $\rho_1$ ,  $\rho_2$  and  $\rho_3$  from Eqns (4.109)-(4.111) using  $c_1$  and  $c_3$ . Use Eqn (4.86) to calculate updated  $\mathbf{r}_1$ ,  $\mathbf{r}_2$  and  $\mathbf{r}_3$ . Use Eqn (4.118) and the  $f$  and  $g$  values to calculate updated  $\mathbf{v}_2$ . Later, repeat all of these process until there is not further change in  $\rho_1$ ,  $\rho_2$  and  $\rho_3$  to the desired degree of precision. Finally, compute orbital elements using  $\mathbf{r}_2$  and  $\mathbf{v}_2$  [32].

#### 4.9.2. Laplace's method

Laplace apply this method in 1780 to evaluate the middle position and velocity vectors in a span of observational data for the orbits of comets and minor planets. Three sets of angular measurements are needed to find the six independent quantities for orbit determination. Data from different sites at different times can be processed using this method, so it seems improbable firstly but the solution does converge [1].

Line of sight unit vectors,  $\hat{\mathbf{L}}$  to the satellite at each observation time is utilized as notation [1],

$$\hat{\mathbf{L}}_i = \begin{bmatrix} \cos \delta_{ti} \cos \alpha_{ti} \\ \cos \delta_{ti} \sin \alpha_{ti} \\ \sin \delta_{ti} \end{bmatrix} \quad i = 1, 2, 3 \quad (4.119)$$

When the slant range,  $\rho$  to each satellite and the observation site's location is known, the position vectors can be found easily [1],

$$\mathbf{r} = \rho \hat{\mathbf{L}} + \mathbf{R} \quad (4.120)$$

$\mathbf{r} \cdot \mathbf{r}$  yields the satellite's distance [1]

$$r = \sqrt{\rho^2 + 2\rho \hat{\mathbf{L}} \mathbf{R} + R^2} \quad (4.121)$$

Differentiate Eqn (4.120) twice to produce the velocity and acceleration for each observation [1],

$$\begin{aligned}\dot{\mathbf{r}} &= \dot{\rho}\hat{\mathbf{L}} + \rho\dot{\hat{\mathbf{L}}} + \dot{\mathbf{R}} \\ \ddot{\mathbf{r}} &= \ddot{\rho}\hat{\mathbf{L}} + 2\dot{\rho}\dot{\hat{\mathbf{L}}} + \rho\ddot{\hat{\mathbf{L}}} + \ddot{\mathbf{R}}\end{aligned}\tag{4.122}$$

Substituting this expression for the satellite's acceleration above and combining with Eqn (4.120) yields  $-\frac{\mu}{r^3}(\rho\hat{\mathbf{L}} + \mathbf{R}) = \ddot{\rho}\hat{\mathbf{L}} + 2\dot{\rho}\dot{\hat{\mathbf{L}}} + \rho\ddot{\hat{\mathbf{L}}} + \ddot{\mathbf{R}}$ . Rearrange it [1]

$$\ddot{\rho}\hat{\mathbf{L}} + 2\dot{\rho}\dot{\hat{\mathbf{L}}} + \rho\left(\ddot{\hat{\mathbf{L}}} + \frac{\mu}{r^3}\hat{\mathbf{L}}\right) = -\ddot{\mathbf{R}} - \frac{\mu}{r^3}\mathbf{R}\tag{4.123}$$

Utilize the Lagrange interpolation formula due to that each line-of-sight vector is at a particular time and for finding the unknown derivatives [1],

$$\mathbf{r}(t) = \sum_{i=1}^n \mathbf{r}_i \prod_{k \neq i} \frac{t - t_k}{t_i - t_k}\tag{4.124}$$

An approximate expression for  $\hat{\mathbf{L}}(t)$  at any time ( $n = 3$  for three observations) is derived using Lagrange interpolation,  $\hat{\mathbf{L}}(t) = \frac{(t-t_2)(t-t_3)}{(t_1-t_2)(t_1-t_3)}\hat{\mathbf{L}}_1 + \frac{(t-t_1)(t-t_3)}{(t_2-t_1)(t_2-t_3)}\hat{\mathbf{L}}_2 + \frac{(t-t_1)(t-t_2)}{(t_3-t_1)(t_3-t_2)}\hat{\mathbf{L}}_3$ . Differentiate the expression to obtain  $\dot{\hat{\mathbf{L}}}(t) = \frac{2t-t_2-t_3}{(t_1-t_2)(t_1-t_3)}\hat{\mathbf{L}}_1 + \frac{2t-t_1-t_3}{(t_2-t_1)(t_2-t_3)}\hat{\mathbf{L}}_2 + \frac{2t-t_1-t_2}{(t_3-t_1)(t_3-t_2)}\hat{\mathbf{L}}_3$  and  $\ddot{\hat{\mathbf{L}}}(t) = \frac{2}{(t_1-t_2)(t_1-t_3)}\hat{\mathbf{L}}_1 + \frac{2}{(t_2-t_1)(t_2-t_3)}\hat{\mathbf{L}}_2 + \frac{2}{(t_3-t_1)(t_3-t_2)}\hat{\mathbf{L}}_3$  [1].

When the middle time is supposed to be zero ( $t = t_2 = 0$ ), these expressions are simpler. Differences in times can be used, so this assumption is general [1].

Furthermore, once more observations are obtainable; the first and second derivatives can be evaluated much more accurately by using Lagrange's interpolation formula with additional observations. Additionally, least-square techniques can be utilized to obtain even better estimates. In the condition that the higher derivatives are important, both of these approaches also needed for improved accuracy [1].

Once all the observations happen from one site, the derivatives of the position vector,  $\dot{\mathbf{R}}_2 = \boldsymbol{\omega}_E \times \mathbf{R}_2$  and  $\ddot{\mathbf{R}}_2 = \boldsymbol{\omega}_E \times \dot{\mathbf{R}}_2$ . On the other hand, when all the observation happen from different sites, the derivatives of the position vector are found by using

Lagrange's interpolation formula for the change in the times,  $\tau_i = t_i - t_2$ , so  $\ddot{\mathbf{R}}_2 = -\frac{\tau_3}{\tau_1(\tau_1-\tau_3)}\mathbf{R}_1 - \frac{\tau_3+\tau_1}{\tau_1\tau_3}\mathbf{R}_2 - \frac{\tau_1}{\tau_3(\tau_3-\tau_1)}\mathbf{R}_3$  and  $\ddot{\mathbf{R}}_2 = \frac{2}{\tau_1(\tau_1-\tau_3)}\mathbf{R}_1 + \frac{2}{\tau_1\tau_3}\mathbf{R}_2 + \frac{2}{\tau_3(\tau_3-\tau_1)}\mathbf{R}_3$  [1].

Firstly, assume a value for the position magnitude to find the range  $\rho$  and its derivatives, and the position magnitude  $r$ ,  $\begin{bmatrix} \hat{\mathbf{L}} & : & 2\dot{\hat{\mathbf{L}}} & : & \ddot{\hat{\mathbf{L}}} + \frac{\mu}{r^3}\hat{\mathbf{L}} \end{bmatrix} \begin{bmatrix} \ddot{\rho} \\ \dot{\rho} \\ \rho \end{bmatrix} = -\left[\ddot{\mathbf{R}} + \frac{\mu}{r^3}\mathbf{R}\right]$ . Use determinants and Cramer's rule to solve this expression. The determinant,  $D$  for the system of equations in slant range [1],

$$D = \begin{vmatrix} \hat{\mathbf{L}} & : & 2\dot{\hat{\mathbf{L}}} & : & \ddot{\hat{\mathbf{L}}} + \frac{\mu}{r^3}\hat{\mathbf{L}} \end{vmatrix} \quad (4.125)$$

Subtract  $\frac{\mu}{r^3}$  times the first column from the third to reduce the complexity slightly and factor out the 2 from the second column to obtain,  $D = 2\begin{vmatrix} \hat{\mathbf{L}} & : & 2\dot{\hat{\mathbf{L}}} & : & \ddot{\hat{\mathbf{L}}} \end{vmatrix}$ . Utilize Eqn (4.123) to apply Cramer's rule and replace the third column with the right-hand side of Eqn (4.123) for the reason that the column represent the slant-range component (factor out the  $-1$  from the column),  $D\rho = -2\begin{vmatrix} \hat{\mathbf{L}} & : & \dot{\hat{\mathbf{L}}} & : & \ddot{\mathbf{R}} + \frac{\mu}{r^3}\mathbf{R} \end{vmatrix}$ . Splitting this determinant yields,  $D\rho = -2\begin{vmatrix} \hat{\mathbf{L}} & : & \dot{\hat{\mathbf{L}}} & : & \ddot{\mathbf{R}} \end{vmatrix} - 2\frac{\mu}{r^3}\begin{vmatrix} \hat{\mathbf{L}} & : & \dot{\hat{\mathbf{L}}} & : & \mathbf{R} \end{vmatrix}$ . Suppose  $D_1$  is the first determinant and  $D_2$  is the second determinant, so the range is [1]

$$\rho = \frac{-2D_1}{D} - \frac{2\mu D_2}{r^3 D} \quad (4.126)$$

If the site is located at the great circle that encompasses the satellite's orbit, the determinant could be zero and create numerical difficulties [1].

Guessing is needed at the slant range, so determine the final value for  $\rho$  by iterating. Substitute Eqn (4.126) into (4.121) to obtain [1],

$$r_2^2 = \left(\frac{-2D_1}{D} - \frac{2\mu D_2}{r_2^3 D}\right)^2 + 2\left(\frac{-2D_1}{D} - \frac{2\mu D_2}{r_2^3 D}\right)\hat{\mathbf{L}}_2 \cdot \mathbf{R}_2 + \mathbf{R}_2^2 \quad (4.127)$$

Expand this expression and let  $C$  equal the dot product to produce an eight-order polynomial [1],

$$C = \hat{\mathbf{L}}_2 \cdot \mathbf{R}_2$$

$$r_2^8 + \left( \frac{4CD_1}{D} - \frac{4D_1^2}{D^2} - \mathbf{R}_2^2 \right) r_2^6 + \mu \left( \frac{4CD_2}{D} - \frac{8D_1D_2}{D^2} \right) r_2^3 - \frac{4\mu^2D_2}{D^2} = 0 \quad (4.128)$$

Real root from this expression is the correct root(s), but try each root and compare to a priori data or process more observations to isolate the correct root in the case of multiple roots. Thus, it is very difficult process while designing multi-purpose routines [1].

Solve Eqn (4.126) to find the slant range at the middle time. Therefore, make one more time this process for the velocity, which is the middle term in the determinant expression, using Cramer's rule starting from Eqn (4.123). Thus,  $D\dot{\rho} = -\left| \hat{\mathbf{L}} : \ddot{\mathbf{R}} + \frac{\mu}{r^3} \mathbf{R} : \ddot{\hat{\mathbf{L}}} \right|$ . Splitting this determinant yields  $D\dot{\rho} = -\left| \hat{\mathbf{L}} : \ddot{\mathbf{R}} : \ddot{\hat{\mathbf{L}}} \right| - \frac{\mu}{r^3} \left| \hat{\mathbf{L}} : \mathbf{R} : \ddot{\hat{\mathbf{L}}} \right|$ . Suppose  $D_3$  is the first velocity determinant and  $D_4$  is the second determinant, so the range rate is [1]

$$\dot{\rho} = -\frac{D_3}{D} - \frac{\mu D_4}{r^3 D} \quad (4.129)$$

Consequently, the middle velocity vector in Eqn (4.122) is found by using the velocity determinants [1],

$$\mathbf{v}_2 = \dot{\rho} \hat{\mathbf{L}}_2 + \rho \dot{\hat{\mathbf{L}}}_2 + \dot{\mathbf{R}}_2 \quad (4.130)$$

Iteration is not necessary when Eqn (4.128) gives the correct root the first time. The line-of-sight unit vectors for solution must be greatly modified for satellites near Earth. However, this process is not acceptable trusty for routine satellite observations utilizing merely sparse data (3-5 points/pass). On the other hand, it is trustworthy for interplanetary observations once used with precise orbit determination methods [1].

#### 4.9.3. Double r-iteration

Double r-iteration is an interesting combination of numerical and dynamical techniques for solving the angle-only problem is more adapted for observations that



are far apart in which Gauss method does not work very well. Days apart observations can be solved by this method but iterations are difficult. There are four steps to find a solution: the first step connects the guesses from the available information, the second step is the actual double r-iteration that is described below and gives intermediate guesses, and the formal iterative process is done in the third step to align the times with the estimated values of the orbits. Lastly, a type of differential correction is done to determine the answer in the final step. Check Methods of Orbit Determination book of Escobal, Pedro P. ([1965] 1985,281) for hyperbolic relations, and  $t_m$  identifies the orbital motion that is (+1) for direct and (-1) for retrograde orbits and [1].

Double r-iteration formulations [1]:

$$\begin{aligned}\tau_1 &= JD_1 - JD_2 \\ \tau_3 &= JD_3 - JD_2\end{aligned}\tag{4.131}$$

Guess  $r_1$  and  $r_2$  or assume [1]

$$\begin{aligned}r_1 &= 1.0 \text{ ER} \\ r_2 &= 1.1 \text{ ER}\end{aligned}\tag{4.132}$$

Then [1],

$$c_i = 2\hat{\mathbf{L}}_i \cdot \mathbf{R}_i \quad i = 1,2\tag{4.133}$$

Loop is starting [1],

$$\rho_i = \frac{-c_i + \sqrt{c_i^2 - 4(R_i^2 - r_i^2)}}{2} \quad i = 1,2\tag{4.134}$$

$$\mathbf{r}_i = \rho_i \hat{\mathbf{L}}_i + \mathbf{R}_i \quad i = 1,2\tag{4.135}$$

$$\widehat{\mathbf{W}} = \frac{\mathbf{r}_1 \times \mathbf{r}_2}{|\mathbf{r}_1||\mathbf{r}_2|}\tag{4.136}$$

$$\rho_3 = \frac{\mathbf{R}_3 \cdot \widehat{\mathbf{W}}}{\hat{\mathbf{L}}_3 \cdot \widehat{\mathbf{W}}}\tag{4.137}$$

$$\mathbf{r}_3 = \rho_3 \hat{\mathbf{L}}_3 + \mathbf{R}_3\tag{4.138}$$

$$\begin{aligned}\cos(\Delta v_{jk}) &= \frac{\mathbf{r}_j \cdot \mathbf{r}_k}{r_j r_k} \\ \sin(\Delta v_{jk}) &= t_m \sqrt{1 - \cos^2(\Delta v_{jk})}\end{aligned} \quad j = 2,3 \text{ and } k = 1,2 \quad (4.139)$$

$$\left[ \begin{array}{lll} \text{if } \Delta v_{31} > 180^\circ \\ c_1 = \frac{r_2 \sin(\Delta v_{32})}{r_1 \sin(\Delta v_{31})} & c_3 = \frac{r_2 \sin(\Delta v_{21})}{r_3 \sin(\Delta v_{31})} & p = \frac{c_1 r_1 + c_3 r_3 - r_2}{c_1 + c_3 - 1} \\ \text{else} \\ c_1 = \frac{r_1 \sin(\Delta v_{31})}{r_2 \sin(\Delta v_{32})} & c_3 = \frac{r_1 \sin(\Delta v_{21})}{r_3 \sin(\Delta v_{32})} & p = \frac{c_3 r_3 - c_1 r_2 + r_1}{-c_1 + c_3 + 1} \end{array} \right. \quad (4.140)$$

$$e \cos(v_i) = \frac{p}{r_1} - 1 \quad i = 1,2,3 \quad (4.141)$$

$$\left[ \begin{array}{l} \text{if } \Delta v_{21} \neq 180^\circ \\ e \sin(v_2) = \frac{-\cos(\Delta v_{21}) e \cos(v_2) + e \cos(v_1)}{\sin(\Delta v_{21})} \\ \text{else} \\ e \sin(v_2) = \frac{\cos(\Delta v_{32}) e \cos(v_2) - e \cos(v_3)}{\sin(\Delta v_{31})} \end{array} \right. \quad (4.142)$$

$$e = \sqrt{(e \cos(v_2))^2 + (e \sin(v_2))^2} \quad (4.143)$$

$$a = \frac{p}{1 - e^2} \quad n = \sqrt{\frac{\mu}{a^3}} \quad (4.144)$$

$$S = \frac{r_2}{p} \sqrt{1 - e^2} e \sin(v_2) \quad C = \frac{r_2}{p} [e^2 + e \cos(v_2)] \quad (4.145)$$

$$\sin(\Delta E_{32}) = \frac{r_3}{\sqrt{ap}} \sin(\Delta v_{32}) - \frac{r_3}{p} (1 - \cos(\Delta v_{32})) S \quad (4.146)$$

$$\cos(\Delta E_{32}) = 1 - \frac{r_2 r_3}{ap} (1 - \cos(\Delta v_{32}))$$

$$\sin(\Delta E_{21}) = \frac{r_1}{\sqrt{ap}} \sin(\Delta v_{21}) + \frac{r_1}{p} (1 - \cos(\Delta v_{21})) S \quad (4.147)$$

$$\cos(\Delta E_{21}) = 1 - \frac{r_2 r_1}{ap} (1 - \cos(\Delta v_{21}))$$

$$\Delta M_{32} = \Delta E_{32} + 2S \sin^2 \left( \frac{\Delta E_{32}}{2} \right) - C \sin(\Delta E_{32}) \quad (4.148)$$

$$\Delta M_{12} = -\Delta E_{21} + 2S \sin^2\left(\frac{\Delta E_{21}}{2}\right) + C \sin(\Delta E_{21})$$

$$F_1 = \tau_1 - \frac{\Delta M_{12}}{n} \quad F_2 = \tau_3 - \frac{\Delta M_{32}}{n} \quad (4.149)$$

Estimating the accuracy of each pass yields [1]

$$Q = \sqrt{F_1^2 + F_2^2} \quad (4.150)$$

Repeat all calculations for  $F_1(r_1 + \Delta r_1, r_2)$ . Assume  $\Delta r_1 \approx 0.04r_1$  [1]

$$\begin{aligned} \frac{\partial F_1}{\partial r_1} &= \frac{F_1(r_1 + \Delta r_1, r_2) - F_1(r_1, r_2)}{\Delta r_1} \\ \frac{\partial F_2}{\partial r_1} &= \frac{F_2(r_1 + \Delta r_1, r_2) - F_2(r_1, r_2)}{\Delta r_1} \end{aligned} \quad (4.151)$$

Repeat all calculations for  $F_2(r_1 + \Delta r_1, r_2)$ . Assume  $\Delta r_1 \approx 0.04r_1$  [1]

$$\begin{aligned} \frac{\partial F_1}{\partial r_2} &= \frac{F_1(r_1, r_2 + \Delta r_2) - F_1(r_1, r_2)}{\Delta r_2} \\ \frac{\partial F_2}{\partial r_2} &= \frac{F_2(r_1, r_2 + \Delta r_2) - F_2(r_1, r_2)}{\Delta r_2} \end{aligned} \quad (4.152)$$

$$\begin{aligned} \Delta &= \frac{\partial F_1}{\partial r_1} \left( \frac{\partial F_2}{\partial r_2} \right) - \frac{\partial F_2}{\partial r_1} \left( \frac{\partial F_1}{\partial r_2} \right) \\ \Delta_1 &= \frac{\partial F_2}{\partial r_2} F_1 - \frac{\partial F_1}{\partial r_2} F_2 \end{aligned} \quad (4.153)$$

$$\Delta_2 = \frac{\partial F_1}{\partial r_1} F_2 - \frac{\partial F_2}{\partial r_1} F_1$$

$$\Delta r_1 = -\frac{\Delta_1}{\Delta} \quad \Delta r_2 = -\frac{\Delta_2}{\Delta} \quad (4.154)$$

Until converged (if not, set  $r_1 = r_1 + \Delta r_1$  and  $r_2 = r_2 + \Delta r_2$ ) [1]

$$\begin{aligned} f &= 1 - \frac{a}{r_2} (1 - \cos(\Delta E_{32})) \\ g &= \tau_3 - \sqrt{\frac{a^3}{\mu}} (\Delta E_{32} - \sin(\Delta E_{32})) \end{aligned} \quad (4.155)$$

$$\boldsymbol{v}_2 = \frac{\boldsymbol{r}_3 - f\boldsymbol{r}_2}{g} \tag{4.156}$$

## 5. EXAMPLES USING GAUSS and GIBBS METHODS

### 5.1. Telescope and Antenna Characteristics

Characteristics of telescope and antenna, which are used for optic and radar measurements in Turksat, are explained below.

- **Telescope**

Turksat Observatory is located at Turksat Main Campus since 2013 and has the biggest telescope of Ankara and special improved telescope system of Turkey. Moreover, it is only autonomous observatory of Turkey consists of observatory building and control office as shown in Figure 5.1.



**Figure 5.1: Observatory building and control office of Turksat observatory.**

Optic system specialties are professional Officina Stellare telescope with 50 cm diameter, GM4000 HPS equatorial mount, auto guider telescope with 8 cm diameter, TCS automatic focuser, FLI ProLine 4240 CCD camera with  $2048 \times 2048$  resolution.

Furthermore, filter wheel with FLI 12, Astro-Don/Badeer UBVRI and LRGBC filter sets, Celestron Nexstar 8 SE amatory telescope with 8 cm diameter for direct observations and Canon 60 DA photographic apparatus improved for astrophotography. Telescopes with 50 cm and 8 cm diameters are shown in Figure 5.2.



**Figure 5.2: Telescopes with 50 cm and 8 cm diameters.**

Properties of observatory building are 5 m diameter building area, isolated 2.5 m depth telescope bent bar from the building, Ash Dome full automation chamfer, dual openable gate system, 6 kW uninterruptible power supply, portable air conditioner and dehumidifier.

Additionally, properties of control office are 21 m<sup>2</sup> container office, meteorology station, air quality and rain sensor, 360° sky camera, air conditioner and 6 kW uninterruptible power supply.

- **Antenna**

Characteristics of antenna that was used for Turksat-3A ranging process are listed in Table 5.1.

**Table 5.1: Characteristics of Turksat-3A ranging antenna.**

<b>Polarization</b>	<b>Linear Polarization</b>		
Frequency Band	Tx: 13,95–14,5 GHz Rx: 10,70–12,75 GHz Tracking: 10,70–12,75 GHz		
Antenna Gain	Tx gain min. 60,30 dBi Rx gain min. 59,10 dBi		
Antenna Diameter	9m		
Beamwidth	-3dB	Tx: 0.15°	Rx: 0.18°
	-15 dB	Tx: 0.32°	Rx: 0.37°
G/T	37.30 dB/K (90°K LNA) 35.80 dB/K (150°K LNA)		

Turksat-3A ranging antenna is shown in Figure 5.3.



**Figure 5.3: Turksat-3A ranging antenna.**

## **5.2. Gauss and Gibbs Methods Examples**

Preliminary orbit determination can be found using Laplace method, Gauss method or double r-iteration for angle only observation. As mentioned before, Laplace method is suitable only middle point although it is close to other data points while Gauss method adjusts data to all three points and is trustworthy for all data. Moreover, double r-iteration is efficient for large spreads in data for multiple observing locations [1]. Thus, Gauss method is the most suitable for orbit determination of Turksat satellites for angle only observation.

Programming language Matlab was utilized to determine the orbit in this thesis. Right ascension data, declination data and measurement time were obtained from Turksat Observatory in Turksat Main Campus. Using latitude, longitude, elevation from sea level, measurement time as UT, right ascension and declination as input data satellites (three set of data) yielded state vector ( $r, v$ ) components of satellites. After that, orbital parameters were found easily using state vectors. Additionally, right ascension and declination were computed using azimuth and elevation data of antenna to compare telescope and antenna angular measurements.

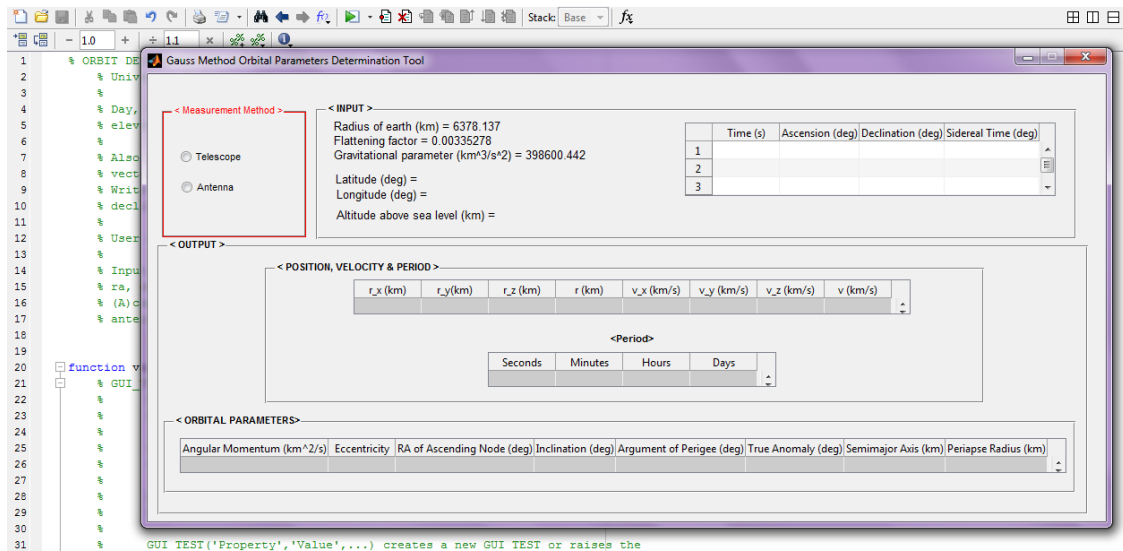


**Figure 5.4: Display image of Gauss method in the beginning.**

Display image of Gauss method in the beginning is shown in Figure 5.4 and display image of Gauss method for the results is shown in Figure 5.5.

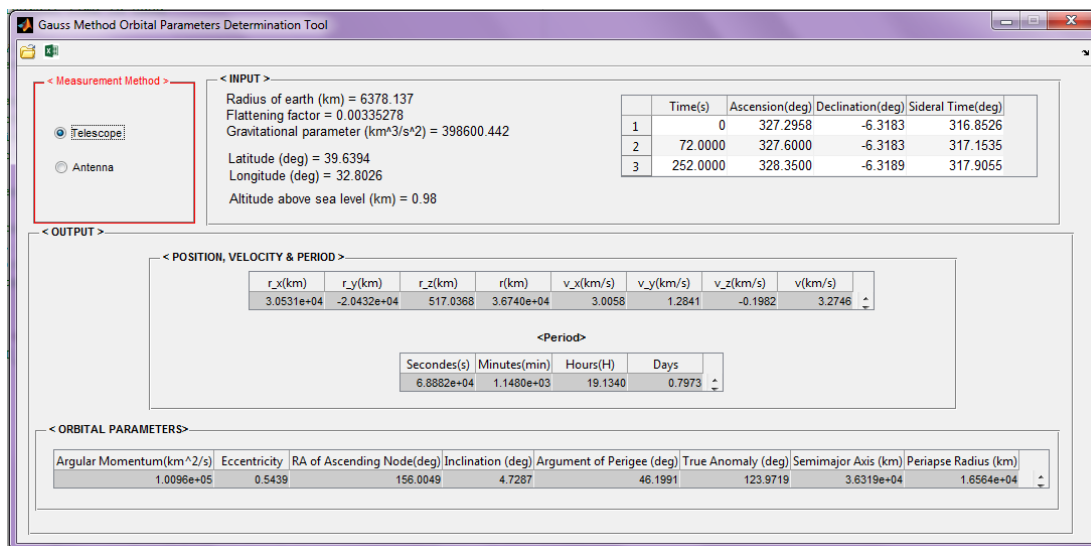


**Figure 5.5: Display image of Gauss method for the results.**

Furthermore, preliminary orbit determination with range measurements can be found using Gibbs method or Lambert's problem. Gauss developed Gauss method really to advance Lambert's problem [1]. Therefore, Gibbs method is used in thesis because Gauss method is already used and there is no need for less improved Lambert's problem.



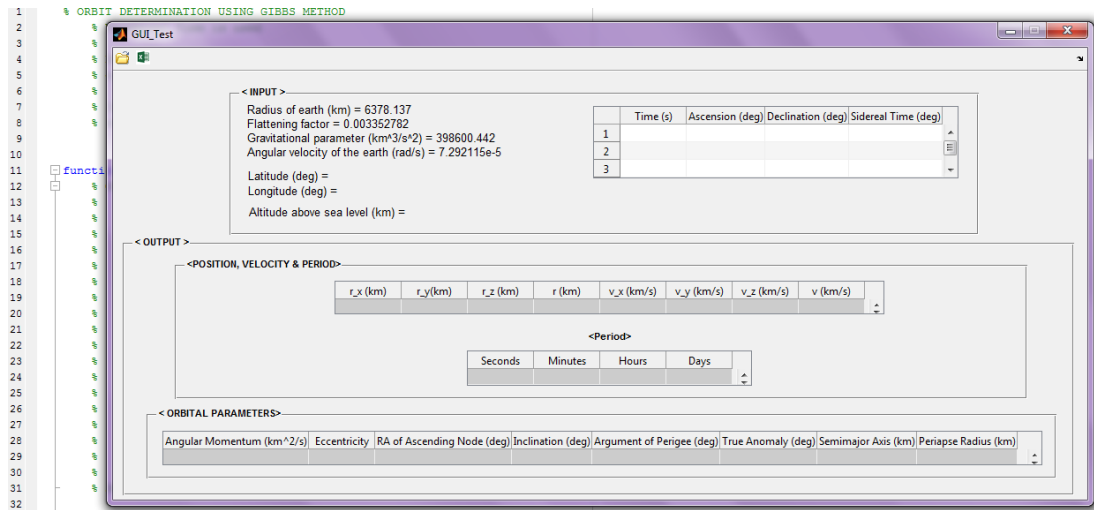


**Figure 5.6: Display image of Gibbs method in the beginning.**

This time, Turksat Satellite Control Directorate in Turksat Main Campus obtained all data from ranging antenna. Latitude, longitude, elevation from sea level and measurement time as UT, azimuth data, elevation data and slant range of satellites (three set of data are obtained by ranging) were required as input data to find state vector ( $r$ ,  $v$ ) components of satellites. Thereafter, orbital parameters were found quickly using state vectors.

Display image of Gibbs method in the beginning is shown in Figure 5.6 and display image of Gibbs method for the results is shown in Figure 5.7.

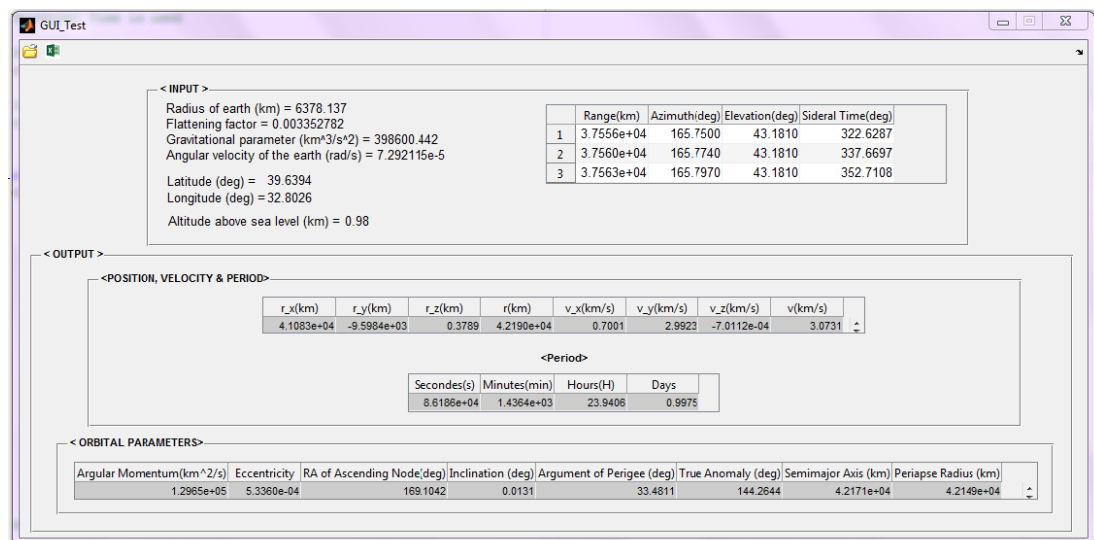


**Figure 5.7: Display image of Gibbs method for the results.**

Additionally, a free open source planetarium software Stellarium, that shows 3D simulation of sky and gives angle and position data, was used to compare results that

were calculated using the measured data in Turksat. Display image of Stellarium software for Turksat-3A is shown in Figure 5.8 [33].



**Figure 5.8: Display image of Stellarium software for Turksat-3A [33].**

International Space Station (ISS) was used as a reference target to control the accuracy of Stellarium. State vector values were compared for same specific time according to National Aeronautics and Space Administration (NASA) and Stellarium [33], [34].

#### Ground track



This map shows the ground track of the International Space Station's next orbit. The crosshair marks its current position.

The blue sections of the ISS' track indicate when the space station is in the earth's shadow. The red sections mark when the ISS is sunlit.

updated: November 17, 2015  
 URL: [iss.astroviewer.net](http://iss.astroviewer.net) | © 2008-2014 by Dirk Matussek  
 Orbital data provided by NASA | Layout based on YAML  
 AstroViewer® is a registered trademark  
 Imprint

**Figure 5.9: ISS orbit according to NASA [34].**

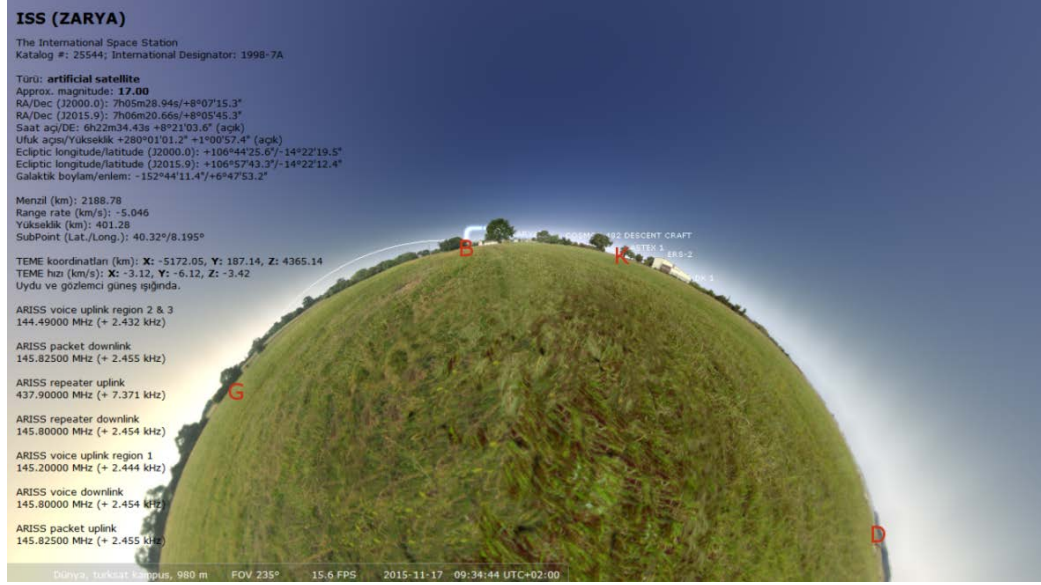


**Figure 5.10: ISS orbit according to Stellarium [33].**

Display of ISS orbit according to NASA and Stellarium at 07:34:44 UTC on 17 November 2015 are seen in Figure 5.9 and Figure 5.10. Moreover, comparison of ISS orbit is seen in Table 5.2.

**Table 5.2: ISS orbit comparison.**

	NASA	Stellarium
<b>r (km)</b>	401	392,3556
<b>v (km/s)</b>	7,677	7,674

Error of Stellarium according to NASA data was 2,156 % for  $r$  and 0,333 % for  $v$ . Error level is acceptable for preliminary orbit determination, so Stellarium can be used to obtain data for preliminary orbit determination.

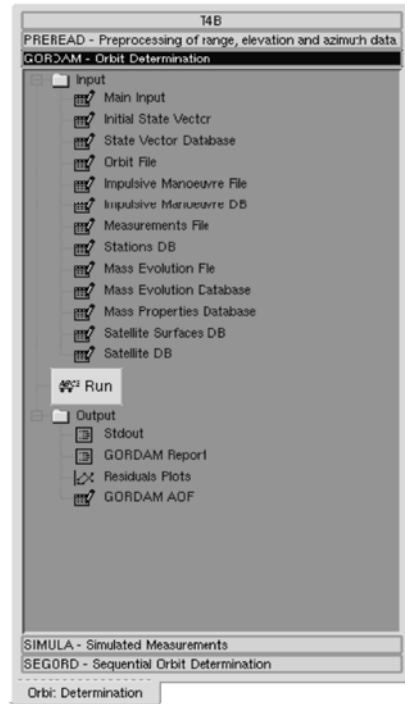


**Figure 5.11: Display image of GORDAM software [35].**

Furthermore, Turksat uses orbit determination software GORDAM that is a product of GMV Innovating Solutions. Additionally, GORDAM was utilized for comparison. An iterated least squares fit of a numerically integrated orbit to the pre-processed tracking data is applied to determine the orbit in GORDAM. Display image of GORDAM software is shown in Figure 5.11 [35]. Least square method is a precise orbit determination method and uses more than three set of measuring data for least square method, so its results are the best in comparison with preliminary orbit determination methods. In other words, the more measuring data used the more results are sensitive.

All Turksat satellites are placed in GEO and characteristic of GEO satellites are shown in Table 5.3 to compare the found results. Preliminary orbit determination results are used as an initial condition to improve precise orbit determination results. Thus, aim of this thesis is to try finding results as close as possible to Table 5.3. Therefore, the results can be utilized as an initial condition for future works.

**Table 5.3: Characteristic of GEO satellite.**

<b>r and semimajor axis (km)</b>	<b>42150 – 42180</b>
<b>v (km/s)</b>	<b>~3,07</b>
<b>Eccentricity</b>	<b>0,00010 – 0,00055</b>
<b>Inclination (deg)</b>	<b>0 – 0,09</b>

In first example, Turksat Observatory personnel measured Turksat-4A satellite using telescope, and Stellarium data for same satellite at same specific time was obtained. Telescope measuring data and Stellarium data was utilized to find state vectors and orbital parameters using Gauss method. Moreover, GORDAM orbital parameter results were acquired from Turksat Satellite Control Directorate.

As shown in Table 5.4 and Table 5.5, Stellarium data gives better results according to Table 5.3 because it is independent of weather conditions and human errors. However, telescope results are also very good for preliminary orbit determination and close to Stellarium results. Telescope error with respect to Stellarium was 0,0991 % for  $r$  and 0,161 % for  $v$ .

**Table 5.4: State vectors of Turksat-4A on 20 October 2015.**

	TELESCOPE	STELLARIUM
$r_x$ (km)	23323,49	39841,74
$r_y$ (km)	35029,97	13683,82
$r_z$ (km)	-105,558	-0,78615
<b><math>r</math> (km)</b>	42084,38	42126,13
$v_x$ (km/s)	-2,55001	-0,99364
$v_y$ (km/s)	1,700378	2,904628
$v_z$ (km/s)	0,008139	-0,00072
<b><math>v</math> (km/s)</b>	3,064946	3,069884

Stellarium results were closer than telescope results to GORDAM, as shown in Table 5.5, because Stellarium is independent from weather conditions and human errors. As a result, of course, Gauss method is not as good as like least square, but it can be used for preliminary orbit determination in condition angle only observations.

**Table 5.5: Orbital parameters of Turksat-4A on 20 October 2015.**

	TELESCOPE	STELLARIUM	GORDAM
Angular Momentum (km <sup>2</sup> /s)	128986,3	129322,2	
<b>Eccentricity</b>	0,008218	0,004186	0,0004374912750
RA of Ascending Node (deg)	99,69244	194,4152	262,81063597907
<b>Inclination (deg)</b>	0,20936	0,013508	0,0610662536364
Argument of Perigee (deg)	141,3863	21,44771	330,47306327290
True Anomaly (deg)	175,2647	163,0924	
<b>Semimajor Axis (km)</b>	41742,55	41958,14	42164,704568070
Periapse Radius (km)	41399,53	41782,49	

In second example, same method was followed for Turksat-3A as shown in Table 5.6 and Table 5.7.

**Table 5.6: State vectors of Turksat-3A on 20 October 2015.**

	<b>TELESCOPE</b>	<b>STELLARIUM</b>
r_x (km)	41992,7951	41731,1556
r_y (km)	4217,2669	-2185,60622
r_z (km)	-133,66061	-245,540285
<b>r (km)</b>	42204,242	41789,0717
v_x (km/s)	-0,4684828	0,09423015
v_y (km/s)	3,02423967	3,04452053
v_z (km/s)	0,01807553	-0,00442245
<b>v (km/s)</b>	3,0603641	3,04598163

**Table 5.7: Orbital parameters of Turksat-3A on 20 October 2015.**

	<b>TELESCOPE</b>	<b>STELLARIUM</b>	<b>GORDAM</b>
Angular Momentum (km <sup>2</sup> /s)	128974,8	127259,7	
<b>Eccentricity</b>	0,054229	0,034666	0,00046822077
RA of Ascending Node (deg)	34,60112	102,0337	147,598670738
<b>Inclination (deg)</b>	0,375863	0,348582	0,05482261972
Argument of Perigee (deg)	73,03467	38,12678	46,7281519603
True Anomaly (deg)	258,0986	216,8418	
<b>Semimajor Axis (km)</b>	41855,33	40678,6	42166,3091798
Periapse Radius (km)	39585,54	39268,43	

Similarly, Stellarium data was better than telescope because it is independent of weather conditions and human errors. Additionally, Turksat-4A results were closer to Table 5.3 than Turksat-3A results.

In third example, Turksat Satellite Control Directorate personnel measured Turksat-3A satellite using the ranging antenna. Normally, antenna measures slant range, azimuth and elevation of satellite, but right ascension and declination can be found from azimuth and elevation via transformation matrix. Thus, antenna right ascension and elevation data can be used for Gauss method. Therefore, Gauss and Gibbs methods can be compared using antenna data. In addition, GORDAM orbital parameter results were acquired from Turksat Satellite Control Directorate.

As shown in Table 5.8 and Table 5.9, Gibbs method gives better results than Gauss method. Inclination is just in range for Gauss while eccentricity, inclination and semimajor axis are in range for Gibbs according to Table 5.3.

**Table 5.8: State vectors of Turksat-3A on 26 October 2015.**

	<b>GAUSS</b>	<b>GIBBS</b>
r_x (km)	40798,32	41083,25
r_y (km)	-9537,12	-9598,41
r_z (km)	26,83011	0,37895
<b>r (km)</b>	41898,21	42189,6
v_x (km/s)	0,694773	0,700076
v_y (km/s)	2,974125	2,992263
v_z (km/s)	-0,0019	-0,0007
<b>v (km/s)</b>	3,054199	3,073068

**Table 5.9: Orbital parameters of Turksat-3A on 26 October 2015.**

	<b>GAUSS</b>	<b>GIBBS</b>	<b>GORDAM</b>
Angular Momentum (km <sup>2</sup> /s)	127965,5	129651,5	
<b>Eccentricity</b>	0,01949	0,000534	0,0004292539670
RA of Ascending Node (deg)	212,6683	169,1042	141,90827579711
<b>Inclination (deg)</b>	0,051156	0,013082	0,0620349031876
Argument of Perigee (deg)	313,745	33,4811	56,398103273979
True Anomaly (deg)	180,4293	144,2644	
<b>Semimajor Axis (km)</b>	41097,25	42171,34	42165,697566675
Periapse Radius (km)	40296,27	42148,84	

Gibbs results were quite close to GORDAM results, because ranging value was used. However, both results can be acceptable and are good results for preliminary orbit determination.

In forth example, Stellarium data was obtained like antenna and telescope to use Gauss method at same specific time for Turksat-2A. Likewise, Stellarium state vector data was used to calculate orbital parameters. Thus, telescope and antenna data, so right ascension-declination and azimuth-elevation can be compared with Gauss method.

As shown in Table 5.10 and Table 5.11, antenna results are closer to Stellarium results than telescope results. Antenna error according to Stellarium was 0,137% for  $r$  and -0,761% for  $v$  while telescope error according to Stellarium was -0,018% for  $r$  and -0,971% for  $v$ . Nevertheless, both results can be acceptable and are good results for preliminary orbit determination. Moreover, Stellarium results were considerably close to the GORDAM results.

**Table 5.10: State vectors of Turksat-2A on 20 October 2015.**

	ANTENNA	TELESCOPE	STELLARIUM
r_x (km)	35928,69	36186,72	35979,21
r_y (km)	-21958	-22261	-21986
r_z (km)	-17,5531	-120,588	-24,78
<b>r (km)</b>	42107,32	42485,82	42165,00
v_x (km/s)	1,603545	1,624782	1,60
v_y (km/s)	2,618591	2,639858	2,62
v_z (km/s)	0,000277	-0,00167	0,00
<b>v (km/s)</b>	3,070566	3,099801	3,07

**Table 5.11: Orbital parameters of Turksat-2A on 20 October 2015.**

	ANTENNA	TELESCOPE	STELLARIUM	GORDAM
Angular Momentum (km <sup>2</sup> /s)	129293,3	131697,6	129443	
<b>Eccentricity</b>	0,004102	0,024176	0,003074	0.00029313
RA of Ascending Node (deg)	46,32935	69,12573	58,5881	37.0459739
<b>Inclination (deg)</b>	0,02444	0,165515	0,033672	0.04461375
Argument of Perigee (deg)	114,6172	258,7246	84,7324	178.103632
True Anomaly (deg)	167,622	0,551132	185,251	
<b>Semimajor Axis (km)</b>	41939,32	43538,34	42036,30	42166.3467

In fifth example, Turksat Observatory personnel measured Turksat-3A on 13 August 2015. As mentioned before, Gauss method works robust especially once data is separated by 10° or less (so by 40 minutes or less). Thus, state vectors, eccentricity and inclination results for short time period (at 19:33:38, 19:40:42 and 19:50:16) and long time period (at 19:33:38, 20:17:22 and 21:08:31) were compared to show sensibility to time period between three measurement data in Table 5.12. As expected, state vectors and inclination are within the boundaries according to Table 5.3 for short time period. Moreover, short time period results are better than long time period results. Short time period data should be used to obtain better results for Gauss method.



**Table 5.12: Short time period and long time period on 13 August 2015.**

	<b>Short time period</b>	<b>Long time period</b>
<b>r (km)</b>	42159,3	40952,74
<b>v (km/s)</b>	3,072757	2,98388
<b>Eccentricity</b>	0,014371	0,085261
<b>Inclination (deg)</b>	0,07038	0,185686

For last example, Turksat Observatory personnel measured Russian communication satellite Cosmos 2397 in GEO while measured Turksat satellites [36]. Cosmos 2397 was out of control and closed to Turksat satellites at that date. Fortunately, collision did not happen. As shown in Table 5.13 and Table 5.14, although state vectors are quite close values to the GEO satellite values, orbital parameters are not close the real values. However, results are acceptable for preliminary orbit determination.

**Table 5.13: State vectors of Cosmos 2397 on 20 October 2015.**

<b>r_x (km)</b>	<b>41992,8</b>
r_y (km)	4217,267
r_z (km)	-133,661
<b>r (km)</b>	42204,24
v_x (km/s)	-0,46848
v_y (km/s)	3,02424
v_z (km/s)	0,018076
<b>v (km/s)</b>	3,060364

**Table 5.14: Orbital parameters of Cosmos 2397 on 20 October 2015.**

<b>Angular Momentum (km<sup>2</sup>/s)</b>	<b>128974,8</b>
<b>Eccentricity</b>	0,054229
RA of Ascending Node (deg)	34,60112
<b>Inclination (deg)</b>	0,375863
Argument of Perigee (deg)	73,03467
True Anomaly (deg)	258,0986
<b>Semimajor Axis (km)</b>	41855,33
Periapse Radius (km)	39585,54

Due to perturbations or out of control conditions of satellite, other satellites can be closer to Turksat satellites and so collision can be occurred. Satellite maneuver should be needed to prevent collision, so Turksat satellite region should be observed to make collision prediction.

Antenna send signal to own satellite to measure range value, however signal cannot be sent to other satellites. Thus, orbit of other satellites only can be determined using

telescope. Data that are more sensible can be obtained using high resolution and automatic telescope. As a consequence, preliminary orbit determination should be done before precise orbit determination to improve results as done in this thesis.

## **6. CONCLUSION AND RECOMMENDATIONS**

Preliminary orbit determination subject via optical and radar systems was studied in this thesis. Gauss and Gibbs methods were used to estimate state vectors and orbital parameters to determine the orbit of satellite. Moreover, data obtained from open source Stellarium software was utilized to compare real measurement results. In addition, GORDAM software that is utilized by Turksat to determine orbit with least square method was used for comparison. Gauss method is the best fit to the telescope measurements while Gibbs method is the best for antenna measurements in the case of preliminary orbit determination.

Weather conditions and sensibility of telescope are very important for optical measurements. Gibbs method gives more sensible results than Gauss method because antenna is more accurate than telescope and ranging value is used. Likewise, human errors are formed due to manual usage of telescope. Stellarium input data always gives fairly good results according to the used telescope because it is independent from weather conditions and human errors. GORDAM results are the best because a precise orbit determination method (least square method) is used. Gauss method works robust especially once data is separated by  $10^\circ$  or less (so by 40 minutes or less). Thus, short period time measurements give better results. Consequently, Gauss method is the best method for angle only observations while Gibbs method is the best method for ranging data in order to determine preliminary orbit.

Precise orbit determination methods can be studied to obtain more sensible results using preliminary orbit determination results as initial conditions for future works. More measuring data should be used to find results that are more sensitive. Orbit trajectory can be drawn to prepare a visual presentation. Software can be integrated to the telescope to see the results immediately. High resolution and automatic telescope can be used to obtain more sensitive data.



## REFERENCES

- [1] **Vallado, D.A.** (2004). *Fundamentals of Astrodynamics and Applications*. Mc Graw-Hill.
- [2] **Xu, T.H., Jiang, N., Sun, Z.Z.** (2012). An improved adaptive Sage filter with applications in GEO orbit determination and GPS kinematic positioning. *Science China*, 55, 892-898.
- [3] **Martin Mur, T.J. & Dow, J.M.** (1997). Satellite navigation using GPS. *ESA Bulletin Nr.*, 90.
- [4] **Wettergren, J., Bonnedal, M., Ingvarson, P., Wastberg, B.** (2009). Antenna for precise orbit determination. *Acta Astronautica*, 65, 1765–1771.
- [5] **Aydın Duru, S.** (2015). *Uydu ve uzay çöplerinin yörüngelerinin yerdeki optic sistemlerle tespiti ve doğrulanması*. (Yüksek lisans tezi). Ankara Üniversitesi, Fen Bilimleri Enstitüsü, Ankara.
- [6] **Abacı, H.** (2008). *Uydu yörünge benzetimi ve yörünge kestirimi*. (Yüksek lisans tezi). Hacettepe Üniversitesi, Fen Bilimleri Enstitüsü, Ankara.
- [7] **Arroyo, V., Cordero, A., Torregrosa, J.R., Vassileva, M.P.** (2015). Artificial satellites preliminary orbit determination by the modified high order Gauss method. *International Journal of Computer Mathematics*, 89:3, 347-356.
- [8] **Montejo, F.J., Lopez Moratalla, T., Abad, C.** (2010). Astrometric positioning and orbit determination of geostationary satellites. *Advances in Space Research*, 47, 1043–1053.
- [9] **Cao, F., Yang, X., Li, Z., Sun, B., Kong, Y., Chen, L., Feng, C.** (2014). Orbit determination and prediction of GEO satellite of BeiDou during repositioning maneuver. *Advances in Space Research*, 54, 1828–1837.
- [10] **Hinagawa, H., Yamaoka, H., Hanada, T.** (2013). Orbit determination by genetic algorithm and application to GEO observation. *Advances in Space Research*, 53, 532–542.
- [11] **Lei, H., Li, Z.G., Yang, X.H., ... Feng, C.G.** (2011). Geostationary orbit determination using SATRE. *Advances in Space Research*, 48, 923–932.
- [12] **Yoshikawa, M., Kawaguchi, J. Yamakawa, H., ... Ishibashi, S.** (2005). Summary of the orbit determination of NOZOMI spacecraft for all the mission period. *Acta Astronautica*, 57, 510 – 519.
- [13] **Guo, R., Hu, X.G., ... He, F.** (2010). Orbit determination for geostationary satellites with the combination of transfer ranging and pseudorange data. *Science China*, 53:9, 1746–1754.

- [14] **Yang, Y., Yang, X.H., Li, Z.G., Feng, C.G.** (2013). Satellite orbit determination combining C-band ranging and differenced ranges by transfer. *Chinese Science Bulletin*, 58:19, 2323-2328.
- [15] **Zhao, G., Zhou, X.H., Wu, B.** (2012). Precise orbit determination of Haiyang-2 using satellite laser ranging. *Chinese Science Bulletin*, 58:6, 589-597.
- [16] **Wang, X.** (2013). A robust method of preliminary orbit determination. *Chinese Astronomy and Astrophysics*, 37, 455–463.
- [17] **Mander, A., Bisnath, S.** (2013). GPS-based precise orbit determination of Low Earth Orbiters with limited resources. *Springer-Verlag Berlin Heidelberg*, 17, 587–594.
- [18] **Helleputte, T.V., Visser, P.** (2008). GPS based orbit determination using accelerometer data. *Aerospace Science and Technology*, 12, 478–484.
- [19] **Hugentobler, U., Beutler, G.** (2003). Strategies for precise orbit determination of low earth orbiters using the GPS. *Space Science Reviews*, 108, 17–26.
- [20] **Giannitrapani, A., Ceccarelli, N., Scortecchi, F., Garulli, A.** (2011). Comparison of EKF and UKF for spacecraft localization via angle measurements. *IEEE TRANSACTIONS ON AEROSPACE AND ELECTRONIC SYSTEMS*, 47:1.
- [21] **Dainty, C.B., Raquet, J., Beckman, C.R.** (2007). Improving Geostationary Satellite GPS Positioning Error Using Dynamic Two-Way Time Transfer Measurements. *39th Annual Precise Time and Time Interval (PTTI) Meeting*, Long Beach, CA : November 26-29.
- [22] **Mikhailov, N.V., Vasil'ev, M.V.** (2011). Autonomous satellite orbit determination using spaceborne GNSS receivers. *Gyroscopy and Navigation*, 2: 1, 1–9.
- [23] **Hwang, Y., Lee, B.S., Kim, H.Y., Kim, H., Kim, J.** (2008). Orbit determination accuracy improvement for geostationary satellite with single station antenna tracking data. *ETRI Journal*, 30:6.
- [24] **Wu, S., Liu, Y.Y., Liu, L. Guo, R., He, F., Li, X.J., Huang, H.** (2012). Precise orbit determination of GEO satellite based on helmert variance component estimation method. *Springer-Verlag Berlin Heidelberg*.
- [25] **Jia, P.Z., Xiong, Y.Q.** (2006). An orbit determination algorithm by means of the satellite-borne GPS data and Kalman filter. *Elsevier B. V.* doi: 10.1016/j.chinastron.2006.04.008.
- [26] **Lee, B.S., Yoon, J.C., Hwang, Y., Kim, J.** (2005). Orbit determination system for the KOMPSAT-2 using GPS measurement data. *Acta Astronautica*, 57, 747 – 753.
- [27] **Choi, J., Jo, J. H., Roh, K. M., Son, J. Y., Kim, M. J., Choi, Y. J., .... Pavlis, E. C.** (2015). Analysis of the angle-only orbit determination for optical tracking strategy of Korea GEO satellite, COMS. *Advance in Space Research*, 56, 1056-1066.
- [28] **Montenbruck, O. & Gill, E.** (2001). *Satellite Orbits: Models, Methods, and Applications*. Springer-Verlag Berlin Heidelberg New York.

- [29] **Scire, G., Santoni, F., Piergentili, F.** (2015). Analysis of orbit determination for space based optical space surveillance system. *Advances in Space Research*, 56, 421–428.
- [30] **Gronchi, G.F.** (2009). Multiple solutions in preliminary orbit determination from three observations. *Celest Mech Dyn Astr*, 103, 301–326.
- [31] **Url-1** <https://www.turksat.com.tr/tr/uydu/turksat-uydu/uydularimiz>, date retrieved: 27.07.2015.
- [32] **Curtis, H.D.** (2014). *Orbital Mechanics for Engineering Mechanics*. Elsevier Ltd.
- [33] **Url-2** <http://www.stellarium.org/tr/>, date retrieved: 13.11.2015.
- [34] **Url-3** <http://iss.astroviewer.net/>, date retrieved: 17.11.2015.
- [35] **Turksat.** (2012). TK4 ground gystem, FDS training [PowerPoint slides].
- [36] **Url-4** <http://nssdc.gsfc.nasa.gov/nmc/masterCatalog.do?sc=2003-015A>, date retrieved: 17.11.2015.





## APPENDICES

### APPENDIX A: GAUSS METHOD

```
% ORBIT DETERMINATION USING GAUSS METHOD

% Universal Time is used

% Day, Time, right ascension, declination, latitude, longitude
and elevation of observation site are used to compute state vectors

% Also azimuth and elevation of antenna can be used to compute
state vectors. Transformation is done from Azimuth-elevation to ra-
dec.

% Write azimuth and elevation instead of right ascension and
declination in input notepad

% User firstly must select measurement metot (telescope or
antenna)

% Input data must be written in notepad as a(does not have a
meaning), day (D-M-Y), time (H-M-S), ra, dec, latitude (phi),
longitude (EW), H, respectively. Azimuth(A)and elevation (a) must
be written instead of ra and dec for antenna selection
function varargout = GUI_Test(varargin)

% GUI_TEST MATLAB code for GUI_Test.fig

%     GUI_TEST, by itself, creates a new GUI_TEST or raises the
existing singleton*.

%     H = GUI_TEST returns the handle to a new GUI_TEST or the
handle to the existing singleton*.

%     GUI_TEST('CALLBACK',hObject,eventData,handles,...) calls
the local function named CALLBACK in GUI_TEST.M with the given input
arguments.

%     GUI_TEST('Property','Value',...) creates a new GUI_TEST
or raises the existing singleton*. Starting from the left, property
value pairs are applied to the GUI before GUI_Test_OpeningFcn gets
called. An unrecognized property name or invalid value makes
property application stop. All inputs are passed to
GUI_Test_OpeningFcn via varargin.

%     *See GUI Options on GUIDE's Tools menu. Choose "GUI
allows only one instance to run (singleton)".

% See also: GUIDE, GUIDATA, GUIHANDLES

% Edit the above text to modify the response to help GUI_Test

% Last Modified by GUIDE v2.5 30-Sep-2015 11:42:15

% Begin initialization code - DO NOT EDIT

gui_Singleton = 1;
gui_State = struct('gui_Name',       mfilename, ...
                  'gui_Singleton',   gui_Singleton, ...
                  'gui_OpeningFcn',  @GUI_Test_OpeningFcn, ...
                  'gui_OutputFcn',   @GUI_Test_OutputFcn, ...
                  'gui_LayoutFcn',   [] , ...
```

```

        'gui_Callback', []);
    if nargin && ischar(varargin{1})
        gui_State.gui_Callback = str2func(varargin{1});
    end
    if nargin
        [varargout{1:nargout}] = gui_mainfcn(gui_State,
varargin{:});
    else
        gui_mainfcn(gui_State, varargin{:});
    end
    % End initialization code - DO NOT EDIT
    % --- Executes just before GUI_Test is made visible.
    function GUI_Test_OpeningFcn(hObject, eventdata, handles,
varargin)
        % This function has no output args, see OutputFcn.
        % hObject    handle to figure
        % eventdata  reserved - to be defined in a future version of
MATLAB
        % handles     structure with handles and user data (see
GUIDATA)
        % varargin    command line arguments to GUI_Test (see
VARARGIN)
        % Choose default command line output for GUI_Test
        handles.output = hObject;
        % Update handles structure
        guidata(hObject, handles);
        % UIWAIT makes GUI_Test wait for user response (see
UIRESUME)
        % uiwait(handles.figure1);
    end
    % --- Outputs from this function are returned to the command
line.
    function varargout = GUI_Test_OutputFcn(hObject, eventdata,
handles)
        % varargout    cell array for returning output args (see
VARARGOUT);
        % hObject    handle to figure
        % eventdata  reserved - to be defined in a future version of
MATLAB
        % handles     structure with handles and user data (see GUIDATA)
        % Get default command line output from handles structure
        varargout{1} = handles.output;
    end
end
end

```

```

% ~~~~~~
%{
This program uses Algorithms 5.5 (Gauss's method) to compute
the state vector from the data provided in Example 5.11.
deg - factor for converting between degrees and radians
pi - 3.1415926...
mu - gravitational parameter (km^3/s^2)
Re - earth's radius (km)
f - earth's flattening factor
H - elevation of observation site (km)
phi - latitude of site (deg)
t - vector of observation times t1, t2, t3 (s)
ra - vector of topocentric equatorial right ascensions
at t1, t2, t3 (deg)
dec - vector of topocentric equatorial right declinations
at t1, t2, t3 (deg)
theta - vector of local sidereal times for t1, t2, t3 (deg)
R - matrix of site position vectors at t1, t2, t3 (km)
rho - matrix of direction cosine vectors at t1, t2, t3
fac1, fac2 - common factors
r, v - the state vector (km, km/s)
coe - vector of orbital elements for r, v:
[h, e, RA, incl, w, TA, a]
where h = angular momentum (km^2/s)
e = eccentricity
incl = inclination (rad)
w = argument of perigee (rad)
TA = true anomaly (rad)
a = semimajor axis (km)
User M-functions required: gauss, coe_from_sv
%}
% -----
function [v0,v1,v2,v3,v4 ] = Calculate(input_args)
%UNTITLED Summary of this function goes here
% Detailed explanation goes here
global mu
global H
global phi
global deg
global EL

```

```

global Method
deg = pi/180;
mu = 398600.442;
Re = 6378.137;
f = 1/298.256;
C=input_args;
%...Data declaration for Example 5.11 of Curtis:
H = C(1,12);
phi = C(1,10)*deg;
ra_1 =C(1,8) *deg;
ra_2 = C(2,8) *deg;
ra_3 = C(3,8) *deg;
dec_1 = C(1,9) *deg;
dec_2 = C(2,9) *deg;
dec_3 = C(3,9) *deg;
%...
% Date:
year_1 = C(1,4);
month_1 = C(1,3);
day_1 = C(1,2);
year_2 = C(2,4);
month_2 = C(2,3);
day_2 = C(2,2);
year_3 = C(3,4);
month_3 = C(3,3);
day_3 = C(3,2);
% Universal time: Local Time-3
hour_1 =C(1,5);
minute_1 =C(1,6);
second_1 = C(1,7);
hour_2 =C(2,5);
minute_2 = C(2,6);
second_2 = C(2,7);
hour_3 =C(3,5);
minute_3 = C(3,6);
second_3 = C(3,7);
%...Convert negative (west) longitude to east longitude:
% if degrees < 0
% degrees = degrees + 360;
% end

```

```

%...Express the longitudes as decimal numbers:
EL=C(1,11);
WL = 360 - EL;

%...Express universal time as a decimal number:
ut_1 = hour_1 + minute_1/60 + second_1/3600;
ut_2 = hour_2 + minute_2/60 + second_2/3600;
ut_3 = hour_3 + minute_3/60 + second_3/3600;

%...Equation 5.46 :
j0_1 = J0(year_1, month_1, day_1);
j0_2 = J0(year_2, month_2, day_2);
j0_3 = J0(year_3, month_3, day_3);

%...Equation 5.47 Julian day number:
jd_1 = j0_1 + ut_1/24;
jd_2 = j0_2 + ut_2/24;
jd_3 = j0_3 + ut_3/24;

%...Algorithm 5.3:
lst_1 = LST(year_1, month_1, day_1, ut_1, EL);
lst_2 = LST(year_2, month_2, day_2, ut_2, EL);
lst_3 = LST(year_3, month_3, day_3, ut_3, EL);

%...Seconds of date
Seconds_1 = 0;
Seconds_2 = (jd_2-jd_1)*86400;
Seconds_3 = (jd_3-jd_1)*86400;

%...Data declaration for Example 5.11:
t = [ Seconds_1 Seconds_2 Seconds_3];
theta = [ lst_1 lst_2 lst_3]*deg;
ra = [ ra_1 ra_2 ra_3];
dec = [dec_1 dec_2 dec_3];

%...
fac1 = Re/sqrt(1-(2*f - f*f)*sin(phi)^2);
fac2 = (Re*(1-f)^2/sqrt(1-(2*f - f*f)*sin(phi)^2) + H)*sin(phi);
for i = 1:3
    R(i,1) = (fac1 + H)*cos(phi)*cos(theta(i));
    R(i,2) = (fac1 + H)*cos(phi)*sin(theta(i));
    R(i,3) = fac2;
end

% If datas are coming from antenna azimuth and elevation
if Method==1
    [ra,dec]=AzEl2RaDec (ra,dec,theta,phi,R)
end

```

```

    for i = 1:3
        rho(i,1) = cos(dec(i))*cos(ra(i));
        rho(i,2) = cos(dec(i))*sin(ra(i));
        rho(i,3) = sin(dec(i));
    end
%...Algorithms 5.5 and 5.6:
    [r, v] = gauss(rho(1,:), rho(2,:), rho(3,:), ...
        R(1,:), R(2,:), R(3,:), ...
        t(1), t(2), t(3));
%...Algorithm 4.2 for the initial estimate of the state vector
% and for the iteratively improved one:
    coe = coe_from_sv(r,v,mu);
%...Echo the input data and output the solution to
% the command window:
fprintf('-----')
fprintf('\n  Example 5.11: Orbit determination by the Gauss
method\n')
fprintf('\n Radius of earth (km) = %g', Re)
fprintf('\n Flattening factor = %g', f)
fprintf('\n Gravitational parameter (km^3/s^2) = %g', mu)
fprintf('\n\n Input data:\n');
fprintf('\n Latitude (deg) = %g', phi/deg);
fprintf('\n Altitude above sea level (km) = %g', H);
fprintf('\n\n Observations:')
fprintf('\n Right')
fprintf(' Local')
fprintf('\n Time (s) Ascension (deg) Declination (deg)')
fprintf(' Sidereal time (deg)')
for i = 1:3
    fprintf('\n %9.4g %11.4f %19.4f %20.4f', ...
        t(i), ra(i)/deg, dec(i)/deg, theta(i)/deg)
end
fprintf('\n\n Solution:\n')
fprintf('\n');
fprintf('\n r (km) = [%g, %g, %g]', ...
    r(1), r(2), r(3))
fprintf('\n v (km/s) = [%g, %g, %g]', ...
    v(1), v(2), v(3))
fprintf('\n');
fprintf('\n Angular momentum (km^2/s) = %g', coe(1))
fprintf('\n Eccentricity = %g', coe(2))

```

```

fprintf('\n RA of ascending node (deg) = %g', coe(3)/deg)
fprintf('\n Inclination (deg) = %g', coe(4)/deg)
fprintf('\n Argument of perigee (deg) = %g', coe(5)/deg)
fprintf('\n True anomaly (deg) = %g', coe(6)/deg)
fprintf('\n Semimajor axis (km) = %g', coe(7))
fprintf('\n Periapse radius (km) = %g', coe(1)^2 ...
/mu/(1 + coe(2)))
%...If the orbit is an ellipse, output the period:
if coe(2)<1
    T1 = 2*pi/sqrt(mu)*coe(7)^1.5;
    fprintf('\n Period:')
    fprintf('\n Seconds = %g', T1)
    fprintf('\n Minutes = %g', T1/60)
    fprintf('\n Hours = %g', T1/3600)
    fprintf('\n Days = %g', T1/24/3600)
else
    fprintf('\n Period:Undefined(Orbit is parabola or hyperbola')
end
fprintf('\n-----\n')
% ~~~~~~
global mes
global yes
global res
global tes
mes=[t;ra/deg;dec/deg;theta/deg]';
yes=[r,norm(r),v, norm(v)];
if coe(2)<1
    res=[T1,T1/60,T1/3600,T1/24/3600];
else
    res=[NaN,NaN,NaN,NaN];
end
tes=[coe(1),coe(2),coe(3)/deg,coe(4)/deg,coe(5)/deg,coe(6)/deg,coe(7)
),coe(1)^2/mu/(1 + coe(2))];
% H,phi/deg,t,ra,dec,theta,coe_old,r_old,v_old,norm (r_old), norm
(v_old),coe,r,v, norm (r), norm (v),T1,T2)
v1=mes;
v2=yes;
v3=res;
v4=tes;
v0=[H,phi/deg,EL];
end

```

```

% -----
--
function OpenFile_ClickedCallback(hObject, eventdata, handles)
% hObject    handle to OpenFile (see GCBO)
% eventdata  reserved - to be defined in a future version of MATLAB
% handles    structure with handles and user data (see GUIDATA)
%           jScrollPane = handles.time_table.jScrollPane;
%           set(jScrollPane,'VerticalScrollBarPolicy',21); % or:
%           jScrollPane.VERTICAL_SCROLLBAR_NEVER
%           jScrollPane.setHorizontalScrollBarPolicy(31); % or:
%           jScrollPane.HORIZONTAL_SCROLLBAR_NEVER
%           jScrollPane.setViewportView;
%           jEditbox = jScrollPane.getComponent(0);
%           jEditbox.setWrapping(false); % do *NOT* use set(...)!!!

global filename
global pName

[filename,pName] = uigetfile('*.txt','Select Your Data
Set');

formatSpec = '%s %u %u %u %u %u %f %f %f %f %f %f';
sizeA = [12 3];
fileID = fopen(filename);
C = fscanf(fileID,formatSpec,sizeA);
fclose(fileID);
C = C';
[v_0,v_1,v_2,v_3,v_4]=Calculate(C);

colnames
{'Time(s)', 'Ascension(deg)', 'Declination(deg)', 'Sideral Time(deg)'};
set(handles.time_table, 'data', v_1, 'ColumnName', colnames);

colnames
{'r_x(km)', 'r_y(km)', 'r_z(km)', 'r(km)', 'v_x(km/s)', 'v_y(km/s)', 'v_z(
km/s)', 'v(km/s)'};
set(handles.Pos_Vel_Table, 'data', v_2, 'ColumnName', colnames);
colnames = {'Secondes(s)', 'Minutes(min)', 'Hours(H)', 'Days'};
set(handles.Per_Table, 'data', v_3, 'ColumnName', colnames);
colnames = {'Angular Momentum(km^2/s)', 'Eccentricity', 'RA of
Ascending Node(deg)', 'Inclination (deg)', 'Argument of Perigee
(deg)', 'True Anomaly (deg)', 'Semimajor Axis (km)', 'Periapse Radius
(km)'};
set(handles.Par_Table, 'data', v_4, 'ColumnName', colnames);
set(handles.LatitudeVal, 'String', v_0(2));
set(handles.HVal, 'String', v_0(1));
set(handles.LongitudeVal, 'String', v_0(3));

end

```



```

% -----
--

function ExpExcel_ClickedCallback(hObject, eventdata, handles)

% hObject    handle to ExpExcel (see GCBO)
% eventdata  reserved - to be defined in a future version of MATLAB
% handles    structure with handles and user data (see GUIDATA)

global mes
global yes
global res
global tes
global filename
global pName
global phi
global H
global deg
global EL

[xFileName,xPathName] = uiputfile('*.xls');

xlswrite(strcat(xPathName,xFileName),{strcat('Data set from file :
',pName,filename)},1,'J1');

xlswrite(strcat(xPathName,xFileName),{'Time(s)'          'Ascension(deg)'
'Declination(deg)' 'Sideral Time(deg)'} ,1, 'J4');

xlswrite(strcat(xPathName,xFileName),mes,1, 'J5');

xlswrite(strcat(xPathName,xFileName),{'r_x(km)', 'r_y(km)', 'r_z(km)',
'r(km)', 'v_x(km/s)', 'v_y(km/s)', 'v_z(km/s)', 'v(km/s)'} ,1, 'H10');

xlswrite(strcat(xPathName,xFileName),yes,1, 'H11');

xlswrite(strcat(xPathName,xFileName),{'Secondes(s)', 'Minutes(min)', '
Hours(H)', 'Days'} ,1, 'J15');

xlswrite(strcat(xPathName,xFileName),res,1, 'J16');

xlswrite(strcat(xPathName,xFileName),{'Angular
Momentum(km^2/s)', 'Eccentricity', 'RA          of          Ascending
Node(deg)', 'Inclination (deg)', ...
'Argument of Perigee (deg)', 'True Anomaly (deg)', 'Semimajor
Axis (km)', 'Periapse Radius (km)'} ,1, 'H20');

xlswrite(strcat(xPathName,xFileName),tes,1, 'H21');

xlswrite(strcat(xPathName,xFileName),{'1';'2';'3'},1, 'I5:I7');

gets=[phi/deg;EL;H];

xlswrite(strcat(xPathName,xFileName),{'Latitude      (deg)';'Longitude
(deg)';'Altitude above sea level (km)'} ,1, 'C4:C6');

xlswrite(strcat(xPathName,xFileName),gets,1, 'D4:D6');

winopen(strcat(xPathName,xFileName));

end

% --- Executes when selected object is changed in MeasurementMethod.
function MeasurementMethod_SelectionChangeFcn(hObject, eventdata,
handles)

```

```

% hObject    handle to the selected object in MeasurementMethod
% eventdata  structure with the following fields (see UIBUTTONGROUP)
%   EventName: string 'SelectionChanged' (read only)
%   OldValue: handle of the previously selected object or empty if
none was selected
%   NewValue: handle of the currently selected object
% handles    structure with handles and user data (see GUIDATA)
    global Method
    Method=get(handles.Antenna,'Value');
    uitoolbar2_ButtonDownFcn(hObject, eventdata, handles);
end
%
function [ras,decl]=AzEl2RaDec (Az,El,theta,phi,R)
%This function calculates the right ascension and the
% declination from azimuth and elevation
for i = 1:3
    % Matrix of transformation from topocentric horizon to
geocentric equatorial
    Q_xX(1,:) = [-sin(theta(1,i))    -sin(phi)*cos(theta(1,i))
cos(phi)*cos(theta(1,i))];
    Q_xX(2,:) = [cos(theta(1,i))    -sin(phi)*sin(theta(1,i))
cos(phi)*sin(theta(1,i))];
    Q_xX(3,:) = [0 cos(phi) sin(phi)];
    %           for           topocentric           horizon           coordinate
rho_x(:,i)=[cos(El(1,i))*sin(Az(1,i));cos(El(1,i))*cos(Az(1,i));sin(
El(1,i))];
    % for geocentric equatorial coordinate
    rho_X(:,i)=Q_xX*rho_x(:,i);
    l = rho_X(1,i);
    m =rho_X(2,i);
    n = rho_X(3,i);
    decl(1,i) = asin(n);
    if m > 0
        ras(1,i) = acos(l/cos(decl(1,i)));
    else
        ras(1,i) = 2*pi - acos(l/cos(decl(1,i)));
    end
end
end
%
% -----
--
function uitoolbar2_ButtonDownFcn(hObject, eventdata, handles)

```

```

% hObject    handle to uitoolbar2 (see GCBO)
% eventdata  reserved - to be defined in a future version of MATLAB
% handles     structure with handles and user data (see GUIDATA)
set(handles.uitoolbar2,'Visible','on');
end

```

## APPENDIX A1: J0

```

% ~~~~~~
function j0 = J0(year, month, day)
% ~~~~~~
%{
This function computes the Julian day number at 0 UT for any year
between 1900 and 2100 using Equation 5.48.
j0 - Julian day at 0 hr UT (Universal Time)
year - range: 1901 - 2099
month - range: 1 - 12
day - range: 1 - 31
User m-functions required: none
%}
% -----
j0 = 367*year - fix(7*(year + fix((month + 9)/12))/4) ...
+ fix(275*month/9) + day + 1721013.5;
% ~~~~~~
end %J0

```

## APPENDIX A2: LST

```

% ~~~~~~
function lst = LST(year, month, day, ut, EL)
% ~~~~~~
%{
This function calculates the local sidereal time.
lst - local sidereal time (degrees)
y - year
m - month
d - day
ut - Universal Time (hours)
EL - east longitude (degrees)

```

```

j0 - Julian day number at 0 hr UT
j - number of centuries since J2000
g0 - Greenwich sidereal time (degrees) at 0 hr UT
gst - Greenwich sidereal time (degrees) at the specified UT
User M-function required: J0
User subfunction required: zeroTo360
%}
% -----
%...Equation 5.48;
j0 = J0(year, month, day);
%...Equation 5.49:
j = (j0 - 2451545)/36525;
%...Equation 5.50:
g0 = 100.4606184 + 36000.77004*j + 0.000387933*j^2 - 2.583e-8*j^3;
%...Reduce g0 so it lies in the range 0 - 360 degrees
g0 = zeroTo360(g0);
%...Equation 5.51:
gst = g0 + 360.98564724*ut/24;
%...Equation 5.52:
lst = gst + EL;
%...Reduce lst to the range 0 - 360 degrees:
lst = lst - 360*fix(lst/360);
return
% ~~~~~~
function y = zeroTo360(x)
% ~~~~~~
%{
This subfunction reduces an angle to the range 0 - 360 degrees.
x - The angle (degrees) to be reduced
y - The reduced value
%}
% -----
if (x >= 360)
x = x - fix(x/360)*360;
elseif (x < 0)
x = x - (fix(x/360) - 1)*360;
end
y = x;
end %zeroTo360
end %LST

```

```
% ~~~~~
```

### APPENDIX A3: gauss

```
% ~~~~~
function [r, v] = ...
gauss(Rho1, Rho2, Rho3, R1, R2, R3, t1, t2, t3)
%~~~~~
%{
This function uses the Gauss method
(Algorithms 5.5) to calculate the state vector of an
orbiting body from angles-only observations at three
closely-spaced times.
mu - the gravitational parameter (km^3/s^2)
t1, t2, t3 - the times of the observations (s)
tau, tau1, tau3 - time intervals between observations (s)
R1, R2, R3 - the observation site position vectors
at t1, t2, t3 (km)
Rho1, Rho2, Rho3 - the direction cosine vectors of the
satellite at t1, t2, t3
p1, p2, p3 - cross products among the three direction
cosine vectors
Do - scalar triple product of Rho1, Rho2 and Rho3
D - Matrix of the nine scalar triple products
of R1, R2 and R3 with p1, p2 and p3
E - dot product of R2 and Rho2
A, B - constants in the expression relating slant range
to geocentric radius
a,b,c - coefficients of the 8th order polynomial
in the estimated geocentric radius x
x - positive root of the 8th order polynomial
rho1, rho2, rho3 - the slant ranges at t1, t2, t3
r1, r2, r3 - the position vectors at t1, t2, t3 (km)
r,v - the estimated state vector at the end of
Algorithm 5.5 (km, km/s)
User m-functions required: kepler_U, f_and_g
User subfunctions required: posroot
%}
% -----
global mu
```

```

%...Equations 5.98:
tau1 = t1 - t2;
tau3 = t3 - t2;
%...Equation 5.101:
tau = tau3 - tau1;
%...Independent cross products among the direction cosine vectors:
p1 = cross(Rho2,Rho3);
p2 = cross(Rho1,Rho3);
p3 = cross(Rho1,Rho2);
%...Equation 5.108:
Do = dot(Rho1,p1);
%...Equations 5.109b, 5.110b and 5.111b:
D = [[dot(R1,p1) dot(R1,p2) dot(R1,p3)]
[dot(R2,p1) dot(R2,p2) dot(R2,p3)]
[dot(R3,p1) dot(R3,p2) dot(R3,p3)]];
%...Equation 5.115b:
E = dot(R2,Rho2);
%...Equations 5.112b and 5.112c:
A = 1/Do*(-D(1,2)*tau3/tau + D(2,2) + D(3,2)*tau1/tau);
B = 1/6/Do*(D(1,2)*(tau3^2 - tau^2)*tau3/tau ...
+ D(3,2)*(tau^2 - tau1^2)*tau1/tau);
%...Equations 5.117:
a = -(A^2 + 2*A*E + norm(R2)^2);
b = -2*mu*B*(A + E);
c = -(mu*B)^2;
%...Calculate the roots of Equation 5.116 using MATLAB's
% polynomial 'roots' solver:
Roots = roots([1 0 a 0 0 b 0 0 c]);
%...Find the positive real root:
x = posroot(Roots);
%...Equations 5.99a and 5.99b:
f1 = 1 - 1/2*mu*tau1^2/x^3;
f3 = 1 - 1/2*mu*tau3^2/x^3;
%...Equations 5.100a and 5.100b:
g1 = tau1 - 1/6*mu*(tau1/x)^3;
g3 = tau3 - 1/6*mu*(tau3/x)^3;
%...Equation 5.112a:
rho2 = A + mu*B/x^3;
%...Equation 5.113:
rho1 = 1/Do*((6*(D(3,1)*tau1/tau3 + D(2,1)*tau/tau3)*x^3 ...

```

```

+ mu*D(3,1)*(tau^2 - tau1^2)*tau1/tau3) ...
/(6*x^3 + mu*(tau^2 - tau3^2)) - D(1,1));
%...Equation 5.114:
rho3 = 1/Do*((6*(D(1,3)*tau3/tau1 - D(2,3)*tau/tau1)*x^3 ...
+ mu*D(1,3)*(tau^2 - tau3^2)*tau3/tau1) ...
/(6*x^3 + mu*(tau^2 - tau1^2)) - D(3,3));
%...Equations 5.86:
r1 = R1 + rho1*Rho1;
r2 = R2 + rho2*Rho2;
r3 = R3 + rho3*Rho3;
%...Equation 5.118:
v2 = (-f3*r1 + f1*r3)/(f1*g3 - f3*g1);
%...Save the initial estimates of r2 and v2:
r = r2;
v= v2;
return
% ~~~~~
function x = posroot(Roots)
% ~~~~~
%{
This subfunction extracts the positive real roots from
those obtained in the call to MATLAB's 'roots' function.
If there is more than one positive root, the user is
prompted to select the one to use.
x - the determined or selected positive root
Roots - the vector of roots of a polynomial
posroots - vector of positive roots
User M-functions required: none
%}
% ~~~~~
%...Construct the vector of positive real roots:
posroots = Roots(find(Roots>0 & ~imag(Roots)));
npositive = length(posroots);
%...Exit if no positive roots exist:
if npositive == 0
fprintf('\n\n ** There are no positive roots. \n\n')
return
end
%...If there is more than one positive root, output the
% roots to the command window and prompt the user to

```

```

% select which one to use:
if npositive == 1
x = posroots;
else
fprintf('\n\n ** There are two or more positive roots.\n')
for i = 1:npositive
fprintf('\n root #%g = %g',i,posroots(i))
end
fprintf('\n\n Make a choice:\n')
nchoice = 0;
while nchoice < 1 | nchoice > npositive
nchoice = input(' Use root #? ');
end
x = posroots(nchoice);
fprintf('\n We will use %g .\n', x)
end
end %posroot
end %gauss
% ~~~~~

```

## APPENDIX A4: kepler\_U

```

% ~~~~~
function x = kepler_U(dt, ro, vro, a)
% ~~~~~
%{
This function uses Newton's method to solve the universal
Kepler equation for the universal anomaly.
mu - gravitational parameter (km^3/s^2)
x - the universal anomaly (km^0.5)
dt - time since x = 0 (s)
ro - radial position (km) when x = 0
vro - radial velocity (km/s) when x = 0
a - reciprocal of the semimajor axis (1/km)
z - auxiliary variable (z = a*x^2)
C - value of Stumpff function C(z)
S - value of Stumpff function S(z)
n - number of iterations for convergence
nMax - maximum allowable number of iterations
User M-functions required: stumpC, stumpS
%}

```



```

%}
% -----
global mu
%...Set an error tolerance and a limit on the number of iterations:
error = 1.e-8;
nMax = 1000;
%...Starting value for x:
x = sqrt(mu)*abs(a)*dt;
%...Iterate on Equation 3.65 until convergence occurs within
%...the error tolerance:
n = 0;
ratio = 1;
while abs(ratio) > error && n <= nMax
n = n + 1;
C = stumpC(a*x^2);
S = stumpS(a*x^2);
F = ro*vro/sqrt(mu)*x^2*C + (1 - a*ro)*x^3*S + ro*x - sqrt(mu)*dt;
dFdx = ro*vro/sqrt(mu)*x*(1 - a*x^2*S) + (1 - a*ro)*x^2*C + ro;
ratio = F/dFdx;
x = x - ratio;
end
%...Deliver a value for x, but report that nMax was reached:
if n > nMax
fprintf('\n **No. iterations of Kepler''s equation = %g', n)
fprintf('\n F/dFdx = %g\n', F/dFdx)
end
% ~~~~~

```

## APPENDIX A5: f\_and\_g

```

% ~~~~~
function [f, g] = f_and_g(x, t, ro, a)
% ~~~~~
%{
This function calculates the Lagrange f and g coefficients.
mu - the gravitational parameter (km^3/s^2)
a - reciprocal of the semimajor axis (1/km)
ro - the radial position at time to (km)
t - the time elapsed since ro (s)
x - the universal anomaly after time t (km^0.5)

```

```

f - the Lagrange f coefficient (dimensionless)
g - the Lagrange g coefficient (s)
User M-functions required: stumpC, stumpS
%}
% -----
global mu
z = a*x^2;
%...Equation 3.69a:
f = 1 - x^2/ro*stumpC(z);
%...Equation 3.69b:
g = t - 1/sqrt(mu)*x^3*stumpS(z);
end
% ~~~~~

```

## APPENDIX A6: coe\_from\_sv

```

% ~~~~~
function coe = coe_from_sv(R,V,mu)
% ~~~~~
%{
% This function computes the classical orbital elements (coe)
% from the state vector (R,V) using Algorithm 4.1.
%
mu - gravitational parameter (km^3/s^2)
R - position vector in the geocentric equatorial frame (km)
V - velocity vector in the geocentric equatorial frame (km)
r, v - the magnitudes of R and V
vr - radial velocity component (km/s)
H - the angular momentum vector (km^2/s)
h - the magnitude of H (km^2/s)
incl - inclination of the orbit (rad)
N - the node line vector (km^2/s)
n - the magnitude of N
cp - cross product of N and R
RA - right ascension of the ascending node (rad)
E - eccentricity vector
e - eccentricity (magnitude of E)
eps - a small number below which the eccentricity is considered
to be zero
w - argument of perigee (rad)

```

```

TA - true anomaly (rad)
a - semimajor axis (km)
pi - 3.1415926...
coe - vector of orbital elements [h e RA incl w TA a]
User M-functions required: None
%}
% -----

eps = 1.e-10;
r = norm(R);
v = norm(V);
vr = dot(R,V)/r;
H = cross(R,V);
h = norm(H);
%...Equation 4.7:
incl = acos(H(3)/h);
%...Equation 4.8:
N = cross([0 0 1],H);
n = norm(N);
%...Equation 4.9:
if n ~= 0
RA = acos(N(1)/n);
if N(2) < 0
RA = 2*pi - RA;
end
else
RA = 0;
end
%...Equation 4.10:
E = 1/mu*((v^2 - mu/r)*R - r*vr*V);
e = norm(E);
%...Equation 4.12 (incorporating the case e = 0):
if n ~= 0
if e > eps
w = acos(dot(N,E)/n/e);
if E(3) < 0
w = 2*pi - w;
end
else
w = 0;
end
end

```

```

else
w = 0;
end
%...Equation 4.13a (incorporating the case e = 0):
if e > eps
TA = acos(dot(E,R)/e/r);
if vr < 0
TA = 2*pi - TA;
end
else
cp = cross(N,R);
if cp(3) >= 0
TA = acos(dot(N,R)/n/r);
else
TA = 2*pi - acos(dot(N,R)/n/r);
end
end
%...Equation 4.62 (a < 0 for a hyperbola):
a = h^2/mu/(1 - e^2);
coe = [h e RA incl w TA a];
end %coe_from_sv
% ~~~~~

```

## APPENDIX B: GIBBS METHOD

```

% ORBIT DETERMINATION USING GIBBS METHOD
% Universal Time is used
% Day, Time, slant range of object, azimuth, elevation,
latitude, longitude and
% elevation of observation site are used to compute state
vectors
% Input data must be written in notepad as day (D-M-Y), time (H-
M-S),
% slant range of object (rho), azimuth (A), elevation (a),
latitude (phi), longitude (EW), H, respectively
function varargout = GUI_Test(varargin)
% GUI_TEST MATLAB code for GUI_Test.fig
% GUI_TEST, by itself, creates a new GUI_TEST or raises the
existing singleton*.
% H = GUI_TEST returns the handle to a new GUI_TEST or the
handle to the existing singleton*.

```

```

%      GUI_TEST('CALLBACK',hObject,eventData,handles,...) calls
the local function named CALLBACK in GUI_TEST.M with the given input
arguments.

%      GUI_TEST('Property','Value',...) creates a new GUI_TEST
or raises the existing singleton*. Starting from the left, property
value pairs are applied to the GUI before GUI_Test_OpeningFcn gets
called. An unrecognized property name or invalid value makes
property application stop. All inputs are passed to
GUI_Test_OpeningFcn via varargin.

%      *See GUI Options on GUIDE's Tools menu. Choose "GUI
allows only one instance to run (singleton)".

% See also: GUIDE, GUIDATA, GUIHANDLES

% Edit the above text to modify the response to help GUI_Test
% Last Modified by GUIDE v2.5 27-Apr-2015 15:01:55
% Begin initialization code - DO NOT EDIT
gui_Singleton = 1;
gui_State = struct('gui_Name',       mfilename, ...
                  'gui_Singleton',   gui_Singleton, ...
                  'gui_OpeningFcn', @GUI_Test_OpeningFcn, ...
                  'gui_OutputFcn',  @GUI_Test_OutputFcn, ...
                  'gui_LayoutFcn',   [] , ...
                  'gui_Callback',    []);

if nargin && ischar(varargin{1})
    gui_State.gui_Callback = str2func(varargin{1});
end

if nargin
    [varargout{1:nargout}] = gui_mainfcn(gui_State,
varargin{:});
else
    gui_mainfcn(gui_State, varargin{:});
end

% End initialization code - DO NOT EDIT
% --- Executes just before GUI_Test is made visible.
function GUI_Test_OpeningFcn(hObject, eventdata, handles,
varargin)

% This function has no output args, see OutputFcn.
% hObject    handle to figure
% eventdata  reserved - to be defined in a future version of
MATLAB
% handles     structure with handles and user data (see
GUIDATA)
% varargin    command line arguments to GUI_Test (see
VARARGIN)

% Choose default command line output for GUI_Test
handles.output = hObject;

```

```

        % Update handles structure
        guidata(hObject, handles);

        % UIWAIT makes GUI_Test wait for user response (see
UIRESUME)
        % uiwait(handles.figure1);
    end

    % --- Outputs from this function are returned to the command
line.
    function varargout = GUI_Test_OutputFcn(hObject, eventdata,
handles)
        % varargout    cell array for returning output args (see
VARARGOUT);
        % hObject      handle to figure
        % eventdata    reserved - to be defined in a future version of
MATLAB
        % handles      structure with handles and user data (see GUIDATA)
        % Get default command line output from handles structure
        varargout{1} = handles.output;
    end

    % --- Executes during object deletion, before destroying
properties.
    function uitable12_DeleteFcn(hObject, eventdata, handles)
        % hObject      handle to uitable12 (see GCBO)
        % eventdata    reserved - to be defined in a future version of
MATLAB
        % handles      structure with handles and user data (see
GUIDATA)
    end

    % -----
    -----

    function OpenInputFile_ClickedCallback(hObject, eventdata,
handles)
        % hObject      handle to OpenInputFile (see GCBO)
        % eventdata    reserved - to be defined in a future version of
MATLAB
        % handles      structure with handles and user data (see
GUIDATA)
    end

    % --- Executes on button press in Loadnewfile.
    function Loadnewfile_Callback(hObject, eventdata, handles)
        % hObject      handle to Loadnewfile (see GCBO)
        % eventdata    reserved - to be defined in a future version of
MATLAB
        % handles      structure with handles and user data (see
GUIDATA)

```

```

end

% -----
--

function OpenFile_ClickedCallback(hObject, eventdata, handles)
    % hObject    handle to OpenFile (see GCBO)
    % eventdata  reserved - to be defined in a future version of
MATLAB
    % handles     structure with handles and user data (see
GUIDATA)
end
end

%
% ~~~~~~
% Example_5_10
% ~~~~~~
%
% This program uses Algorithms 5.4 and 4.2 to obtain the orbital
% elements from the observational data provided in Example 5.10.
%
% deg - conversion factor between degrees and radians
% pi - 3.1415926...
% mu - gravitational parameter (km^3/s^2)
% Re - equatorial radius of the earth (km)
% f - earth's flattening factor
% wE - angular velocity of the earth (rad/s)
% omega - earth's angular velocity vector (rad/s) in the
% geocentric equatorial frame
% rho - slant range of object (km)
% A - azimuth (deg) of object relative to observation site
% a - elevation angle (deg) of object relative to observation site
% theta - local sidereal time (deg) of tracking site
% phi - geodetic latitude (deg) of site
% H - elevation of site (km)
% r - geocentric equatorial position vector of object (km)
% v - geocentric equatorial velocity vector of object (km)
% coe - orbital elements [h e RA incl w TA a]
% where
% h = angular momentum (km^2/s)
% e = eccentricity
% RA = right ascension of the ascending node (rad)
% incl = inclination of the orbit (rad)
% w = argument of perigee (rad)

```

```

% TA = true anomaly (rad)
% a = semimajor axis (km)
% rp - perigee radius (km)
% T - period of elliptical orbit (s)
%
% User M-functions required: r_from_observe, coe_from_sv
% -----
--

function [v0,v1,v12,v3,v4 ] = Calculate(input_args)
global f Re wE H phi deg mu EL
deg = pi/180;
f = 1/298.256;
Re = 6378.137;
wE = 7.292115e-5;
mu = 398600.442;
deg = pi/180;
C=input_args;
%...Data declaration for Example 5.10:
phi = C(1,10);
H = C(1,12);
rho_1 = C(1,7);
rho_2 = C(2,7);
rho_3 = C(3,7);
A_1 = C(1,8);
A_2 = C(2,8);
A_3 = C(3,8);
a_1 = C(1,9);
a_2 = C(1,9);
a_3 = C(1,9);
% Date:
year_1 = C(1,3);
month_1 = C(1,2);
day_1 = C(1,1);
year_2 = C(2,3);
month_2 = C(2,2);
day_2 = C(2,1);
year_3 = C(3,3);
month_3 = C(3,2);
day_3 = C(3,1);
% Universal time: Local Time-3
hour_1 =C(1,4);

```



```

minute_1 =C(1,5);
second_1 = C(1,6);
hour_2 =C(2,4);
minute_2 = C(2,5);
second_2 = C(2,6);
hour_3 =C(3,4);
minute_3 = C(3,5);
second_3 = C(3,6);

%...Convert negative (west) longitude to east longitude:
% if degrees < 0
% degrees = degrees + 360;
% end

%...Express the longitudes as decimal numbers:
EL=C(1,11);
WL = 360 - EL;

%...Express universal time as a decimal number:
ut_1 = hour_1 + minute_1/60 + second_1/3600;
ut_2 = hour_2 + minute_2/60 + second_2/3600;
ut_3 = hour_3 + minute_3/60 + second_3/3600;

%...Equation 5.46 :
j0_1 = J0(year_1, month_1, day_1);
j0_2 = J0(year_2, month_2, day_2);
j0_3 = J0(year_3, month_3, day_3);

%...Equation 5.47 Julian day number:
jd_1 = j0_1 + ut_1/24;
jd_2 = j0_2 + ut_2/24;
jd_3 = j0_3 + ut_3/24;

%...Algorithm 5.3:
lst_1 = LST(year_1, month_1, day_1, ut_1, EL);
lst_2 = LST(year_2, month_2, day_2, ut_2, EL);
lst_3 = LST(year_3, month_3, day_3, ut_3, EL);

%...Data declaration for Example 5.10:
rho = [rho_1 rho_2 rho_3];
A = [A_1 A_2 A_3];
a = [a_1 a_2 a_3];
theta = [ lst_1 lst_2 lst_3];

%...
%...

%...Algorithm 5.4:
[r1] = r_from_observe(rho_1, A_1, a_1, lst_1, phi, H);

```

```

[r2] = r_from_observe(rho_2, A_2, a_2, lst_2, phi, H);
[r3] = r_from_observe(rho_3, A_3, a_3, lst_3, phi, H);
%...GIBBS
% ~~~~~~
% Example_5_01
% ~~~~~~
%{
This program uses Algorithm 5.1 (Gibbs method) and Algorithm 4.2
to obtain the orbital elements from the data provided in Example
5.1.

deg - factor for converting between degrees and radians
pi - 3.1415926...
mu - gravitational parameter (km^3/s^2)
r1, r2, r3 - three coplanar geocentric position vectors (km)
ierr - 0 if r1, r2, r3 are found to be coplanar
1 otherwise
v2 - the velocity corresponding to r2 (km/s)
coe - orbital elements [h e RA incl w TA a]
where h = angular momentum (km^2/s)
e = eccentricity
RA = right ascension of the ascending node (rad)
incl = orbit inclination (rad)
w = argument of perigee (rad)
TA = true anomaly (rad)
a = semimajor axis (km)
T - period of elliptic orbit (s)
User M-functions required: gibbs, coe_from_sv
%}
% -----
%...Data declaration for Example 5.1:
    r1 = [r1];
    r2 = [r2];
    r3 = [r3];
%...
    %...Echo the input data to the command window:
    fprintf('-----\n')
    fprintf('\n Example 5.1: Gibbs Method\n')
    fprintf('\n\n Input data:\n')
    fprintf('\n Gravitational parameter (km^3/s^2) = %g\n', mu)
    fprintf('\n r1 (km) = [%g %g %g]', r1(1), r1(2), r1(3))
    fprintf('\n r2 (km) = [%g %g %g]', r2(1), r2(2), r2(3))

```

```

    fprintf('\n r3 (km) = [%g %g %g]', r3(1), r3(2), r3(3))
    fprintf('\n\n');
%...Algorithm 5.1:
    [v2, ierr] = gibbs(r1, r2, r3);
%...If the vectors r1, r2, r3, are not coplanar, abort:
if ierr == 1
    fprintf('\n These vectors are not coplanar.\n\n')
    v0= [H, phi,EL];
    v1= [rho;A;a;theta]';
    v12= [NaN,NaN,NaN,NaN,NaN,NaN,NaN,NaN];
    v3= [NaN,NaN,NaN,NaN];
    v4= [NaN,NaN,NaN,NaN,NaN,NaN,NaN,NaN];
    der= msgbox('These vectors are not coplanar','Error','error');
else
    %...Algorithm 4.2:
    coe = coe_from_sv(r2,v2,mu);
    h = coe(1);
    e = coe(2);
    RA = coe(3);
    incl = coe(4);
    w = coe(5);
    TA = coe(6);
    %a = coe(7);
    %...Equation 2.40
    rp = h^2/mu/(1 + e);
    %...Output the results to the command window:
    fprintf(' Solution:')
    fprintf('\n');
    fprintf('\n r2 (km/s) = [%g %g %g]', r2(1), r2(2), r2(3))
    fprintf('\n v2 (km/s) = [%g %g %g]', v2(1), v2(2), v2(3))
    fprintf('\n\n Orbital elements:');
    fprintf('\n Angular momentum (km^2/s) = %g', h)
    fprintf('\n Eccentricity = %g', e)
    fprintf('\n Inclination (deg) = %g', incl/deg)
    fprintf('\n RA of ascending node (deg) = %g', RA/deg)
    fprintf('\n Argument of perigee (deg) = %g', w/deg)
    fprintf('\n True anomaly (deg) = %g', TA/deg)
    fprintf('\n Semimajor axis (km) = %g', coe(7))
    fprintf('\n Perigee radius (km) = %g', rp)
    %...If the orbit is an ellipse, output the period:

```

```

    if e < 1
    T = 2*pi/sqrt(mu)*coe(7)^1.5;
    fprintf('\n Period:')
    fprintf('\n Seconds = %g', T)
    fprintf('\n Minutes = %g', T/60)
    fprintf('\n Hours = %g', T/3600)
    fprintf('\n Days = %g', T/24/3600)
    end
    fprintf('\n-----\n')
%
%%%%%%%%%%%%%%%%%%%%%%%%%%%%%%%%%%%%%%%%%%%%%%%%%%%%%%%%%%%%%%%%%%%%%%%%

    global mes
    global yes
    global res
    global tes
    mes=[rho;A;a;theta]';
    yes=[r2,norm(r2),v2, norm(v2)];
    if coe(2)<1
        res=[T,T/60,T/3600,T/24/3600];
    else
        res=[NaN,NaN,NaN,NaN];
    end

    tes=[coe(1),coe(2),coe(3)/deg,coe(4)/deg,coe(5)/deg,coe(6)/deg,coe(7)
    ),coe(1)^2/mu/(1 + coe(2))];

    v1=mes;
    v12=yes;
    v3=res;
    v4=tes;
    v0=[H, phi,EL];

end
end
% -----
--

function OpenFile_ClickedCallback(hObject, eventdata, handles)
% hObject    handle to OpenFile (see GCBO)
% eventdata  reserved - to be defined in a future version of MATLAB
% handles    structure with handles and user data (see GUIDATA)
%
%       jScrollPane = handles.time_table(jScrollPane);
%
%       set(jScrollPane,'VerticalScrollBarPolicy',21); % or:
jScrollPane.VERTICAL_SCROLLBAR_NEVER

```

```

%           jScrollPane.setHorizontalScrollBarPolicy(31);    % or:
jScrollPane.HORIZONTAL_SCROLLBAR_NEVER

%jViewport = jScrollPane.getViewport;
%jEditbox = jViewport.getComponent(0);
%jEditbox.setWrapping(false); % do *NOT* use set(...)!!!

global filename
global pName

[filename,pName] = uigetfile('*.txt','Select Your Data
Set');

formatSpec = '%u %u %u %u %u %f %f %f %f %f %f %f';
sizeA = [12 3];
fileID = fopen(filename);
C = fscanf(fileID,formatSpec,sizeA);
fclose(fileID);
C = C';
[v_0,v_1,v_2,v_3,v_4]=Calculate(C);
colnames =
{'Range(km)', 'Azimuth(deg)', 'Elevation(deg)', 'Sideral Time(deg)'};
set(handles.time_table, 'data', v_1, 'ColumnName', colnames);
colnames =
{'r_x(km)', 'r_y(km)', 'r_z(km)', 'r(km)', 'v_x(km/s)', 'v_y(km/s)', 'v_z(
km/s)', 'v(km/s)'};
set(handles.Pos_Vel_Table, 'data', v_2, 'ColumnName', colnames);
colnames = {'Secondes(s)', 'Minutes(min)', 'Hours(H)', 'Days'};
set(handles.Per_Table, 'data', v_3, 'ColumnName', colnames);
colnames = {'Angular Momentum(km^2/s)', 'Eccentricity', 'RA of
Ascending Node(deg)', 'Inclination (deg)', 'Argument of Perigee
(deg)', 'True Anomaly (deg)', 'Semimajor Axis (km)', 'Periapse Radius
(km)'};
set(handles.Par_Table, 'data', v_4, 'ColumnName', colnames);
set(handles.LatitudeVal, 'String', v_0(2));
set(handles.HVal, 'String', v_0(1));
set(handles.LongitudeVal, 'String', v_0(3));

end

% -----
--

function ExpExcel_ClickedCallback(hObject, eventdata, handles)
% hObject    handle to ExpExcel (see GCBO)
% eventdata  reserved - to be defined in a future version of MATLAB
% handles    structure with handles and user data (see GUIDATA)

global mes
global yes
global res

```

```

global tes
global filename
global pName
global phi
global H
global deg
global EL

[xFileName,xPathName] = uiputfile('*.xls');
xlswrite(strcat(xPathName,xFileName),{strcat('Data set from file :
',pName,filename)},1,'J1');

xlswrite(strcat(xPathName,xFileName),{'Range(km)', 'Azimuth(deg)', 'El
vation(deg)', 'Sideral Time(deg)'},1,'J4');

xlswrite(strcat(xPathName,xFileName),mes,1,'J5');

xlswrite(strcat(xPathName,xFileName),{'r_x(km)', 'r_y(km)', 'r_z(km)',
'r(km)', 'v_x(km/s)', 'v_y(km/s)', 'v_z(km/s)', 'v(km/s)'},1,'H10');

xlswrite(strcat(xPathName,xFileName),yes,1,'H11');

xlswrite(strcat(xPathName,xFileName),{'Secondes(s)', 'Minutes(min)', '
Hours(H)', 'Days'},1,'J15');

xlswrite(strcat(xPathName,xFileName),res,1,'J16');

xlswrite(strcat(xPathName,xFileName),{'Angular
Momentum(km^2/s)', 'Eccentricity', 'RA          of          Ascending
Node(deg)', 'Inclination (deg)', ...
    'Argument of Perigee (deg)', 'True Anomaly (deg)', 'Semimajor
Axis (km)', 'Periapse Radius (km)'},1,'H20');

xlswrite(strcat(xPathName,xFileName),tes,1,'H21');

gets=[phi;EL;H];

xlswrite(strcat(xPathName,xFileName),{'Latitude      (deg)'; 'Longitude
(deg)'; 'Altitude above sea level (km)'},1,'C4:C6');

xlswrite(strcat(xPathName,xFileName),gets,1,'D4:D6');

winopen(strcat(xPathName,xFileName));

end

```

## APPENDIX B1: r\_from\_observe

```

%
~~~~~

function [r] = r_from_observe(rho, A, a, theta, phi, H)

%
~~~~~

%{This function calculates the geocentric equatorial position of an
object from radar observations of range, azimuth, elevation angle
and their rates.

deg - conversion factor between degrees and radians
pi - 3.1415926...

```

```

Re - equatorial radius of the earth (km)
f - earth's flattening factor
wE - angular velocity of the earth (rad/s)
omega - earth's angular velocity vector (rad/s) in the
geocentric equatorial frame
theta - local sidereal time (degrees) of tracking site
phi - geodetic latitude (degrees) of site
H - elevation of site (km)
R - geocentric equatorial position vector (km) of tracking site
Rdot - inertial velocity (km/s) of site
rho - slant range of object (km)
A - azimuth (degrees) of object relative to observation site
a - elevation angle (degrees) of object relative to observation site
dec - topocentric equatorial declination of object (rad)
h - hour angle of object (rad)
RA - topocentric equatorial right ascension of object (rad)
Rho - unit vector from site to object
r - geocentric equatorial position vector of object (km)
v - geocentric equatorial velocity vector of object (km)
User M-functions required: none
%}
% -----
--

global f Re wE
deg = pi/180;
omega = [0 0 wE];
%...Convert angular quantities from degrees to radians:
A = A *deg;
a = a *deg;
theta = theta*deg;
phi = phi *deg;
%...Equation 5.56:
R = [(Re/sqrt(1-(2*f - f*f)*sin(phi)^2) + H)*cos(phi)*cos(theta),
(Re/sqrt(1-(2*f - f*f)*sin(phi)^2) + H)*cos(phi)*sin(theta), (Re*(1 -
f)^2/sqrt(1-(2*f - f*f)*sin(phi)^2) + H)*sin(phi)];
%...Equation 5.66:
Rdot = cross(omega, R);
%...Equation 5.83a:
dec = asin(cos(phi)*cos(A)*cos(a) + sin(phi)*sin(a));
%...Equation 5.83b:
h = acos((cos(phi)*sin(a) - sin(phi)*cos(A)*cos(a))/cos(dec));

```

```

if (A > 0) & (A < pi)
    h = 2*pi - h;
end
%...Equation 5.83c:
RA = theta - h;
%...Equations 5.57:
Rho = [cos(RA)*cos(dec) sin(RA)*cos(dec) sin(dec)];
%...Equation 5.63:
r = R + rho*Rho;
end %r_from_observe
%
~~~~~

```

## APPENDIX B2: gibbs

```

% ~~~~~
function [V2, ierr] = gibbs(R1, R2, R3)
% ~~~~~
%{
This function uses the Gibbs method of orbit determination to
to compute the velocity corresponding to the second of three
supplied position vectors.
mu - gravitational parameter (km^3/s^2
R1, R2, R3 - three coplanar geocentric position vectors (km)
r1, r2, r3 - the magnitudes of R1, R2 and R3 (km)
c12, c23, c31 - three independent cross products among
R1, R2 and R3
N, D, S - vectors formed from R1, R2 and R3 during
the Gibbs' procedure
tol - tolerance for determining if R1, R2 and R3
are coplanar
ierr - = 0 if R1, R2, R3 are found to be coplanar
= 1 otherwise
V2 - the velocity corresponding to R2 (km/s)
User M-functions required: none
%}
% -----
global mu
tol = 1e-4;
ierr = 0;

```



```

%...Magnitudes of R1, R2 and R3:
r1 = norm(R1);
r2 = norm(R2);
r3 = norm(R3);
%...Cross products among R1, R2 and R3:
c12 = cross(R1,R2);
c23 = cross(R2,R3);
c31 = cross(R3,R1);
%...Check that R1, R2 and R3 are coplanar; if not set error flag:
if abs(dot(R1,c23)/r1/norm(c23)) > tol
ierr = 1;
end
%...Equation 5.13:
N = r1*c23 + r2*c31 + r3*c12;
%...Equation 5.14:
D = c12 + c23 + c31;
%...Equation 5.21:
S = R1*(r2 - r3) + R2*(r3 - r1) + R3*(r1 - r2);
%...Equation 5.22:
V2 = sqrt(mu/norm(N)/norm(D))*(cross(D,R2)/r2 + S);
% ~~~~~~
end %gibbs

```



## CURRICULUM VITAE



**Name Surname:** Derya Baş

**Place and Date of Birth:** Kastamonu / 09.03.89

**E-Mail:** bash.derya@gmail.com

**B.Sc.:** 2012, Istanbul Technical University, Faculty of Aeronautics and Astronautics, Astronautical Engineering

**M.Sc.:** 2016, Istanbul Technical University, Department of Aeronautical and Astronautical Engineering , Astronautics and Aeronautics Engineering Programme

### Projects and Theses:

- Turksat-6A Project, Electrical Propulsion Responsible, Tubitak Space (February 2015-Present)
- Turksat-4A/4B Direct Participation Project, Propulsion Responsible, Mitsubishi Electric Kamakura Works / JAXA Assembly& Integration Building (February 2013-Present)
- Team Leader of Hunter Project Team (2012)
- Project Hunter is designating for the Mission Idea Contest 2, which held by Japan Aerospace Exploration Agency (JAXA).
- Tubitak Research Project Competition Between High School Students, Member of Physics Division (Eliminated second phase)
- **Undergraduate Thesis:** Plasma Flow Modeling of Pulsed Plasma Thruster (2012)  
**Thesis Advisor:** Assist. Prof. Dr. Cuma YARIM
- **Master's Thesis:** Satellite Orbit Determination Via Optical and Radar Systems (continue)  
**Thesis Advisor:** Prof. Dr. Cengiz HACIZADE

## **List of Publications:**

Baş, D., Bulut, M., Sözbir, N., Gülgönül, Ş. 2014. Haberleşme Uydularında Çift Yakıtlı İtici Sistem Bileşenleri ve Uygulanan Testler, Ulusal Havacılık ve Uzay Konferansı, Eylül 2014

## **Certificates:**

- Brief Introduction of Jaxa & Environmental Test Technology Unit (JAXA – 2015)
- Introduction to JERG-2-130 Test Requirements (JAXA – 2015)
- Thermal Testing and Verification (JAXA – 2015)
- Practical Guide and Technology of Environmental Test (JAXA – 2015)
- Basic and Advanced Theory and Technology of Mechanical Tests (JAXA – 2015)
- Obligatory Satellites System Assembly and Integration Course (MELCO – 2013)
- Satellites System Assembly and Integration Skills Course (MELCO – 2013)
- Adhesive Treatment Module (MELCO – 2013)
- Alignment Measurement Training of Mechanical Ground Support Equipment (MGSE) Module (MELCO – 2013)
- Introduction of JAXA Environmental Test Center's Activities (JAXA-2013)
- JAXA Environmental Test Facilities, Environmental Test Technology for Space Vehicle (JAXA-2013)
- General Test Strategies in Spacecraft (JAXA-2013)
- The 2<sup>nd</sup> Mission Idea Contest for Micro/Nano Satellite Utilization, Tokyo (June 2012)